Chemical and Physical Properties of Australian Fine Particles: A Pilot Study

Final Report to Environment Australia
from the
Division of Atmospheric Research, CSIRO
and the
Australian Nuclear Science and Technology Organisation

G.P. Ayers, M.D. Keywood and J.L. Gras
Division of Atmospheric Research, CSIRO
PMB 1
Aspendale
Victoria 3195
Australia
tel (03) 9239 4400
fax (03) 9239 4688
e_mail chief@dar.csiro.au

D. Cohen, D. Garton and G.M. Bailey
ANSTO
Physics Division
PMB1
Menai
New South Wales 2234
Australia
tel (02) 9717 3042
fax (02) 9717 3257

CONTENTS

Summary

This report presents results and interpretation from a pilot study entitled ***Chemical and Physical Properties of Australian Fine Particles (AFP Study),*** carried out between August 1996 and December 1997. This pilot study was commissioned by Environment Australia, and was carried out by the CSIRO and ANSTO in conjunction with the relevant agencies responsible for ambient air quality monitoring in Sydney, Brisbane, Melbourne, Canberra, Launceston and Adelaide. The study, although of limited duration, employed a comprehensive package of aerosol measurement equipment (listed in Table 2 in the body of the report) to generate a large database on a wide variety of chemical and physical properties of atmospheric aerosol particles measured at six locations across eastern Australia. Major conclusions and recommendations that can be reached from analysis of the AFP database concern:

Comparability of Measurement Systems

At the fine particle levels encountered in the six locations studied, the various measurements of aerosol mass concentration regularly differed by more than the expected levels of measurement system uncertainty. In routine operation, the levels of performance for co-located samplers implied in the Australian PM10 standards [AS 3580.9.6-1990/AS 3580.9.9-1990] and relevant US standards [summarised by Chow, 1995] were not always achieved.

The key source of variance between aerosol measurement systems appears to be the extent to which semi-volatile aerosol material is collected and determined. One component of this is atmospheric water, which may readily exchange with aerosol material sampled on filters in response to change in humidity. Although this fact is well known and allowed for in the standard (gravimetric) PM10 methods, tighter control of humidity during the gravimetric analysis of filters appears desirable. In this regard, it is noteworthy that the least variance between gravimetric data pairs was achieved by the MOUDI (Micro-Orifice Uniform Deposit Impactor) and Solar-Vol samplers: both were operated by the CSIRO group, which had the strictest control of humidity during filter weighing.

A second component of semi-volatile aerosol material occurs in the organic fraction. In general, systematically lower PM2.5 and PM1 values were determined by TEOM (Tapered Element Oscillating Microbalance) measurement systems in comparison with the manual, gravimetric systems. The discrepancy was of order 30% between the CSIRO PM2.5 TEOM and the MOUDI in the AFP Study. The principal difference between these systems is that the TEOMs operate at elevated temperatures (commonly 35ºC to 50ºC) whereas the manual gravimetric systems collect aerosol material at ambient temperature. Evidence in the international literature supports the view that volatilisation of semi-volatile organic material is a cause of systematically lower TEOM data.

Comparison of the two measurement systems used extensively to estimate aerosol elemental carbon (EC) content in previous Australian fine particle studies revealed a systematic difference approaching a factor of two. Differences of this magnitude have been found internationally in comparisons between aerosol carbon measurement systems, underlining the difficulties inherent in these measurements.

Taking into consideration all these findings we recommend that:

(1) a nationally coherent approach to particle measurement systems should be developed, incorporating performance standards for PM parameters that are amenable to validation on a regular basis (for example by comparison of operational instruments in routine use with a single national "calibration" sampler operated by a single agency);

(2) consideration should be given to seeking a common sampling system for particle measurements in all jurisdictions, to avoid differences between different sampler types and different operational procedures;

(3) care should be exercised in the use of heating to achieve humidity control for measurement systems such as the nephelometer or TEOM; where heating is operationally used the extent of loss of semi-volatile aerosol material should be assessed by comparison with manual, gravimetric measurements undertaken at ambient temperature;

(4) consideration should be given to employing alternate methods of humidity control (drying) in Australian fine particle measurement systems;

(5) comparisons between absolute EC levels reported from previous Australian fine particle studies should be made with caution; research should be undertaken to evaluate available methods of aerosol carbon measurement with a view to developing a single method of measurement for aerosol carbon that is appropriate for Australian conditions.

Relationships Between PM10, PM2.5 and PM1

The MOUDI has been used in the AFP study to provide data on aerosol mass and chemical composition over the TSP, PM10, PM2.5 and PM1 aerosol fractions simultaneously, without the additional error that must intrude if these four parameters are measured by four separate instruments.

While PM10 and PM2.5 data show a strong structural relationship, variability in PM10 was found to be dominated by variability in the PM2.5 fraction, rather than the PM10-PM2.5 fraction. Thus, the statistical relationships noted between health outcomes and PM10 are most likely caused by the PM2.5 component of the size fraction, rather than the PM10-PM2.5 fraction. This would appear to provide an argument for an ambient aerosol standard based on PM2.5 mass concentration rather than the current PM10 mass concentration. It suggests that stronger relationships might be observed between PM2.5 and health outcomes, than are currently observed between PM10 and health outcomes, if more PM2.5 data were available, *i.e*. if PM2.5 data were regularly monitored and reported.

On the other hand, the high correlations between each of PM2.5, PM1 and PM2.5-PM1 suggest that in terms of analysis of variance in conjunction with health indicator variables, there would be little to gain by moving from PM2.5 to PM1.

Therefore, we recommend that:

(6) PM2.5 measurements should be undertaken routinely in Australia (initially in conjunction with existing PM10 measurements so as to provide a quantitative basis for determining which is the better indicator of health effects of atmospheric particles);

(7) given high correlations found between PM1, PM2.5-PM1 and PM2.5, PM1 measurements offer no clear advantage over PM2.5 measurements as a mass-based indicator of potential health effects of ambient particles.

Continuous Particle Measurement Systems: Nephelometer, TEOM, Ultrafine Particle Measurement Systems

The advantages of a continuous monitoring systems compared with 24 hour average sampling on a 6 day cycle should be self-evident. Where high particle loadings occur on an event basis, as in most Australian cities, this avoids the 5 in 6 probability of missing events, provides greater insights into physical processes, opens the prospects for examining lagged particle-health relationships (over varying lag times) and allows much better statistics for health determinations where statistics are usually severely limited. However any measurement system has limitations as well as advantages, as noted above in the case of the TEOM.

Use of nephelometers to determine aerosol scattering coefficient (b_{spd}) at multiple sites in a number of Australian locales has a long history, going back as much as two decades. Although scattering coefficient as determined by a nephelometer is an integral property of the aerosol size distribution, the physics of the interaction between aerosol particles and visible radiation is weighted towards particles in the sub-micrometre size range. Within the context of an emerging focus internationally on the PM2.5 aerosol fraction, it is relevant to consider the possibility that the extensive historical records of b_{spd} might provide a surrogate historical record for PM2.5, because this latter mass-based integral measure tends also to be dominated by a mode in the mass distribution at diameters below 1 μm.

In the AFP Study we have confirmed that linear relationships can be found between b_{spd} (measured by nephelometer) and PM2.5 (measured by TEOM) in each city studied. However differences in the scattering-mass relationships were identified, caused by site-specific aerosol (size distribution) properties. Thus if b_{spd} were to be used as a surrogate historical record for PM2.5 the slope of the relationship would have to be determined for each site. An additional complication is that at any given site this relationship may vary with season (not investigated in the AFP study), so clearly caution would be required in any project aimed at harmonising the historical b_{spd} data records with new and ongoing PM2.5 records. Other complicating matters are the significant dependence of nephelometer output on humidity, and the strong implication from the TEOM results that humidity reduction via a heating, often used for nephelometers as well as for the TEOM, may not be appropriate.

Ultrafine particle number concentration is also readily amenable to continuous measurement: such measurements were included in the AFP Study. The AFP study data show that ultrafine particle number concentrations do not correlate with the ambient mass-based data normally reported, *i.e*. PM10 and PM2.5, nor with measures of ultrafine particle mass derived from MOUDI data (*i.e*. estimates of PM0.15). We conclude that mass-based integral properties of the aerosol do not provide surrogates for ultrafine particle number concentration.

Taking into consideration these findings we recommend that:

(8) a rigorous determination of the relationship between b_{spd} and PM2.5 must be carried out at each locality (over at least one complete annual cycle) where historical b_{spd} data are to be used as a surrogate for fine mass data.

(9) ultrafine particle number concentrations cannot be inferred from mass-based aerosol measurements so must be determined directly using independent ultrafine particle (or condensation nucleus) measurement systems.

Gaps in Knowledge

The AFP study has highlighted a number of areas where further understanding is required to underpin sound policy development. The most important lack of knowledge concerns semi-volatile aerosol material. A related issue, given the probable role of organic material as a major fraction of the semi-volatile aerosol material, and the possible role of toxic organic constituents in health effects, is a lack of certainty about the amount and types of carbonaceous material in the aerosol. In this regard we recommend that:

(10) studies be undertaken to characterise the semi-volatile component of aerosol material in the major urban airsheds in Australia, in terms of its contribution to PM10 and PM2.5 mass loading, its composition, sources, and variability with location and season;

(11) uniform methods be developed and agreed between jurisdictions for the determination of carbonaceous aerosol material, in particular the components elemental carbon (EC) and organic carbon (OC).

Discussions between the AFP Study team and representatives of the various State/Territory agencies assisting with the measurement program suggest that a number of aspects of fine particle monitoring and assessment may have been the subject of in-house investigations carried out by some of these agencies. Useful information may have been generated, but remains not widely known or available. Therefore we recommend that:

(12) agencies be encouraged to make available to a central database, located in Environment Australia, copies of all published and unpublished work in their possession related to aerosol monitoring and assessment in Australia.

Finally, taking into consideration all the foregoing comments we recommend that:

(13) given the current uncertainty world-wide over the implications for human health of exposure to fine particles, the uncertainty over choice of ambient indicator for fine particles, the disparity of approaches taken to date by different agencies within Australia, and the evident differences between results from different measurement systems employed in the AFP Study, a national conference on fine particle monitoring and assessment should be held. The aim would be to bring together the relevant regulatory agencies and research institutions to seek a consensus on the development of a nationally uniform approach to fine particle monitoring and assessment within Australia.

1. Introduction

This report presents results and interpretation from a pilot study on the ***Chemical and Physical Properties of Australian Fine Particles (AFP Study)***, carried out by CSIRO and ANSTO over an 18 month period from mid 1996. The AFP Study was sponsored by Environment Australia, and was carried out in collaboration with six of the relevant State/Territory regulatory agencies, as listed in Table 1. Western Australia and the Northern Territory did not take part in the study as a major aerosol study has recently been completed in Perth [Gras, 1996] and the Northern Territory does not currently monitor particles.

Table 1. AFP Participants

Institution	*Role*
CSIRO, Division of Atmospheric Research	Sampling equipment, personnel, analysis, reporting
ANSTO, Physics Division	Sampling equipment, personnel, analysis, reporting
Environment Australia	Funding
Environment Protection Authority Victoria (EPA Vic)	Site, air quality data
Environment Protection Authority New South Wales (EPA NSW)	Site, air quality data
Department of Environment Queensland	Site, personnel, air quality data
Environment Protection Authority South Australia	Site
Department of Environment and Land Management Tasmania, Environment and Planning Division	Site, personnel, air quality data
ACT Analytical Laboratories, Environment ACT	Site, personnel, air quality data

2. Scope

The AFP Study was commissioned by Environment Australia in 1996 as an 18 month project with the following rationale[1]:

In Australia responsibility for monitoring the exposure of the population to fine particles resides in the relevant State and Territory authorities, with the consequence that the data available for a national assessment of fine particle issues may be of variable type, completeness and quality. Moreover, in Australia as elsewhere debate about which size range of particles should be monitored has yet to reach a consensus, with existing aerosol data comprising a mixture of TSP, PM10 and PM2.5 information, plus many years of b_{sp} (aerosol scattering coefficient) data[2]. Additionally, the majority of extant data in Australia consist of mass concentration data, with little knowledge available about the variation with particle size of potentially harmful components (*e.g.* sulfate, acidity, organics), nor about the relationships between mass-based parameters and other aerosol properties. For example, the number concentration of particles < 100 - 200 nm aerodynamic diameter, rather than mass concentration, has been proposed recently to be of great significance to human health effects [Seaton *et al.*, 1995].

This work confronts these issues via a pilot study to investigate their relevance in Australia. It addresses three key questions:

1) how comparable are the fine particle measurements made by various State/Territory EPAs?
2) how are key chemical species distributed across the fine particle size range (10 nm to 20 μm diameter), and how well do PM10 and PM2.5 (and PM1) measurements discriminate between different chemical species?
3) what number distributions of particles are found in urban Australian environments and how does particle number concentration (particles > 3 nm diameter) relate to the currently employed mass-based fine particle measurement methods and to b_{sp} derived from nephelometer records?

[1] See letter of offer from Environment Australia.

[2] A glossary of terms is provided in Appendix A.

3. Aims

The specific aims of the pilot study were:

1) to determine a comprehensive range of fine particle physical and chemical properties during a 1 month period in parallel with existing routine aerosol measurements at one site in each of the six major urban centres in Australia;
2) to use these data to provide a preliminary analysis of the comparability of the separate State/Territory measurement systems for the aerosol parameters measured;
3) to analyse in detail the chemical and physical relationships between PM10, PM2.5 (and PM1) under the various Australian conditions studied, and to summarise the advantages and disadvantages of these measurements;
4) to make recommendations, if necessary, concerning steps required to achieve uniformity in measurements system performance across Australia;
5) to make recommendations for additional work, if necessary, based upon the pilot study findings.

4. Sampling Program

The AFP Study involved a measurement program based on a "travelling" package of aerosol measurement equipment operated for one month at a monitoring site in each of six State/Territory jurisdictions. Each set of measurements was carried out in parallel with the existing State/Territory samplers at the site for comparison purposes. The pilot study package deployed consisted of the instrumentation listed in Table 2. Initially, the equipment was shipped to sites and installed alongside existing state or territory authority equipment, however this resulted in working in small and equipment-overcrowded spaces and damage to equipment during shipping. To avoid this, in 1997 a caravan laboratory was used for transportation of the package and operation of the equipment adjacent to the given authority air quality site.

Table 2. Instrumentation used in the Aerosol Pilot Study

Instrument	*Information*
Micro-Orifice Uniform Deposit Impactor (MOUDI)	mass and chemical concentration data from particles from 0.056 to 18 µm in aerodynamic diameter
ANSTO PM10 sampler (SFU; stacked filter unit)	mass and chemical concentration data for particles 2.5 – 10 µm and less than 2.5 µm in diameter
ANSTO PM2.5 sampler (ASP-type; cyclone inlet)	mass and chemical concentration data for particles less than 2.5 µm in diameter
PM2.5 Aerosol Sampler (ECOTECH Solar-Vol 1100)	mass and chemical concentration data for particles less than 2.5 µm in diameter
Aerosol Differential Mobility Analyser including an Ultrafine Particle Counter	number concentration data for particles from 15 nm to 300 nm in diameter
Active-cavity Laser Particle Size Spectrometer	number concentration data for particles from 100 nm to 3 µm in diameter
Nephelometers	particle scattering coefficient, at 530 nm, one measurement at ambient humidity, one at reduced humidity
Ultrafine particle counter	particle number concentration for >3nm in diameter
PM2.5 TEOM	mass concentration particles less than 2.5 µm diameter

The first four devices were operated on a 6-day cycle (a 24 hour sample taken each 6th day) in parallel with the co-located State/Territory samplers. The collected aerosol material was subsequently analysed by ANSTO and CSIRO for a wide range of elemental and chemical species. The remaining devices were used to carry out continuous measurements for specific periods, at intervals throughout each 1 month period. These devices produced time series data on aerosol number concentration and size distribution from the ultrafine range (~3 nm

diameter) to 3 µm diameter, as well as aerosol scattering coefficient and PM2.5 mass concentration.

Sampling was carried out in 6 cities (Sydney, Brisbane, Melbourne, Canberra, Launceston and Adelaide) between July 1996 and August 1997, for a period of approximately 4 weeks in each city. Sample sites and times within each city were chosen after consultation with the relevant State/Territory regulatory agencies. Considerations included: the typical month in the year for worst haze episodes, existing particle monitoring activities, availability of space and power. The sample locations, number of days sampled for the 6 day samplers and timing are listed in Table 3.

Table 3. Sampling locations, times and number of days sampled for 6 day samplers.

Sampling Locality	*Sampling Period*	*No. of 6 day samples*
Sydney, Liverpool	20/8/96-15/9/96	5
Brisbane, Rocklea	25/9/96-24/11/96	8
Melbourne, Footscray	3/4/97-27/4/97	5
Canberra, Monash	3/5/97-4/6/97	5
Launceston, Ti Tree Bend	10/6/97-25/7/97	8
Adelaide, Therbaton	1/8/97-27/8/97	5

5. Instrumentation

A key measurement within this comprehensive package was that of the MOUDI, a device hitherto unused in Australia. The MOUDI provides data on aerosol mass and chemical composition over the whole size range that constitutes the TSP, PM10, PM2.5 and PM1 aerosol fractions, so yields data on all four aerosol parameters simultaneously, from a single sample. This ensures completely consistent TSP, PM10, PM2.5 and PM1 data without the additional error that must intrude if these four parameters are measured by four separate instruments, having separate operational characteristics such as flow measurement, size dependent collection characteristics *etc*.

5.1 MOUDI[3]

The MOUDI (Micro-Orifice Uniform Deposit Impactor) is a 10 stage cascade impactor (effectively 12 stage when the inlet stage and final filter are included, as in this work) with the stages having 50% cut-points ranging from 0.056 µm to 18 µm in aerodynamic diameter. The principle of operation is straightforward. A jet of particle-laden air is directed at an impaction plate. When the jet encounters the plate the flow streamlines are forced to make a sharp 90º turn so that the air can flow around the plate and exit the impaction area. Large particles having significant inertia are unable to make the sharp 90º turn and are carried forward to impact on, and thus be collected by, the impaction plate. Particles below a threshold inertia do not impact, but follow the airflow out of the impaction area. Subsequent discussion of the MOUDI data in terms of PM10, PM2.5 and PM1 size fractions does not directly use the individual stage data, but is based on a numerical inversion procedure discussed in detail below, that yields a smooth size distribution from which each fraction is determined.

Table 4. Cut-point size and number of nozzles for each stage of the MOUDI.

Stage	*Cut-point, µm*	*Number of Nozzles*
Inlet	18	1
1	10	1
2	5.6	10
3	3.2	10
4	1.8	20
5	1	40
6	0.56	80
7	0.32	900
8	0.18	900
9	0.1	2000
10	0.056	2000
11	Back-up filter	1

[3]The name Micro-Orifice Uniform Deposit Impactor is a misnomer: in the "non-rotating" version of this device employed in the AFP study the aerosol is actually collected non-uniformly in an array of spots distributed across the collection substrate.

Particles in discrete size ranges are collected by passing the aerosol through a series of impaction stages, with higher jet velocities in each subsequent stage ensuring collection of particles smaller than collected by the previous stage. In the MOUDI each stage is comprised of an arrangement of nozzles and an impaction plate. Table 4 lists the nominal cut size and number of nozzles for each stage in the MOUDI. It is important to note that the sum of all the MOUDI stage collections is a true measure of TSP, since the inlet collects all particles larger than 10 µm, while the backup filter is a high efficiency teflon filter with 100% collection efficiency for particles below the stage 10 cut-point size. MOUDI calibration data and stage collection efficiencies at a flow rate of 30 l min^{-1} have been detailed by Marple *et al.* [1991].

In this project the MOUDI samples were taken over 24 hours at the designed flow rate of 30 l min^{-1}. At this flowrate the MOUDI acts as a "critical orifice" ensuring a very well-defined, essentially invariant flow (to within 1 l min^{-1}). This advantageous characteristic of the MOUDI was checked with high precision during each installation of the MOUDI using a Gillibrator soap-bubble flowmeter attached to the exhaust of the pump. During routine operation, flow and total sample volume were measured using a gasmeter having a prime calibration against the Gillibrator.

The collection substrates used on the first 11 stages (Inlet to Stage 10) were polycarbonate Poretics filters 47mm in diameter with 0.4µm pore size. The final stage (Stage 11) substrate was a teflon-backed Fluoropore filter 37mm in diameter with 1µm pore size[4].

5.2 ANSTO SFU and ASP Samplers

The ANSTO SFU (Stacked Filter Unit) is designed to operate at an average flowrate of 16 l min^{-1} and should be maintained in the range 14 to 18 min^{-1}. It employs a PM10 inlet to exclude particles larger than 10 µm, followed by a pair of filters in series. The filters collect, respectively, the PM10-PM2.5 size fraction (collected on polycarbonate Nuclepore filters 47mm in diameter with 8 µm pore size) and the PM2.5 fraction (polycarbonate Nuclepore filters 47mm in diameter with 0.4µm pore size).

The ANSTO ASP sampler employs a PM2.5 cyclone inlet that excludes particles larger than 2.5 µm, transmitting the PM2.5 fraction which is collected on a 25mm stretched teflon filter [ERDC, 1995]. The cyclone inlet collection efficiencies have been described by John and Reischl [1980]. The ASP sampler is designed for an average flow rate of 22 l min^{-1} and this was maintained during sampling by a critical orifice. The flow rate was calibrated during installation at each site. To comply with the 2.5 µm 50% cut-point flow rates should be maintained within the range 20 and 24 l min^{-1}. At flow rates less than 16 l min^{-1} the 50% cut-point rises sharply to above 3 µm.

5.3 Solar-Vol 1100

The Solar-Vol 1100 is a solar-powered low volume aerosol sampler lent to the project by Ecotech Pty Ltd. In the AFP study the Solar-Vol was operated with a PM2.5 cyclone inlet, at 3 l min^{-1}. The collection characteristics of this cyclone were determined by the University of Minnesota Particle Technology Laboratory [Ecotech, 1996] and the flow rate was maintained with a mass flow controller and periodically checked using the Gillibrator soap bubble flow meter. The collection substrate used was a polycarbonate Poretics filter 47mm in diameter with 0.4µm pore size.

[4]Note that for the teflon filters pore size bears no relationship to collection efficiency for atmospheric particles: the filters used have 100% collection efficiency for sub-micrometre particles.

5.4 Active-cavity-laser Particle Size Spectrometer, ASASP-X

The ASASP-X is a Particle Measuring Systems Inc. (PMS) active-cavity-laser particle size spectrometer. This high-resolution spectrometer uses light scatter in an open-cavity laser system to size individual particles over the diameter range of 100 nm to 3 μm (nominal) into 60 size channels (in four overlapping ranges). Size calibration was carried out at the start and end of each sampling period using monodisperse polystyrene latex particles. Usually this included six sizes 0.234, 0.33, 0.5, 0.76, 0.945 and 2.02 μm. From these calibrations individual calibration relationships were derived for each sample period. The inlet to the ASASP is heated to 40 °C to reduce humidity effects on particle size. A sample flow rate of 3 l min^{-1} was maintained through the external inlet and this was sub-sampled isokinetically to match the spectrometer inlet flow of 1.5 $cm^3 s^{-1}$. Particle sizes reported for this spectrometer are dry, polystyrene equivalent - no conversions to ambient refractive index have been included. Size distributions were usually obtained for every second hour, with ten distributions per hour later integrated to give one distribution every second hour.

5.5 Differential Mobility Size Spectrometer, TSI DMA

Particle size distribution in the range 15 nm - 300 nm was determined using a differential mobility analyser (TSI 3071) and a CN or UCN counter. In most locations the UCN (a TSI 3025A) was used but in Brisbane when the UCN malfunctioned this was replaced with a TSI 3760 CN counter. When used in conjunction with the UCN the DMA was operated at a sample inlet flow of 300 $cm^3 min^{-1}$ (and a sheath flow of 3 l min^{-1}); with the CN counter it was operated at 1 l min^{-1} sample and 10 l min^{-1} sheath. In both cases it was operated with a slow scan giving three distributions of 22 size channels per hour. Each distribution included 10 scans. Flow rates to the spectrometer were all regulated using active flow regulation. Flow calibration was carried out regularly at each site. Size calibration depends only on correct flow and geometric parameters of the mobility analyser, no other calibration is required. Inlet to the DMA was via a diffusion drier and the sheath stream was also dried chemically using silica-gel. Reported particle sizes are as dry particles (r.h. ~ 20 % or less).

5.6 Nephelometers

Aerosol scattering coefficient at a wavelength of 530 nm was determined using Radiance Research type M903 nephelometers. Two instruments were operated in parallel, one was operated at 40 °C using a heated inlet and enclosure, the second was operated unheated in the sampling van. In some locations (for example Launceston) the sample van was heated at night to around 15 - 20 °C for stable operation of all instruments, resulting in sample humidities (for b_{sp}) below ambient, in this instrument, during these periods. Scattering coefficient was calibrated using the fluorocarbon gas R22 and filtered air, usually once per sample period.

5.7 Ultrafine Particle Counters

Two ultrafine particle counters were used during the study, a TSI 3025A UCN (ultrafine condensation nucleus) counter (Sydney and Brisbane) and Nolan Pollak UCN counter. The TSI 3025A is a continuous flow instrument. Initially this was time-shared with the DMA spectrometer but after the UCN counter failed in Brisbane the Nolan -Pollak instrument was used. The Nolan-Pollak counter is an expansion CN counter and was operated to give approximately 45 samples per hour. Both counters have a lower size detection limit of 3 nm and give the number concentration of particles greater than this diameter. The principal calibration required by the TSI 3025A is for flow rate, which was checked for each sampling

session using a Gillibrator bubble flow meter. The Nolan-Pollak counter was calibrated against a standard counter maintained at CSIRO for the Cape Grim Baseline program.

5.8 TEOM

A Rupprecht and Patashnick TEOM series 1400 continuous mass balance, with an URG PM2.5 cyclone inlet was operated to give PM2.5 mass concentration at locations where the CSIRO sampling van was employed. The sample inlet was maintained at 50 °C in Melbourne but was reduced to 35 °C in Canberra, and maintained at 35 °C in Launceston and Adelaide to reduce volatilisation loss. The TEOM mass response was calibrated using a series of filters with measured masses (using the CSIRO microbalance) and was within 1% of the instrument calibration. Flow rate was regulated using an active flow controller; the calibration of which was performed with a Gillibrator bubble flow meter. This was also within 1% of the instrument setting.

6. Sample Analysis Methods

6.1 Filter Handling

All MOUDI filters had optical absorbance measured, were dried in a desiccator for 24 hours at humidity of ≤20% prior to being weighed, then loaded onto impaction plates. The impaction plates in turn were loaded onto the MOUDI stages and held in place magnetically. After sample collection, filters were unloaded from the impaction plates, placed in a desiccator for 24 hours, re-weighed and the absorbance re-measured. Filters for the Solar-Vol were prepared as for the MOUDI filters.

Aerosol mass and elemental carbon mass collected on each MOUDI and Solar-Vol filter were calculated from the gravimetric and absorbance data, and the filters were sent to ANSTO for PIXE analyses. After the PIXE analysis the filters were returned CSIRO for the determination of major soluble ions and organic acids by ion chromatography (IC), and determination of pH by electrode methods, on aqueous filter extracts.

Filters from the ASP and SFU were prepared in a similar fashion at ANSTO. After sampling, these filters were returned to ANSTO for re-weighing and absorbance determination and analysis by accelerator based methods such as PIXE, PIGME and forward recoil analysis. The filters were then sent to CSIRO for IC and pH analyses.

6.2 Gravimetric Analysis (Mass Determination): CSIRO

Filters were weighed using a Mettler MT5 ultra-microbalance with a "tailored" filter pan. Electrostatic charging was reduced by the presence of radioactive static discharge sources within the balance chamber. The resolution of the balance is 0.0001mg (0.1 µg). Each filter was weighed repeatedly until three weights within 0.001mg were obtained. Measuring 6 filters over 5 consecutive days tested reproducibility of the measurement. The results of this test are shown in Table 5.

Table 5. Reproducibility of mass measurements on 6 Poretics polycarbonate filters measured each day over a 5-day period.

Filter	1	2	3	4	5	6
Average mg	15.0538	15.0103	14.9396	15.2412	15.2576	15.0693
Stdev mg	0.0019	0.0017	0.0012	0.0013	0.0008	0.0015
Range mg	0.0048	0.0043	0.0030	0.0034	0.0020	0.0038

The results of a second experiment that simulated the typical time between measurement of the exposed and unexposed filters are shown in Figure 1. Over a period of two months a single filter was weighed at intervals on a total of nine occasions, with storage throughout in plastic Petrie dishes as used for the ambient samples. The weighed filter mass varied by a maximum of 0.05% over the two-month period (0.008 mg difference between the extreme minimum and maximum values).

The first experiment showed a maximum range in results of repeated weighing over 5 days of 0.005 mg (filter number 1), while the range shown in the second experiment was 0.008 mg between extreme values, but only 0.004 mg if the last point in Figure 1 is excluded.

Based on our experience that laboratory tests are usually optimistic in comparison with precision obtained under field conditions, we adopt a conservative value of 0.006 mg for uncertainty in an individual measurement of filter mass. If this value is adopted, it may be compared with the sample masses obtained during the study to provide a perspective on the uncertainty to be associated with the measurements. The two measurements returning the lowest absolute sample masses, and hence the worst case in terms of experimental error in the mass determination, were the Solar-Vol PM2.5 sampler that operated at only 3 l min^{-1}, and the MOUDI, which operated at 10 times the Solar-Vol sampling rate, but distributed the sample over 12 separate collection stages. Table 6 contains data on the mean masses obtained by these instruments at two of the sampling sites.

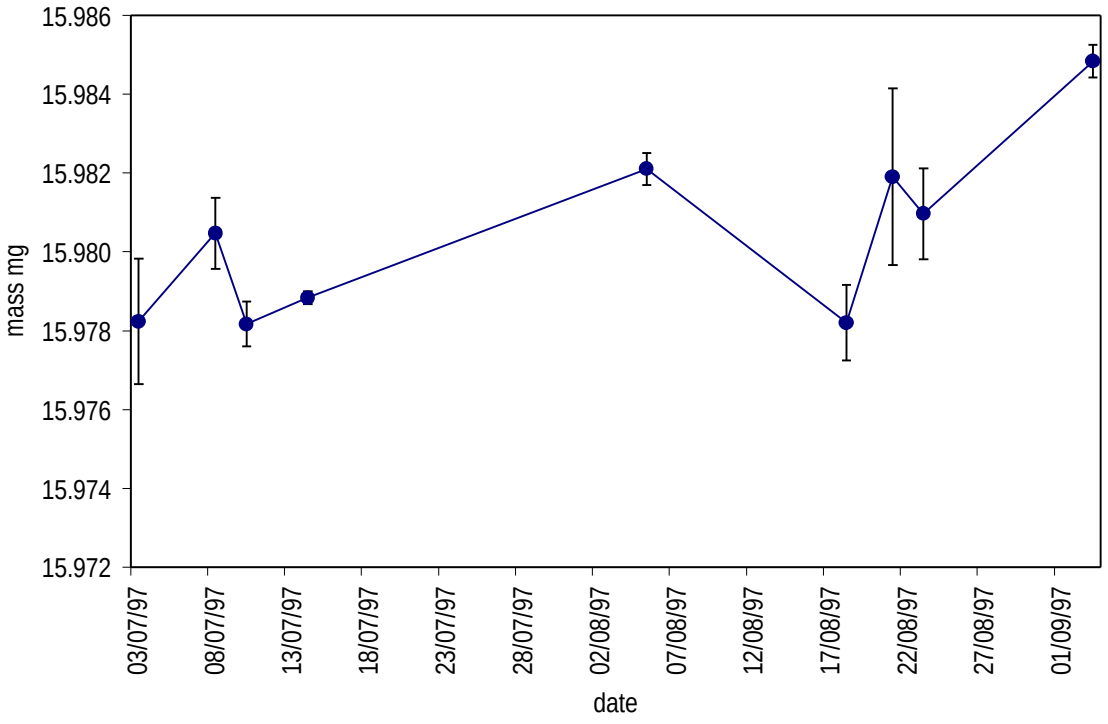

Figure 1. Mean mass plus 95% confidence range from repeated weighing of a Poretics filter between August and September 1996.

Combining the estimated uncertainty of 0.006 mg per measurement with the mean masses in Table 6 implies a typical uncertainty of ±9% for the Solar-Vol in Brisbane, and uncertainties of this magnitude or less for all the MOUDI stages other than stage 11. Propagation of errors through the summation of all MOUDI stages to provide a total mass estimate suggests a much reduced uncertainty. In the illustration in Table 6 based on the Adelaide samples, the total mass determined is 1.20 ± 0.07 mg, or an uncertainty of ±6%.

6.3 Gravimetric Analysis (Mass Determination): ANSTO

Gravimetric methods employed by ANSTO are similar to those employed by CSIRO, and have been documented in ERDC [1995]. Resolution of the Mettler balance employed was 0.001mg, and the two standard deviation range in uncertainty determined by repeated weighing of a standard weight over a 6 month period was about 0.003 mg [Figure 4.11, ERDC, 1995]. All filters were equilibrated for at least 24 hours in a controlled weighing room with temperatures between 20°C and 22°C and relative humidity between 40% and 50%. Typical experimental error for the ANSTO determinations was listed as 3 – 5% [Table 4.4, ERDC, 1995], reflecting the large absolute mass collected by the higher flow ANSTO samplers.

Table 6. Mean gravimetric masses per sample (or impactor stage) and 95% range for the distribution of masses from 5 Solar-Vol PM2.5 samples (Brisbane) and 5 MOUDI samples (Adelaide).

Sample	Mean Mass, mg	95% Range
Solar-Vol (Brisbane, N=5)	0.066	0.015
MOUDI (Adelaide, N=5)		
stage 0	0.093	0.046
1	0.088	0.048
2	0.138	0.060
3	0.173	0.067
4	0.096	0.018
5	0.096	0.042
6	0.074	0.026
7	0.109	0.054
8	0.124	0.058
9	0.105	0.035
10	0.063	0.017
11	0.038	0.012
Total	1.20	

One difference between the CSIRO and ANSTO methods concerns the filter equilibration before weighing. At CSIRO filters were equilibrated and weighed in a temperature and humidity controlled chamber at low relative humidity (≤20%) over silica gel, whereas the ANSTO filters were equilibrated for 24 hours with a higher weighing room relative humidity (40-50%).

6.4 Elemental (Soot) Carbon (EC): CSIRO

Elemental carbon was determined via light absorption at the wavelength of red light using the integrated plate method described in Lin *et al.*, [1973]. The system was calibrated for elemental carbon using an aerosol produced by pyrolysis of acetylene [Gras, 1996], which yielded a specific mass absorption of 10.4 m^2 g^{-1}.

The absorption of light obeys the Lambert-Beer Law

$$I(x) = I_o e^{-bx}$$

where I_o is the intensity of the initial light beam, I(x) is its intensity after travelling distance x and b is the extinction coefficient. We measure the intensity of light transmitted through Poretics filters both with and without aerosol and calculate the absorbance according to

$$A = \ln(\frac{I_o}{I})$$

We calculate the difference in absorbance (*DA*) between the exposed (A_{exp}) and unexposed filter (A_{un}) as

$$DA = A_{exp} - A_{un}$$

Elemental carbon concentration is calculated from

$$EC = \frac{\Delta A x^{-1}(m)}{10.4(m^2 g^{-1})} * 10^6$$

Here *x* is the (notional) length of a tube of sampled air with cross-sectional area equal to that of the filter (of 4.1 cm diameter) and volume of 43.2 m^3 in the case of the MOUDI. In this procedure no allowance is made for light scattering by the sample.

The absorbance reader used previously at CSIRO measures the absorbance of a beam <10 mm in diameter. For the non-uniformly deposited MOUDI samples, an absorbance reader that could measure the entire area (40 mm diameter) on which the sample was deposited was constructed. The response of the new absorbance reader was tied to the prime laboratory calibration of the original reader by using both units to read stage 9 and10 MOUDI samples from this project, since the 2000 jets per stage produce a reasonable approximation to a uniform deposit.

Measurement of absorbance of more than 30 uniformly deposited PM2.5 samples by both absorbance readers enabled an estimate of experimental precision. The 95% confidence range for the difference between the two values was ±0.013 absorbance units, which we adopt as an estimate of precision for an individual measurement. For a MOUDI sample of 43.2 m^3 this translates into an uncertainty of 0.038 μg m^{-3} of EC, whereas for the low-volume Solar-Vol sampler the corresponding uncertainty is a factor of 10 higher at 0.38 μg m^{-3}.

As in the case of gravimetric mass determination, a comparison of the estimated precision of the EC determination with the lowest volume samples, the Solar-Vol samples and the individual MOUDI stage samples, provides an estimate of the worst-case uncertainty to be attached to this measurement. Table 7 contains illustrative EC concentration data, in this case from Launceston for the Solar-Vol, and Melbourne for the MOUDI. These examples provide worst-case illustrations, since both reflect cases when EC was low in absolute terms.

For the Solar-Vol the data combination of the mean loading of 3.4 µg m^{-3} with an uncertainty of 0.38 µg m^{-3} implies an uncertainty of about ±11%. For the MOUDI, it is clear that some of the individual stages returned EC values close to zero and would show individually a large relative uncertainty. The total EC value produced by summing all 12 stages was low in the Melbourne samples, at 1.90 µg m^{-3}. Accumulating an uncertainty of ±0.038 µg m^{-3} per stage over 12 stages yields overall a figure of ±0.46 µg m^{-3}, or a fractional uncertainty for the Melbourne samples of ±24%.

Table 7. Mean EC concentration per sample (or impactor state) and 95% range for the distribution of EC concentrations from 5 Solar-Vol PM2.5 samples (Launceston) and 5 MOUDI samples (Melbourne).

Sample	EC , µg m^{-3}	95% Range
Solar-Vol (Launceston, N=5)	3.4	1.2
MOUDI (Melbourne, N=5)		
stage 0	0.083	0.103
1	0.080	0.110
2	0.081	0.096
3	0.090	0.110
4	0.111	0.113
5	0.169	0.141
6	0.171	0.139
7	0.278	0.101
8	0.256	0.152
9	0.165	0.145
10	0.248	0.143
11	0.171	0.130
Total	1.90	

6.5 Elemental (Soot) Carbon (EC): ANSTO

Elemental carbon was determined by ANSTO using the Laser Integrated Plate Method (LIPM), a variation of the light absorption method. The application of this method by ANSTO has been documented in detail in ERDC [1995], with typical experimental errors listed as 4-9%, depending on mass loading [see Table 4.4, ERDC, 1995]. The LIPM technique has been calibrated at ANSTO for PM2.5 elemental carbon using an aerosol produced by the burning of a common candle. The system was found to be very linear over large absorption ranges corresponding to $0< \ln[I_0/I] <6$ with corresponding elemental carbon loading up to 100 µg cm^{-2} . A specific mass absorption of (10.4±0.9) m^2 g^{-1} was obtained which was identical to that obtained by CSIRO.

A number of differences exist between the CSIRO and ANSTO determinations of EC by optical absorption methods: (1) the CSIRO absorbance readers employed lower intensity monochromatic LED light sources, whereas the ANSTO instrument employs a HeNe laser light source (633nm); (2) the CSIRO filter substrates were polycarbonate sheet filters (Poretics – a "surface" collection medium) while the ANSTO filter substrates were stretched teflon

(Gelman- a "depth" collection medium), and (3) the ANSTO method employed a scale factor to correct for "layering" of the aerosol on the filter, with the factor averaging ~2 [see Section 4.1.5 in ERDC, 1995]. In a review of methods used to measure EC, Heintzenberg *et al.*, [1997] discuss the advantages and disadvantages of these different measurement methods. Surface collection filters are thought to produce a simpler sample/substrate optical geometry that results in less interaction of scattered light between the particles and the filter medium.

6.6 PIXE (Proton Induced X-ray Emission) Analyses

Nuclear methods, primarily the PIXE techniques, were used to analyse the elements H, F, Na, Al, Si, P, S, Cl, K, Ca, Ti, V, Cr, Mn, Fe, Cu, Co, Ni, Zn, Br, Pb. These measurements were carried out by the Nuclear Science Applications group at ANSTO. Typical minimum detection limits (mdl) for each species measured on a MOUDI filters (*i.e*. the worst case in terms of loading per filter) are listed in Table 8. Minimum detection limits for the PIXE method on teflon and Nuclepore filters are significantly lower (better) than those given in Table 8.

Table 8. Typical minimum detection limits for elements analysed by PIXE in µg m^{-3} on MOUDI filters assuming a sample volume of 43.2 m^3.

Element	*minimum detection limit*
F	0.0192
Na	0.0769
Al	0.0096
Si	0.0050
P	0.0046
Si	0.0038
Cl	0.0038
K	0.0027
Ca	0.0023
Ti	0.0019
V	0.0015
Cr	0.0015
Mn	0.0012
Fe	0.0008
Cu	0.0008
Co	0.0008
Ni	0.0008
Zn	0.0008
Br	0.0012
Pb	0.0031

The PIXE techniques involve bombarding samples within an evacuated chamber with 2.6 MeV protons. An 8 mm diameter beam is used to maintain the integrity of the filters; teflon filters which are more prone to damage are hit with an incident proton charge of 3 µC, while the Nuclepore MOUDI filters, because of the small amount of material on these filters,

were hit with an incident proton charge of 30 µC. An example of a typical PIXE spectrum from a Teflon filter is shown in Figure 2.

It is important to note that a few of the elements analysed in some MOUDI samples were well below the mdl for those elements, particularly on some finer stage filters as the sample was spread across the twelve separate stages. However the major aerosol parameters, gravimetric mass, EC and total ionic mass, and commonly occurring elements such as S, Cl, K, Fe, Zn, Br and Pb, were above the detection limits.

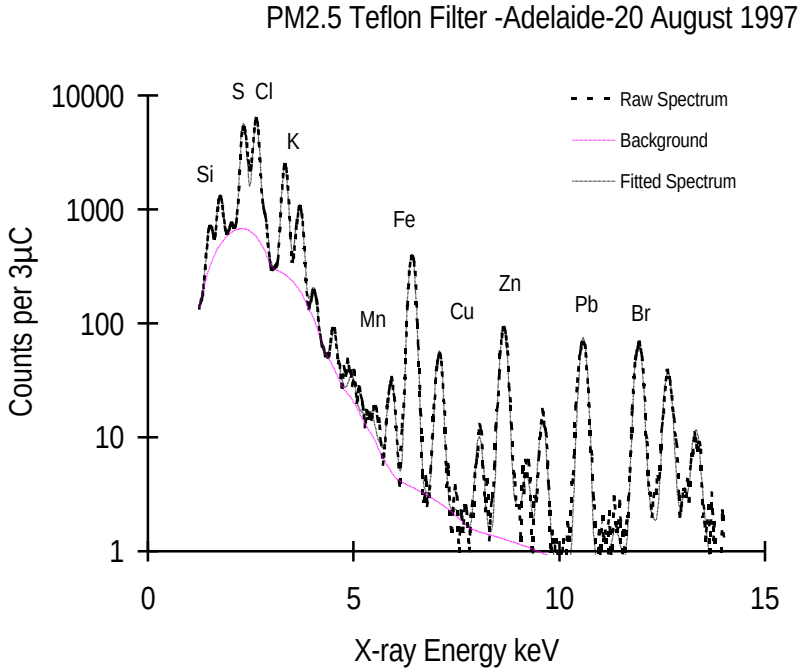

Figure 2. A Typical PIXE spectrum for an exposed Teflon filter obtained in a few minutes of exposure to 2.6 MeV protons.

6.7 Ion Chromatography (IC) Analyses

Suppressed ion chromatography (IC) was used to determine the concentration of soluble ions Na^+, NH_4^+, K^+, Mg^{2+}, Ca^{2+}, Cl^-, NO_3^-, SO_4^{2-}, Br^-, NO_2^-, PO_4^{3-}, F^-, acetate, formate, oxalate and methanesulfonic acid (MSA). IC was carried out within the Acidity and Aerosols Group of the CSIRO Division of Atmospheric Research. Filters were extracted in 12 ml of Milli-Q HPLC grade (high purity de-ionised) water. The hydrophobic Teflon filters were wetted with 100 µl AR grade methanol before extraction to ensure proper aqueous wetting, and a bactericide (120 µl of chloroform) was added to preserve the extracted sample from biological degradation after extraction.

The ions were determined using a Dionex DX500 gradient ion chromatograph employing Dionex IC columns, an AS11 column and ARS1 suppressor for anions, a CS12 column and CRS1 suppressor for the cations. Table 9 shows the detection limits (dl) for each species assuming an air sample volume of 43.2 m^3, typical for the MOUDI operating for 24 hours. Detection limits for the lowest volume sampler employed, the Solar-Vol PM2.5 sampler, are a factor of 10 higher than those given in Table 9.

Table 9. Detection limits for ions analysed by IC assuming sample volume of 43.2 m^3 and peak height 3 times the chromatogram baseline S/N ratio.

Ion	*Detection Limit (ng m^{-3})*
Na^+	0.064
NH_4^+	0.053
K^+	0.109
Mg^{2+}	0.068
Ca^{2+}	0.111
Cl^-	0.171
NO_2^-	0.552
Br^-	0.377
NO_3^-	0.293
SO_4^{2-}	0.213
Oxalate	0.264
Acetate	0.285
Formate	0.268
F^-	0.472
MSA	0.221

One of the routine quality assurance components employed in the IC laboratory is a program of “blind” duplicate analyses. A few percent of samples, randomly selected, are subjected to "blind" duplicate analyses as a means of objectively determining analytical precision on the actual samples under study. Table 10 lists average and median % fractional difference between duplicates for selected ions, together with the average aqueous ion concentration across one set of duplicates.

Table 10. Mean ion concentrations, average % differences and median % differences derived from 15 pairs of “blind’ duplicate analyses carried out on randomly selected samples.

	Mean conc. µmol l^{-1}	*Average % deviation*	*Median % deviation*
Na^+	48.3	4.8	1.4
K^+	3.7	10.1	3.4
Mg^{2+}	7.2	6.5	2.5
Ca^{2+}	5.7	4.3	1.0
NH_4^+	90.0	3.7	1.1
Cl^-	59.7	5.9	3.7
NO_3^-	16.1	5.1	3.9
SO_4^{2-}	18.8	4.4	3.4
PO_4^{3-}	5.6	4.1	4.5
$C_2O_4^{2-}$	2.4	6.2	4.2
HCOOH	15.2	6.3	2.8
CH_3COOH	9.5	6.7	4.5

6.8 pH Determination

Since aerosol acidity as acid sulfate has been suggested as one possible causative agent behind health affects of respirable particles [*e.g.* see Vedal, 1997], three measures were taken to ensure that pH measurements would be of the highest possible precision and accuracy. The first was to use a state-of-art, research grade pH electrode: in the AFP Study an Orion Ross electrode which has internal (chemical) temperature compensation was used. The second was to employ special low ionic strength buffers and ionic strength adjustment solution available from Orion, to ensure calibration and measurements were carried out at similar ionic strengths. The third was to independently check the validity of the standard electrode calibrations made using pH 4 and 7 buffers, by using accurately made up standards of dilute strong acids (both methanesulfonic acid, MSA, and hydrochloric acid, HCl, were used). Results of these calibration checks are presented in Table 11 for MSA standards and Table 12 for HCl standards. Table 13 contains the overall mean results and 95% confidence limits for the pooled pH data for each of the six standards employed.

Table 11. pH of dilute MSA (methanesulfonic acid) standards.

expected pH	*MSA*	*MSA*	*MSA*	*MSA*	*MSA*	*MSA*	*MSA*
4.000	4.035	4.020	3.991	3.995	4.020	4.026	4.022
4.301	4.308	4.301	4.292	4.320	4.301	4.326	4.325
4.602	4.587	4.603	4.563	4.609	4.603	4.628	4.632
4.903	4.875	4.884	4.812	4.913	4.884	4.915	4.914
5.204	5.131	5.134	5.093	5.144	5.134	5.175	5.183
5.505	5.310	5.345	5.300	5.343	5.345	5.405	5.362

Table 12. pH of dilute HCl (hydrochloric acid) standards.

expected pH	*HCl*	*HCl*	*HCl*	*HCl*
4.000	4.067	4.022	4.028	4.037
4.301	4.318	4.300	4.318	4.336
4.602	4.617	4.592	4.605	4.615
4.903	4.901	4.875	4.899	4.898
5.204	5.165	5.132	5.145	5.141
5.505	5.326	5.323	5.360	5.375

The data in all three tables shows an increasing deviation towards lower than expected pH as pH increases. However this is precisely what is expected for solutions in contact with atmospheric CO_2, since CO_2 is a weak acid. As the acid standard is made more dilute, the importance of CO_2 as an additional source of acidity increases, until at pH levels above 5 it becomes a significant source of H^+ ions in the standards. This effect is very clear in the mean data in Table 13. However, it is straightforward to calculate the contribution to acidity made by atmospheric CO_2 to the dilute standards.

Table 13. Mean pH and 95% confidence limits for dilute acid standards.

expected pH	*mean*	*95%c.l.*
4.000	4.022	0.041
4.301	4.312	0.027
4.602	4.605	0.037
4.903	4.889	0.056
5.204	5.148	0.059
5.505	5.358	0.109

In Figure 3 the mean calibration data from Table 13 are plotted with a theoretical pH curve produced by adding to the dilute acid standard the additional CO_2-derived acidity calculated from the known solubility and acidity constants for CO_2, and an assumed atmospheric mixing ratio of 370 ppm in the laboratory air. Clearly the deviation from the 1:1 line may be ascribed quantitatively to the effects of atmospheric CO_2, and the performance of the pH measurement system in the AFP Study can be rated as excellent.

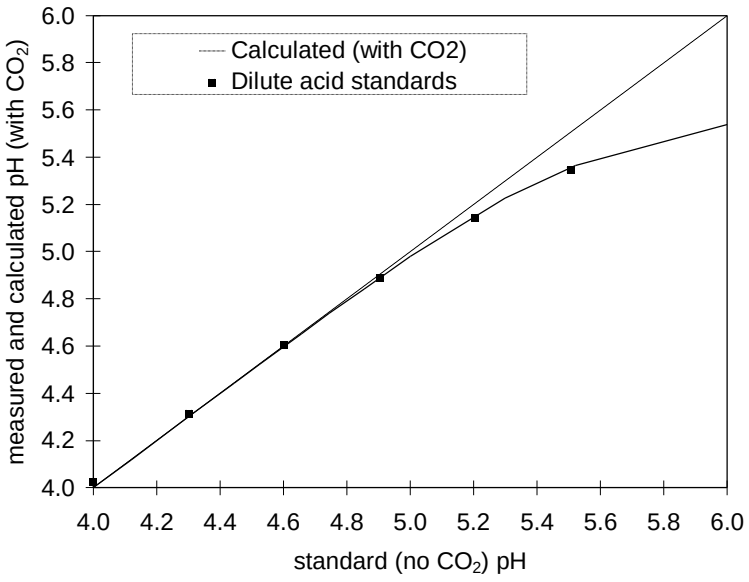

Figure 3. Mean values from laboratory from pH calibration checks, based on dilute strong acid standard solutions (Table 13). The dashed line depicts unity slope. The calculated curve shows the expected pH assuming equilibrium between the standards and atmospheric CO_2.

6.9 MOUDI Data Analysis

6.9.1 Blank Subtractions

PIXE and IC analyses were performed on unexposed new Poretics, Nuclepore and Fluoropore filters with each batch of analyses. For IC, concentrations determined from the blank filter were always below the IC detection limit. As some of the species determined on the MOUDI samples by PIXE were below the PIXE minimum detection limit it was necessary to subtract the blank filter measurements made with each batch from the PIXE results.

6.9.2 Scaling PIXE data

The PIXE analysis returns the average mass per unit area of a species over the proton beam diameter used. For all the analyses an 8 mm diameter beam was used. For uniformly deposited filters such as those from the ANSTO PM2.5 sampler, the relationship between the IC and PIXE results is a simple geometric factor: the ratio of the PIXE beam area to the total exposed filter area. However for the MOUDI, which has non-uniformly deposited samples, with the non-uniformity differing for different stages because the jet number differs (see Table 4), an individual scaling factor is required for each stage in order to relate the IC and PIXE results. This factor for the MOUDI filters will vary with the number of jets that occur within the 8 mm diameter beam for any given filter stage.

In this study we have determined empirically the individual stage scaling factors, on the assumption that sulfur is determined quantitatively by both techniques. Previous comparisons between IC and PIXE-derived aerosol sulfur data using uniformly deposited filters have consistently shown good agreement [*e.g.* ERDC, 1995], and similar results were obtained in this work from the ANSTO PM2.5 sampler (Figure 4).

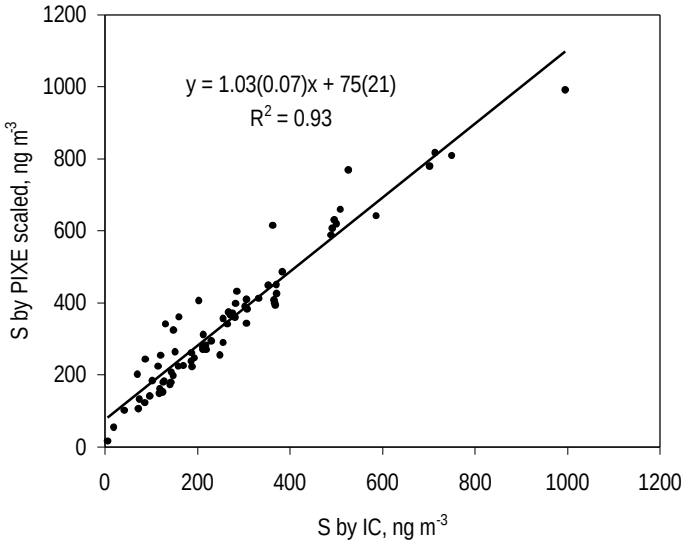

Figure 4. Aerosol sulfur from PIXE analyses vs aerosol sulfur from IC sulfate analyses, ANSTO PM2.5 sampler. The numbers in parentheses are the 95% confidence ranges.

Given the different jet geometries in each MOUDI stage, different scaling factors were anticipated for each stage. This was confirmed to be the case from a comparison of the ratio

of IC/PIXE sulfur values for all 28 MOUDI samples collected during the AFP study (see Figure 5). The median scaling factors derived in this way were employed to scale all PIXE data to the same scale as the IC data, from which the final air concentrations were determined.

Comparison of scaled MOUDI PIXE data and the MOUDI IC data for an element other than sulfur that is also determined by both methods provides a check on the validity of the scaling procedure. Figure 6 shows such a plot for MOUDI chloride, which confirms that the scaling produces, on average, good agreement between the scaled PIXE and IC data.

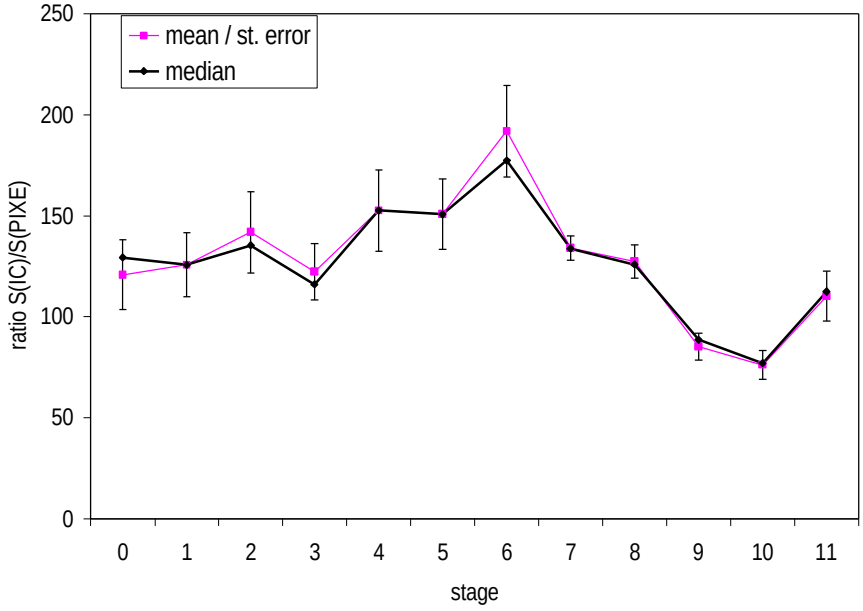

Figure 5. Ratio S (IC) to S(PIXE) for different MOUDI stages, 28 AFP samples.

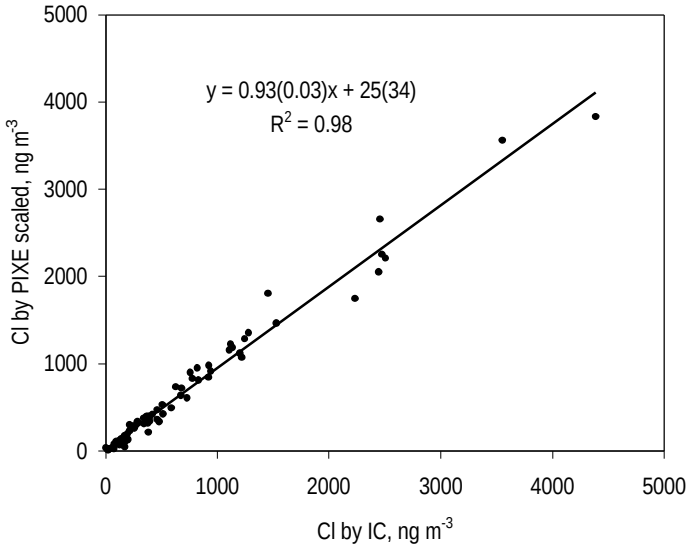

Figure 6. Comparison between MOUDI chloride data derived from scaled PIXE data and directly determined IC data. The numbers in parentheses are the 95% confidence ranges.

6.9.3 Data Inversion

The MOUDI collects the ambient aerosol in 12 discrete, size-fractionated samples so as to provide information on the distribution of chemical components as a function of particle size. While useful information may be gained simply by plotting the MOUDI data in histogram form, a considerably more powerful result can be achieved by utilising the known size-dependence of each collection stage with a numerical inversion procedure to yield a smooth aerosol mass distribution [Winklmayr *et al*.,1990].

The MOUDI inversion routine developed by CSIRO was based on the efficient, non-linear iterative inversion procedure of Twomey and Zalabsky [1981], with the MOUDI stage transmission kernels derived from the Manufacturer's calibration supplied with the CSIRO MOUDI. The individual stage calibration curves were digitised by CSIRO, and fitted with Winklmayr functions [Winklmayr *et al*.,1990], to yield the suite of kernels shown graphically in Figure 7. Smooth distributions of both the stage kernels and MOUDI mass distributions were obtained by carrying out the calculations using 20 points per decade in logarithmic particle diameter, over the particle diameter range 0.01 to 100 µm.

Note that a "fictitious" stage function was generated to represent the MOUDI backup filter (stage 11), having the same shape as the function for stage 10, but a 50% cut-size half that of stage 10.

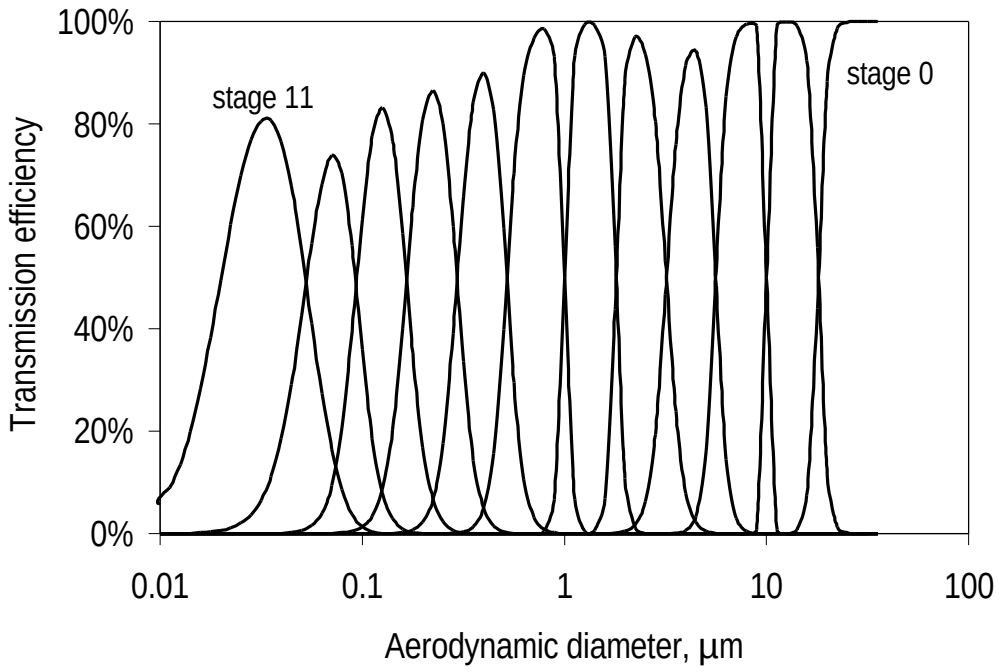

Figure 7. MOUDI kernel functions for each stage.

The inversion procedure convolves an initial "guess" (mass-size) distribution sequentially with each of the stage kernels, compares the resultant calculated stage mass with the measured stage mass, and adjusts the input "guess" distribution to make the calculated and measured stage masses agree. The stage kernel function was used in each case as the

adjustment function, so the overall effect of the procedure was to construct a smooth input distribution from a linear combination of the kernel functions shown in Figure 7. The inversion was constrained to conserve total mass.

The procedure was terminated when either of two conditions was met: (1) the procedure converged, defined by the change in root-mean-square (rms) residual between fitted and observed stage masses changing by less than 1% between successive iterations, or (2) condition (1) was not met but 10 iterations were reached. In the vast majority of cases the inversion converged in < 6 iterations, with rms residuals of less than 3%. A few inversions were not accepted: those that did not meet the convergence criterion with 10 iterations, and those that did meet the convergence criterion but had rms residuals of 4% or greater.

The robustness of the inversion procedure was tested by carrying out numerical experiments based on typical measured mass distributions from each of the sites. The experiments involved carrying out 25 inversions with random error introduced numerically to the measured stage mass data used as input. Four sets of experiments were carried out, reflecting random error distributions (at 95% confidence) of ±5%, ±10%, ±20% and ±25% applied to the input data. The means of the 25 inverted distributions with added random error were in each case found to reproduce almost precisely the original inverted distribution, indicating the absence of any systematic error in the mean response introduced by the increasing uncertainty added to the input data. Figure 8 shows results from three of the numerical experiments, where the initial "no added error" distribution is plotted along with the mean from the 25 inversions with randomly added error, and the 95% confidence range derived from the range in the 25 inverted results with added error.

Plots of the 95% confidence ranges against the mass at each diameter are shown in Figure 9. For almost all of the points it is apparent that the output uncertainty scales linearly with the added input uncertainty, *i.e*. a random input uncertainty of x% results in a 95% range in output of about x%, as shown by the slopes of 0.043 (for 5% random error), 0.12 (for 15% random error) and 0.16 (for 20% random error) in Figure 9.

However, each of the plots in Figure 9 also shows a series of ~7 points near the origin where the fractional output uncertainty error is much larger than the input fractional uncertainty. These points correspond to the lowest 7 size bins (diameters <0.02 μm). It is not surprising that the fractional error increases substantially towards the ends of the inverted distribution, as the inversion procedure effectively has no capability to adjust the size distribution at particle sizes beyond those in which the kernels have significant curvature (note that the kernel for stage 11 is "fictitious" at sizes below ~0.03 μm). Therefore, in all subsequent inversions the procedure was truncated at a lower size cut-off of 0.05 μm, to confine the inversion to the diameter range between 0.05 and 30 μm over which size dependent information is contained in the stage collection characteristics.

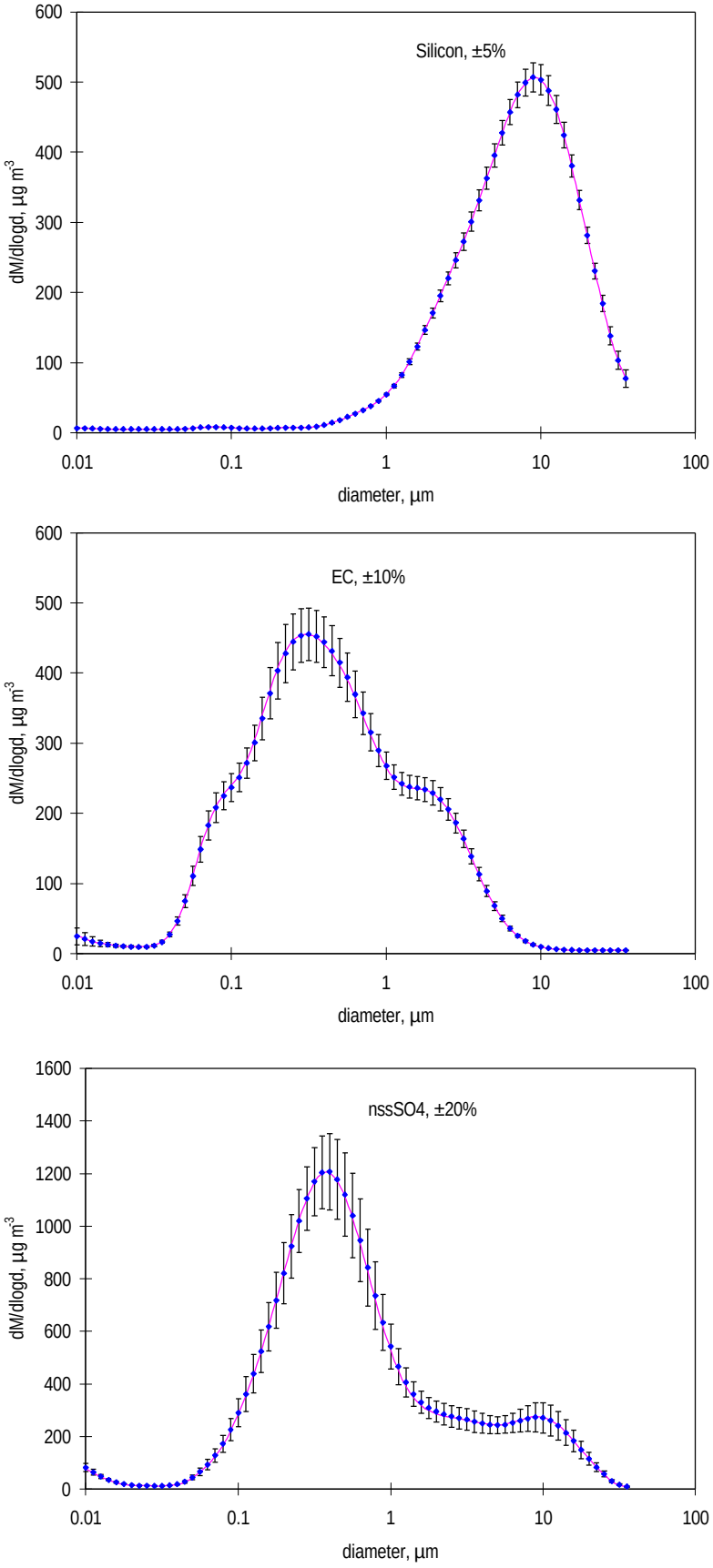

Figure 8. Initial MOUDI distribution (line) and mean distribution plus 95% confidence range derived from 25 numerical experiments with random error at the indicated level added to input data.

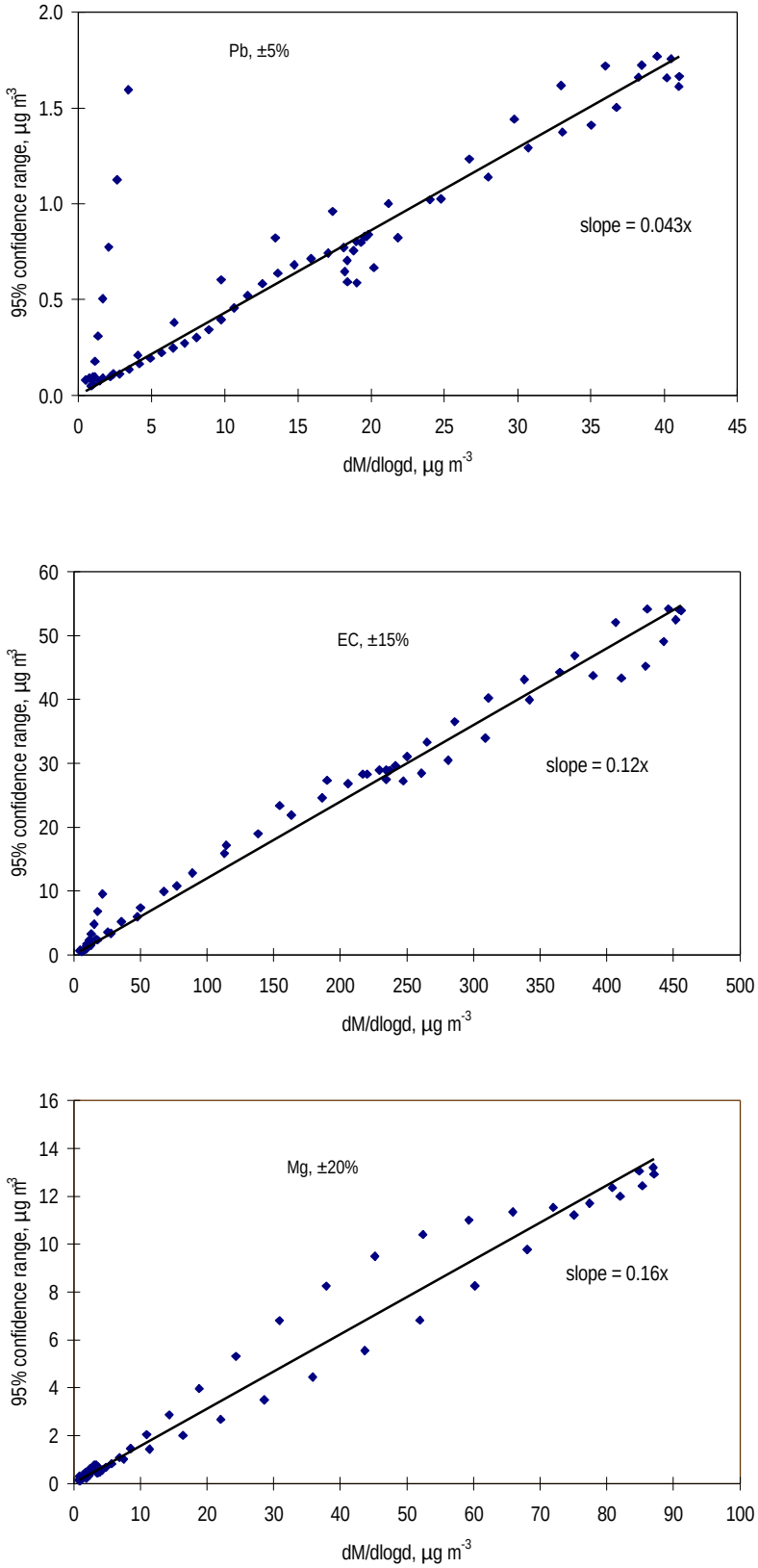

Figure 9. 95% confidence range vs absolute mass in each size bin, derived from 25 numerical experiments with random error at the indicated level added to input data.

6.9.4 Interstage losses

The transmission characteristic of the MOUDI include small, size-dependent particle losses during sample flow path through the device, that were taken into account to remove any resultant small systematic bias in the MOUDI data. Marple *et al.* [1991] measured the interstage losses in the MOUDI for both solid and liquid particles. Their data were fitted to smooth functions, which are shown in Figure 10. Maximum loss occurs at ~10 µm and at less than 0.1 µm, with quite small losses between 0.1 and about 5 µm.

All MOUDI distributions discussed in this work were corrected for interstage losses using the average of the curves in Figure 10, on the assumption that at ambient humidities encountered in this work at least the subset of particles containing soluble material would be deliquesced. Any error introduced by simply averaging the two curves is insignificant, as the overall effect of the interstage loss correction is itself only very minor, as shown in Figure 11.

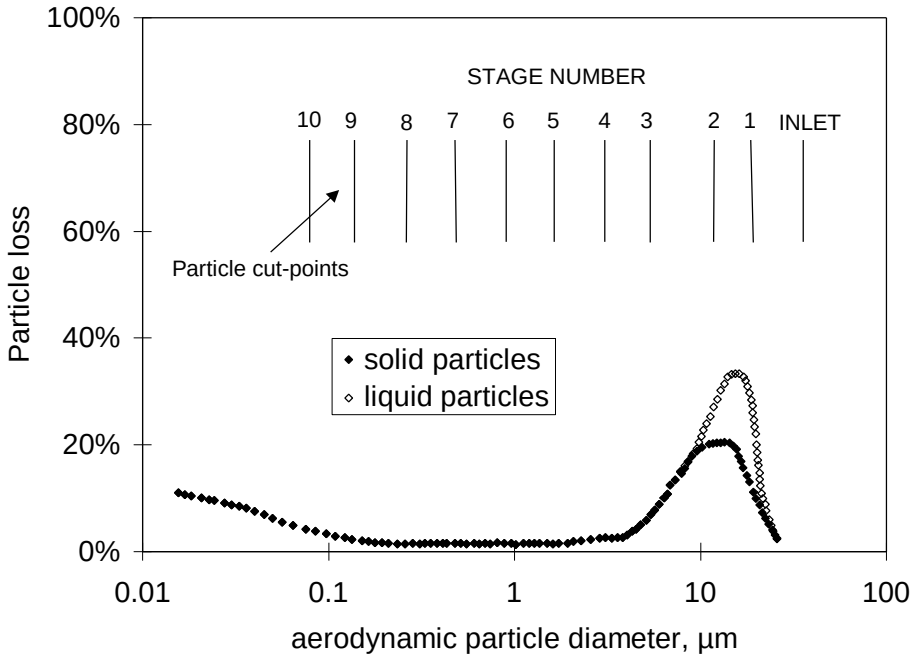

Figure 10. Interstage loss function for the MOUDI (Marple *et al.*, 1991).

6.9.5 Standard Temperature and Pressure.

Australian air quality data are reported at conditions of standard temperature and pressure, 273.15 K and 101.3 hPa. The MOUDI flow data were recorded at ambient temperature and pressure, so require correction to achieve consistency with the other sampling devices used in the study. These corrections were carried out for each sample using the 24 hour mean ambient temperatures and pressures recorded at each site. The importance of accounting for the systematic difference between ambient conditions and STP is clearly evident in Figure 11, which contrasts the magnitude of this correction with the considerably smaller correction required to account for interstage losses.

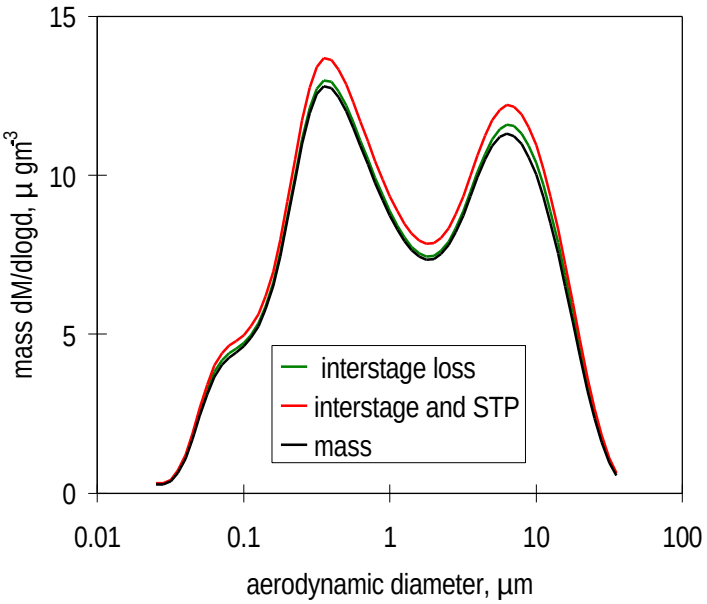

Figure 11. Example of change in size distribution due to corrections for interstage losses and standard temperature and pressure.

It should be noted that the MOUDI distributions are presented in terms of aerodynamic particle diameter – an idealised equivalent diameter for spherical particles of unit density. This procedure facilitates comparison of integrated fractions such as PM10 or PM2.5 where the data are all reported according to the specified standard conditions, as noted above. Differences between aerodynamic diameter and true physical diameter may be as much as 50%.

7. Results

In this chapter an overview of the aerosol data collected during the study is tabulated by site, in chronological order. The purpose of this overview is to provide a broad-scale picture of the average aerosol properties determined at each site, to set an overall perspective from within which, in subsequent chapters, detailed properties of the aerosol on individual days will be discussed, along with comparisons between different instruments.

It is important to note that to generate the overview in this chapter we have taken simple averages over all available data from each measurement system at each site. In many instances the number of samples averaged differs between instruments, as does the number of days on which different systems operated, these disparities arising from a variety of instrument malfunctions or other local operational constraints. Thus while the average data in this chapter do provide a valid perspective on broad-scale aerosol properties, these somewhat disparate (in terms of sample numbers per instrument) averages should not be used to draw inferences concerning relative instrument performance. The important issue of relative instrument performance is specifically addressed in a subsequent chapter using only concurrent data.

7.1 Overview of Aerosol Data by Site

Average values of gravimetric aerosol mass concentration (GM), inorganic mass concentration (IM[5]), estimated organic matter concentration (EOM[6]), elemental carbon (EC) mass concentration and elemental/ionic components are presented in Table 14 – 19. Mean data on aerosol mass determined by the CSIRO TEOM, aerosol scattering coefficient determined by the CSIRO nephelometer, and ultrafine particle concentration from the CSIRO CN counter at each site are presented in Table 20. Note that these latter three data records do not cover all sites or all days at a given site. It should also be noted that the definition of EOM used here assumes total mass closure, that is, that all the gravimetric mass is accounted for by the organic matter plus EC and the mass associated with the 24 chemical species listed in the definition of IM given by Brook *et al*. [1997]. It specifically does not include water which maybe 8 to 10% of the total mass [ERDC 1995] if the filters are not totally dried before hand. Other definitions of EOM which do not assume total mass closure may be used where the total hydrogen and sulfur content of the filters has been determined [Malm *et al*., 1994; ERDC 1995]. These methods have the advantage that they do not rely on the measurement of so many different chemical species some of which only occur in trace quantities and consequently have a lower standard deviation associated with them. For example, in Table 14, for the ANSTO PM2.5 sampler the EOM = 2.9±12.2 μg m^{-3} by the Brook method applied here and 3.6±3.1 μg m^{-3} by the Malm method. However EOM is calculated and discussed later in this report primarily as a check on the consistency of the GM, EC and IM data, not for the purpose of analysing properties of the organic matter content in the aerosol.

One further point to note is that the H measurements for PM2.5 ANSTO samplers listed in Tables 14 - 19 are for total hydrogen, including hydrogen in organic matter,

---

[5]Inorganic Mass is calculated as follows [after Brook *et al*, 1997]:

$IM=H^{+}+Na^{+}+1.41K^{+}+NH_4^{+}+1.63Ca^{2+}+Mg^{2+}+Cl^{-}+NO_3^{-}+NO_2^{-}+SO_4^{2-}+PO_4^{3-}$
$+Pb+Br+1.79V+2.2Al+1.24Zn+2.5Si+1.58Fe+1.94Ti+Cr+Mn+Co+Ni+Cu$

[6]Estimated Organic Matter (EOM) is estimated as follows: EOM=GM-IM-EC

ammonium ions, hydrogen ions and water. The H^+ ions quoted with the IC results represent the soluble hydrogen ion concentrations (free acidity) only and hence are not directly comparable with the H total values.

Reference to the PM10 averages in Tables 14 – 19 obtained from the MOUDI suggests that the six sets of results fall into two distinct groupings. The four major cities, Sydney, Brisbane, Melbourne and Adelaide yielded average MOUDI PM10 concentrations in the range 20 – 25 μg m^{-3}, whereas Canberra and Launceston yielded averages 2 – 3 times higher at 43 and 63 μg m^{-3}. Similar systematic differences are evident in the average IM (inorganic mass) concentrations, which for the four major cities accounts for 30 – 50% of the PM10 loading, but only about 20% for Canberra and Launceston. In the case of EC (elemental carbon) loading the major cities such as Sydney and Adelaide have EC providing ≥10% of PM10, while for Canberra and Launceston the contribution is less than 10%. Finally, the importance of EOM (estimated organic matter) is systematically higher in the case of Canberra and Launceston, at about 75% of PM10, whereas in the major cities the contribution to PM10 made by EOM is less, down to only about 40% in the Brisbane data.

The means of the physical measurements shown in Table 20 also suggest this pattern of aerosol loading in the 6 cities, with Canberra and Launceston displaying the highest TEOM PM2.5 concentrations and scattering coefficients.

These absolute values and systematic differences in average aerosol properties sit within previous results from various Australian locations such as the Latrobe Valley, Melbourne, Sydney, Perth, Launceston and Brisbane [Ayers *et al*., 1990; Gras *et al*. 1992; ERDC, 1995; Gras, 1996; Working Party, 1996; Chan *et al*., 1997], and point towards the different aerosol sources already identified for the regions in question.

The major difference evident in the AFP data is that in Canberra and Launceston, the winter-time aerosol is dominated by emissions from domestic wood-burning (relatively high PM loadings; EOM; $nssK^+$; with relatively low EC), while in the major cities the wintertime aerosol, while having some wood smoke component, has a greater fractional contribution from automotive emissions.

It is notable that the PM10 loadings of all samples from the four major cities fall below the proposed national standard of 50 μg m^{-3}, 24 hour average, while both Canberra and Launceston have individual samples greater than this value. More notable is the Launceston data, with the average of the five 24h means, at 63 μg m^{-3}, being well above the proposed 24 hour figure.

Table 14. Means ±stdev Sydney August 1996

	ANSTO SAMPLERS				MOUDI			
MASSES µg cm^{-3}	PM10		PM2.5		PM10		PM2.5	
mass	18.3 ± 11.6		9.6 ± 7.1		24.7 ± 9.6		18.5 ± 14.3	
IM	6.1 ± 2.9		2.2 ± 1.3		7.5 ± 2.4		5.1 ± 3.8	
EC	3.7 ± 3.3		4.4 ± 3.8		2.4 ± 1.0		2.1 ± 1.7	
EOM	8.5 ± 17.9		2.9 ± 12.2		14.8 ± 13.1		11.2 ± 19.8	

	ANSTO SAMPLERS				MOUDI			
PIXE ng m^{-3}	PM10		PM2.5		PM10		PM2.5	
H[7]			409 ± 324					
Na	1366 ± 1409		224 ± 383		671 ± 531		196 ± 57	
Al	215 ± 106		28 ± 21		49 ± 32			
Si	885 ± 443		62 ± 44		257 ± 161		71 ± 41	
P	20 ± 12.1		5.2 ± 3.5					
S	361 ± 266		339 ± 228		324 ± 146		293 ± 139	
Cl	840 ± 723		295 ± 254		130 ± 158		16 ± 14	
K	141 ± 86		80 ± 47		113 ± 55		70 ± 48	
Ca	216 ± 134		30 ± 18		120 ± 124		22 ± 11	
Ti	37 ± 23.5		3.7 ± 3.1		13 ± 7			
V	5.4 ± 1.9							
Cr	4.9 ± 2.0				2.8 ± 0.5		2.0 ± 0.4	
Mn	13 ± 11		3.0 ± 3.3		5.0 ± 2		3.0 ± 1	
Fe	350 ± 262		59 ± 53		155 ± 98		61 ± 39	
Co	4.2 ± 2.1				5.6 ± 2.2		3.6 ± 1.9	
Ni	4.7 ± 1.7							
Cu	14.3 ± 5.7		7.1 ± 9.8		30 ± 60		7 ± 10	
Zn	29 ± 20		25 ± 18		38 ± 33		25 ± 24	
Br	42 ± 20		31 ± 19		34 ± 16		31 ± 15	
Pb	95 ± 71		77 ± 48		94 ± 52		85 ± 48	

	ANSTO SAMPLERS				MOUDI			
IC ng m^{-3}	PM10		PM2.5		PM10		PM2.5	
H^+	1.8 ± 0.4		1.2 ± 0.9		11 ± 3		9.2 ± 3	
Na	624 ± 355		217 ± 158		520 ± 321		228 ± 77	
NH_4^+	95 ± 115		224 ± 248		392 ± 187		380 ± 183	
K^+	98 ± 59		71 ± 50		133 ± 63		111 ± 61	
$nssK^+$	81 ± 55		65 ± 51		115 ± 63		106 ± 60	
Mg^{2+}	87 ± 46		28 ± 20		58 ± 40		18 ± 8	
Ca^{2+}	165 ± 95		27 ± 10		112 ± 44		54 ± 15	
Cl^-	682 ± 562		311 ± 239		372 ± 384		132 ± 82	
NO_2^-	1.9 ± 0.2		0.9 ± 0.3		16 ± 16		14 ± 17	
Br^-	12 ± 10.9		19 ± 16		11 ± 7		9.7 ± 7	
NO_3^-	395 ± 398		269 ± 278		741 ± 318		356 ± 156	
SO_4^{2-}	631 ± 516		611 ± 490		971 ± 435		875 ± 421	
$nssSO_4^{2-}$	584 ± 503		596 ± 493		852 ± 428		828 ± 418	
Oxalic acid	44 ± 43		35 ± 38		135 ± 102		109 ± 83	
PO_4^{3-}	19 ± 20				3.0 ± 2		1.9 ± 1	
Acetic acid	18 ± 4		6.1 ± 2		119 ± 61		104 ± 61	
Formic acid	54 ± 10		8.9 ± 2		90 ± 24		70 ± 21	
MSA	11 ± 5		10.9 ± 6.8		4.0 ± 2.3		3.7 ± 2.3	

[7] Note that H (total H) determined by PIXE and H^+ (soluble H^+ ion concentration) determined from pH are not comparable measurements.

Table 15. Means ±stdev Brisbane September, October, November 1996

	ANSTO SAMPLERS				MOUDI			
MASSES µg cm^{-3}	PM10		PM2.5		PM10		PM2.5	
mass	18.1 ± 5.9		6.0 ± 2.4		20.0 ± 7.8		11.2 ± 7.7	
IM	8.7 ± 3.5		2.4 ± 0.8		10.8 ± 3.7		5.6 ± 3.7	
EC	1.6 ± 1.2		1.5 ± 0.8		1.7 ± 0.3		1.6 ± 1.3	
EOM	7.8 ± 10.5		2.0 ± 4.0		7.5 ± 11.8		4.0 ± 12.7	

	ANSTO SAMPLERS		MOUDI	
PIXE ng m^{-3}	PM10	PM2.5	PM10	PM2.5
H		194 ± 99		
Na	2176 ± 1143	314 ± 174	2162 ± 935	482 ± 320
Al	156 ± 78	23 ± 13		
Si	732 ± 296	70 ± 30	210 ± 120	60 ± 38
P	20 ± 5.1	5.0 ± 3.8		
S	409 ± 175	326 ± 154	349 ± 202	281 ± 190
Cl	1297 ± 1205	321 ± 387	900 ± 973	167 ± 194
K	146 ± 75	76 ± 55	199 ± 102	88 ± 80
Ca	190 ± 63	32 ± 7	214 ± 87	31 ± 5
Ti	38 ± 18.5	6.7 ± 4.8	11 ± 8	
V	2 ± 1.7			
Cr	7 ± 1.4			
Mn	7 ± 4	3 ± 2	5 ± 2	3 2
Fe	229 ± 114	48 ± 26	121 ± 94	44 ± 35
Co	3.3 ± 1.5		5.3 ± 2.4	3 2
Ni	3.5 ± 1.6			
Cu	9.7 ± 3.8	3.3 ± 2.1	146 ± 62	43 ± 18
Zn	29 ± 9	20 ± 11	41 ± 13	24 ± 18
Br	22 ± 10	9 ± 6	11 ± 3	8 ± 4
Pb	36 ± 26	31 ± 25	27 ± 15	23 ± 13

	ANSTO SAMPLERS		MOUDI	
IC ng m^{-3}	PM10	PM2.5	PM10	PM2.5
H^+	1.5 ± 0.5	0.6 ± 0.2	9 ± 3	8 ± 3
Na	1479 ± 952	419 ± 224	1532 ± 588	554 ± 295
NH_4^+	71 ± 96	115 ± 74	373 ± 190	347 ± 191
K^+	123 ± 70	68 ± 56	252 ± 157	161 ± 121
$nssK^+$	89 ± 62	58 ± 55	204 ± 146	148 ± 117
Mg^{2+}	180 ± 109	52 ± 26	153 ± 57	41 ± 16
Ca^{2+}	200 ± 61	34 ± 8	186 ± 77	71 ± 33
Cl^-	1400 ± 1392	303 ± 372	1133 ± 818	318 ± 192
NO_2^-		8.4 ± 22.1	34 ± 27	27 ± 21
Br^-		5 ± 3	8 ± 7	6 ± 7
NO_3^-	1297 ± 1100	242 ± 86	2505 ± 1409	895 ± 682
SO_4^{2-}	992 ± 495	745 ± 418	1044 ± 607	838 ± 572
$nssSO_4^{2-}$	896 ± 468	717 ± 416	765 ± 598	744 ± 570
Oxalic acid	78 ± 67	62 ± 57	130 ± 113	94 ± 85
PO_4^{3-}				
Acetic acid	19 ± 3	6 ± 1	211 ± 165	160 ± 120
Formic acid	82 ± 30	9 ± 2	134 ± 58	92 ± 35
MSA	16 ± 5	16.0 ± 6.1	8.8 ± 8.5	6.8 ± 6.5

Table 16. Means ±stdev Melbourne April 1997

	ANSTO SAMPLERS				MOUDI			
MASSES µg cm^{-3}	PM10	PM2.5	PM10	PM2.5
mass	17.5 ± 4.2	4.9 ± 2.6	23.5 ± 5.4	14.8 ± 10.6
IM	9.5 ± 2.1	2.0 ± 0.2	8.3 ± 2.1	4.2 ± 2.7
EC	1.7 ± 0.8	1.6 ± 0.7	1.8 ± 1.3	1.5 ± 1.2
EOM	6.4 ± 7.0	1.3 ± 3.5	13.3 ± 8.8	9.1 ± 14.5

	ANSTO SAMPLERS		MOUDI	
PIXE ng m^{-3}	PM10	PM2.5	PM10	PM2.5
H		203 ± 110		
Na	2015 ± 645	68 ± 153	1921 ± 777	633 ± 231
Al	223 ± 151	41 ± 10	37 ± 14	
Si	1103 ± 583	136 ± 34	325 ± 126	108 ± 44
P	10 ± 12	10 ± 8.9		
S	348 ± 102	269 ± 97	302 ± 114	231 ± 101
Cl	1178 ± 795	97 ± 87	1136 ± 760	218 ± 155
K	119 ± 56	50 ± 18	70 ± 28	35 ± 18
Ca	317 ± 114	44 ± 8	117 ± 65	25 ± 13
Ti	45 ± 24	7.0 ± 4.3	15 ± 6.2	5.0 ± 1.8
V				
Cr	4.4 ± 2.5			
Mn	12 ± 1.7	3.3 ± 2.3	6.6 ± 3.0	3.8 ± 2.8
Fe	459 ± 185	75 ± 21	208 ± 50	77 ± 19
Co	2.1 ± 1.9		2.6 ± 1.2	1.7 ± 0.7
Ni	2.3 ± 1.1	0.6 ± 0.6		
Cu	5.7 ± 2.8	1.3 ± 0.7		
Zn	332 ± 298	118 ± 161	208 ± 247	145 ± 181
Br	33 ± 18	20 ± 18	22 ± 16	17 ± 14
Pb	60 ± 44	51 ± 36	58 ± 45	50 ± 43

	ANSTO SAMPLERS		MOUDI	
IC ng m^{-3}	PM10	PM2.5	PM10	PM2.5
H^+	0.9 ± 0.6	0.7 ± 0.3	7.2 ± 0.7	5.7 ± 0.6
Na	1146 ± 487	173 ± 45	1139 ± 363	381 ± 69
NH_4^+	32 ± 24	97 ± 71	196 ± 107	186 ± 107
K^+	85 ± 19	44 ± 21	87 ± 28	55 ± 25
$nssK^+$	59 ± 19	41 ± 21	54 ± 22	47 ± 23
Mg^{2+}	136 ± 50	14 ± 3.9	109 ± 46	27 ± 9.2
Ca^{2+}	235 ± 77	35 ± 5.8	153 ± 28	66 ± 18
Cl^-	1399 ± 934	97 ± 82	1208 ± 549	267 ± 96
NO_2^-			18 ± 10.1	13 ± 7.5
Br^-	15 ± 11	8.9 ± 10	16 ± 17	14 ± 16
NO_3^-	560 ± 355	69 ± 35	889 ± 566	340 ± 160
SO_4^{2-}	842 ± 216	558 ± 206	921 ± 333	699 ± 305
$nssSO_4^{2-}$	770 ± 207	550 ± 206	692 ± 282	638 ± 287
Oxalic acid	36 ± 18	20 ± 10	37 ± 24	30 ± 24
PO_4^{3-}	16 ± 15	14 ± 11		
Acetic acid	20 ± 6.6	7.1 ± 2.8	94 ± 53	69 ± 42
Formic acid	95 ± 27	8.9 ± 2.6	110 ± 12	68 ± 12
MSA	15 ± 3.3	14 ± 3.2	6.7 ± 3.1	5.9 ± 2.5

Table 17. Means ±stdev Canberra May 1997

	ANSTO SAMPLERS						MOUDI					
MASSES µg cm^{-3}	PM10			PM2.5			PM10			PM2.5		
mass	16.1	±	7.8	9.1	±	6.7	43.1	±	22.4	34.3	±	24.6
IM	5.1	±	3.8	1.4	±	1.6	8.8	±	1.2	5.8	±	4.1
EC	2.7	±	1.6	2.3	±	1.9	3.4	±	0.6	2.7	±	2.1
EOM	8.3	±	13.1	5.3	±	10.2	30.8	±	24.3	25.8	±	30.8

	ANSTO SAMPLERS						MOUDI					
PIXE ng m^{-3}	PM10			PM2.5			PM10			PM2.5		
H				412	±	320						
Na	1036	±	475				1016	±	498	403	±	113
Al	132	±	127	20	±	22	41	±	14			
Si	688	±	516	44	±	53	306	±	134	88	±	38
P	14.5	±	6.4	6.8	±	3.9						
S	402	±	361	270	±	342	464	±	212	422	±	204
Cl	135	±	138	55	±	51	122	±	82	37	±	38
K	117	±	91	69	±	62	180	±	103	136	±	110
Ca	69	±	50	14	±	16	48	±	28	12	±	7.2
Ti	14	±	14	1.6	±	2.1	8.0	±	2.3			
V	0.8	±	0.4	0.1	±	0.2						
Cr	4.6	±	0.2	0.2	±	0.3						
Mn	5.5	±	3.3	0.6	±	0.9	4.3	±	1.1	2.0	±	0.2
Fe	133	±	118	23	±	27	115	±	30	41	±	15
Co							3.7	±	1.9	2.0	±	0.9
Ni	1.3	±	0.2									
Cu	2.5	±	1.5	0.8	±	0.8	12.3	±	12.8	5.1	±	4.9
Zn	10	±	10	4.7	±	3.8	13	±	6.2	8.7	±	4.5
Br	28	±	11	19	±	18	40	±	37	34	±	34
Pb	50	±	39	46	±	45	103	±	80	91	±	73

	ANSTO SAMPLERS						MOUDI					
IC ng m^{-3}	PM10			PM2.5			PM10			PM2.5		
H^+	2.5	±	0.7	1.8	±	0.8	11.5	±	4.4	9.6	±	4.2
Na	380	±	342	129	±	168	673	±	352	273	±	107
NH_4^+	206	±	256	145	±	150	540	±	226	530	±	222
K^+	87	±	57	67	±	59	274	±	212	228	±	213
$nssK^+$	77	±	49	64	±	55	252	±	214	220	±	211
Mg^{2+}	50	±	46	18	±	23.6	71	±	33	26	±	12.5
Ca^{2+}	119	±	41	19	±	18.0	152	±	38	86	±	23
Cl^-	198	±	187	52	±	37	250	±	76	133	±	100
NO_2^-	2.8	±	1.1	1.3	±	0.9	14	±	5.4	11	±	4.7
Br^-	7.9	±	7.0	7.2	±	6.7	28	±	27	26	±	26
NO_3^-	468	±	370	132	±	116	1289	±	584	497	±	332
SO_4^{2-}	946	±	913	556	±	770	1450	±	603	1318	±	577
$nssSO_4^{2-}$	919	±	897	546	±	758	1298	±	614	1253	±	594
Oxalic acid	42	±	34	35	±	42	89	±	17	69	±	13
PO_4^{3-}	16	±	7	11	±	12						
Acetic acid	23	±	6.6	7.7	±	2.5	65	±	32	53	±	32
Formic acid	49	±	9	12.4	±	2.5	96	±	31	74	±	30
MSA	11.6	±	2.4	7.5	±	5.4	4.3	±	0.9	4.0	±	0.9

Table 18. Means ±stdev Launceston June, July 1997

	ANSTO SAMPLERS				MOUDI			
MASSES µg cm^{-3}	PM10	PM2.5	PM10	PM2.5
mass	35.0 ± 11.3	27.3 ± 8.6	63.0 ± 29.2	49.3 ± 31.9
IM	5.4 ± 2.4	3.8 ± 1.0	13.5 ± 3.2	8.1 ± 5.1
EC	3.1 ± 1.4	4.0 ± 1.2	2.7 ± 1.3	2.2 ± 1.6
EOM	26.5 ± 15.1	19.5 ± 10.8	46.8 ± 33.7	39.0 ± 38.6

	ANSTO SAMPLERS		MOUDI	
PIXE ng m^{-3}	PM10	PM2.5	PM10	PM2.5
H		1153 ± 393		
Na	1624 ± 1020	251 ± 502	1089 ± 832	531 ± 230
Al	97 ± 67	76 ± 45	60 ± 77	41 ± 58
Si	383 ± 180	33 ± 16	184 ± 86	50 ± 21
P	18 ± 6.1	5.3 ± 3.0		
S	391 ± 145	363 ± 72	351 ± 103	294 ± 91
Cl	538 ± 850	730 ± 287	369 ± 191	252 ± 224
K	179 ± 64	210 ± 68	321 ± 137	273 ± 150
Ca	101 ± 46	17 ± 16	75 ± 46	14 ± 8
Ti	11 ± 5.8	1.5 ± 0.8	7.6 ± 3.1	3.0 ± 0.5
V			2.9 ± 0.3	2.1 ± 0.1
Cr	13 ± 7.6		7.7 ± 8.5	6.8 ± 8.5
Mn	79 ± 102	24 ± 28	66 ± 86	27 ± 30
Fe	167 ± 94	60 ± 55	154 ± 87	72 ± 59
Co	0.8 ± 1.3		3.0 ± 1.5	2.3 ± 1.5
Ni	2.8 ± 1.6		2 ± 0.2	1.2 ± 0.2
Cu	3.7 ± 1.4	1.8 ± 0.8	34 ± 13	22 ± 10
Zn	37 ± 19	30 ± 19	36 ± 20	27 ± 13
Br	44 ± 9.2	27 ± 16	27 ± 21	25 ± 20
Pb	52 ± 18	51 ± 11	83 ± 47	75 ± 43

	ANSTO SAMPLERS		MOUDI	
IC ng m^{-3}	PM10	PM2.5	PM10	PM2.5
H^+	5.8 ± 2.6	4.7 ± 2.2	13 ± 5.2	11 ± 4.9
Na	811 ± 886	312 ± 341	1402 ± 1024	647 ± 519
NH_4^+	81 ± 53	476 ± 113	1026 ± 409	812 ± 327
K^+	206 ± 39	201 ± 63	488 ± 200	398 ± 212
$nssK^+$	191 ± 49	196 ± 68	461 ± 209	389 ± 212
Mg^{2+}	81 ± 106	26 ± 37	83 ± 59	26 ± 9
Ca^{2+}	100 ± 45	22 ± 14	172 ± 42	78 ± 23
Cl^-	683 ± 988	667 ± 286	827 ± 417	552 ± 376
NO_2^-	3.5 ± 0.5	2.0 ± 0.4	6.9 ± 2.7	5.1 ± 2.4
Br^-	10 ± 2.9	11 ± 12	27 ± 20	25 ± 20
NO_3^-	474 ± 520	717 ± 295	4836 ± 1792	2343 ± 810
SO_4^{2-}	869 ± 369	713 ± 194	1081 ± 307	891 ± 277
$nssSO_4^{2-}$	826 ± 356	700 ± 185	911 ± 345	829 ± 286
Oxalic acid	81 ± 21	67 ± 18	108 ± 17	86 ± 18
PO_4^{3-}	21 ± 13	39 ± 17	8.5 ± 6.7	7.4 ± 6.5
Acetic acid	50 ± 14	19 ± 15	77 ± 26	63 ± 22
Formic acid	96 ± 15	32 ± 12	89 ± 31	72 ± 26
MSA	13 ± 10	7.0 ± 3.9	5.1 ± 1.9	4.6 ± 1.9

Table 19. Means ±stdev Adelaide August 1997 n=5

	ANSTO SAMPLERS						MOUDI					
MASSES µg cm^{-3}	PM10			PM2.5			PM10			PM2.5		
mass	25.8	±	9.0	15.2	±	6.8	24.6	±	5.4	15.8	±	11.9
IM	8.4	±	3.0	2.8	±	1.0	8.3	±	2.8	3.9	±	2.5
EC	5.8	±	2.0	11.1	±	5.3	2.7	±	0.7	2.4	±	1.9
EOM	11.5	±	14.0	1.2	±	13.2	13.6	±	8.9	9.6	±	16.2

	ANSTO SAMPLERS						MOUDI					
PIXE ng m^{-3}	PM10			PM2.5			PM10			PM2.5		
H				515	±	261						
Na	1731	±	1192	324	±	240	1453	±	1209	259	±	163
Al	244	±	130	81	±	31	42	±	32			
Si	951	±	399	61	±	28	280	±	184	52	±	27
P	5.8	±	2.1	5.4	±	1.4						
S	312	±	70	249	±	69	149	±	45	82	±	22
Cl	1593	±	1440	552	±	447	1194	±	1122	182	±	183
K	178	±	61	82	±	51	94	±	47	40	±	27
Ca	536	±	291	53	±	17	181	±	89	35	±	16
Ti	23	±	9	3.2	±	1.8	7.5	±	4.1			
V												
Cr	5.6	±	3.4									
Mn	10	±	2.4	3.3	±	2.0	7.8	±	4.3	2.7	±	1.1
Fe	376	±	125	73	±	36	193	±	91	48	±	17
Co	2.5	±	1.4				5.8	±	2.3	1.8	±	0.5
Ni	1.7	±	0.9									
Cu	11.9	±	4.8	3.3	±	1.6	5.2	±	5.9	4.7	±	5.9
Zn	51	±	25	40	±	34	33	±	18	22	±	16
Br	184	±	67	162	±	62	101	±	48	74	±	32
Pb	357	±	119	333	±	129	245	±	96	177	±	62

	ANSTO SAMPLERS						MOUDI					
IC ng m^{-3}	PM10			PM2.5			PM10			PM2.5		
H^+	1.3	±	0.2	1.1	±	0.4	5.4	±	0.5	4.6	±	0.5
Na	985	±	759	327	±	232	945	±	614	211	±	93
NH_4^+	21	±	17	104	±	107	145	±	64	126	±	62
K^+	69	±	33	70	±	48	96	±	37	65	±	42
$nssK^+$	45	±	18	61	±	51	60	±	46	56	±	43
Mg^{2+}	125	±	85	43	±	28.0	131	±	86	30	±	13.9
Ca^{2+}	279	±	91	47	±	13.7	277	±	92	92	±	34
Cl^-	1542	±	1408	517	±	428	1361	±	1144	271	±	202
NO_2^-	2.1	±	0.7	1.4	±	0.6	6.0	±	2.1	4.2	±	1.6
Br^-	100	±	44	114.5	±	71	93	±	47	76	±	39
NO_3^-	347	±	222	353	±	420	706	±	375	344	±	230
SO_4^{2-}	337	±	210	306	±	97	422	±	109	222	±	89
$nssSO_4^{2-}$	271	±	178	283	±	107	160	±	101	158	±	100
Oxalic acid	23	±	8.5	21	±	14	20	±	6.2	13	±	3.3
PO_4^{3-}												
Acetic acid	27	±	3.0	12.6	±	4.2	48	±	4.2	34	±	4.6
Formic acid	134	±	57	21.2	±	3.5	122	±	20	74	±	13
MSA	2.8	±	2.6	6.9	±	3.2	5.5	±	4.9	4.6	±	4.3

Table 20. Mean PM2.5 mass concentrations (measured by TEOM), b_{sp} and b_{spd} (measured by nephelometer) and CN measured by TSI-UCPC[#] (Sydney) and CSIRO CN counter[&] (Melbourne, Canberra, Launceston and Adelaide); n = number of days of data.

	TEOM PM2.5 μgm^{-3}	b_{sp} 10^{-5} m^{-1}	b_{spd} 10^{-5} m^{-1}	CN 10^{3} cm^{-3}
Sydney				27 ± 5 n=18[#]
Brisbane				
Melbourne	8 ± 3 n=12	2.8 ± 1.1 n=7	1.6 ± 1.1 n=27	37 ± 79 n=28[&]
Canberra	19 ± 10 n=20	9.6 ± 9.3 n=26	7.0 ± 6.5 n=24	21 ± 72 n=33[&]
Launceston	36 ± 25 n=46	21 ± 13 n=44	13.5 ± 8.6 n=44	24 ± 9 n=50[&]
Adelaide	11 ± 25 n=25	3.0 ± 1.2 n=24	1.9 ± 0.9 n=24	60 ± 23 n=25[&]

7.2 Aerosol Composition as a Function of Particle Size (MOUDI Data)

The MOUDI data provide information on the distribution with size of aerosol properties, at a level of detail hitherto unavailable in Australia. The initial presentation of size distributions in this chapter is made in Figures 12 – 17. These figures illustrate the capability of the MOUDI to reveal definitively the characteristic size ranges inhabited by specific elements and chemical species. The Figures show the distribution with size of tracers for particular aerosol sources, such as Pb, Br and EC which in the Sydney atmosphere derive primarily from automotive emissions (Figure 12). Figure 13 shows distributions for strong acids (sulfuric and nitric) derived from atmospheric oxidation of SO_2 and NO_x, along with the counter ions H^+ and NH_4^+, in a Brisbane sample.

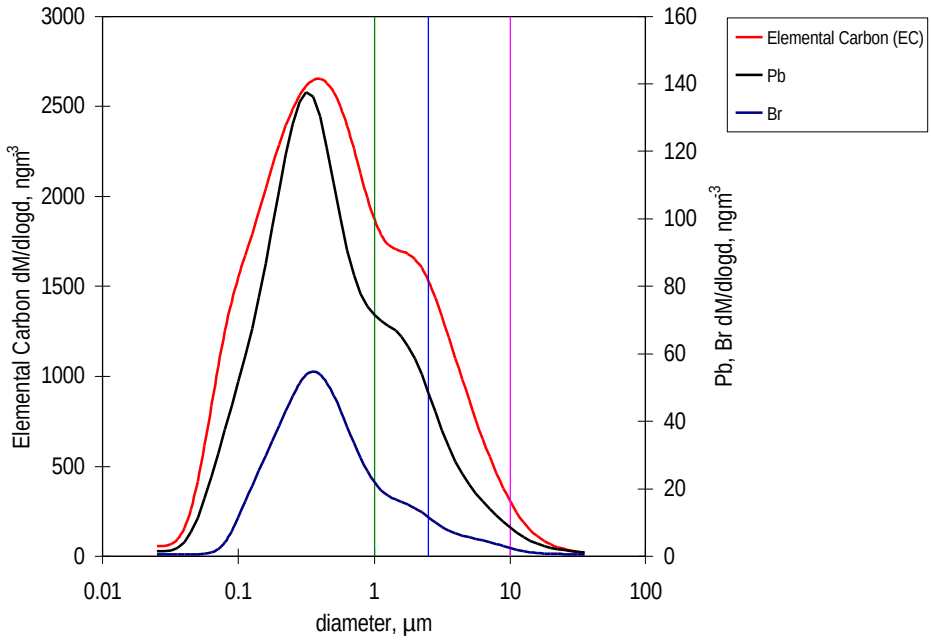

Figure 12. Mass distribution of automotive tracers, Sydney aerosol.

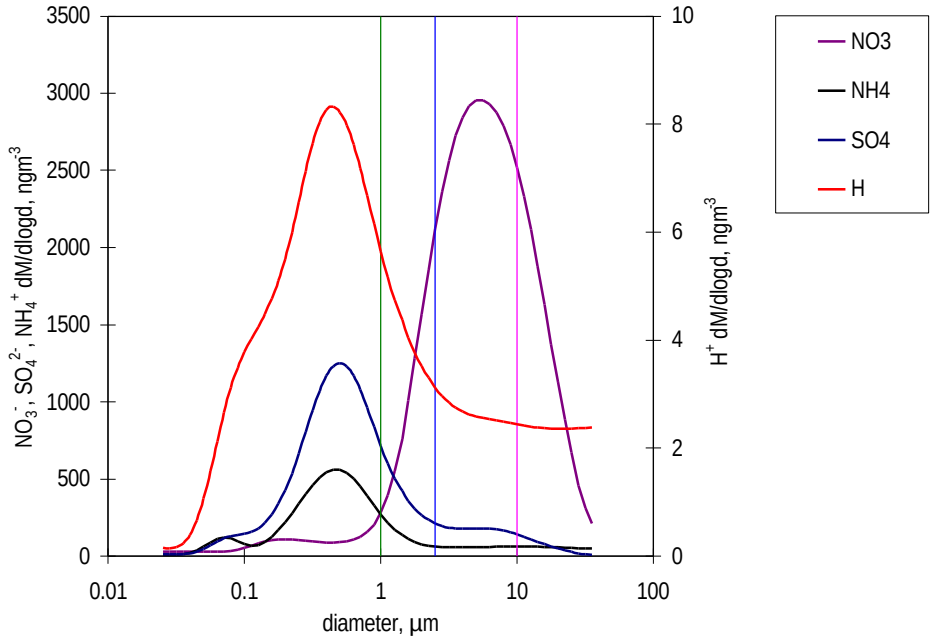

Figure 13. Mass distribution of strong acid species, Brisbane aerosol.

A very clear feature from the distributions in Figure 13 is the fact that nitric acid does not deposit at the "strong acid" part of the size range inhabited by acid sulfate (*i.e.* below 1 µm), but is confined to the more alkaline size range above 1 µm. This is exactly the size range where alkalinity is derived from both soil dust (Figure 14), and sea-salt (Figure 15).

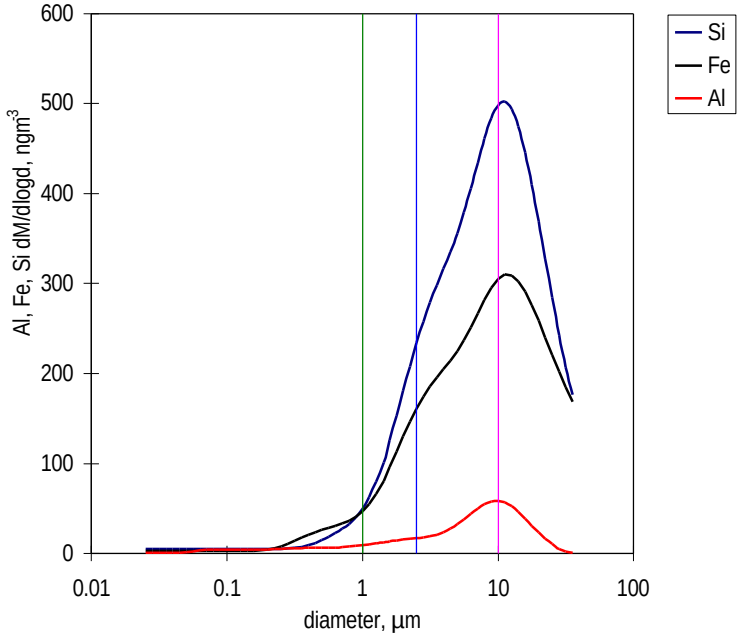

Figure 14. Mass distributions for soil-derived elements, Melbourne aerosol.

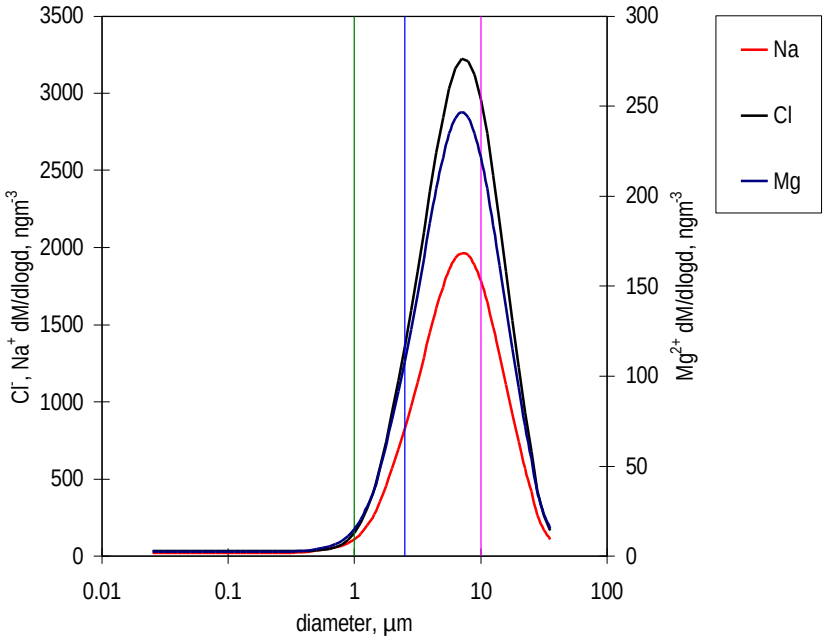

Figure 15. Mass distributions for sea-salt-derived elements, Adelaide aerosol.

Finally, Figure 16 provides evidence of the strong role played by wood-burning ($nssK^+$ is a tracer for smoke from biomass combustion) in dominating the aerosol mass distribution during winter in Launceston, while Figure 17 reveals a more complex picture of the contributions made by different major aerosol components in an aerosol sample from Canberra.

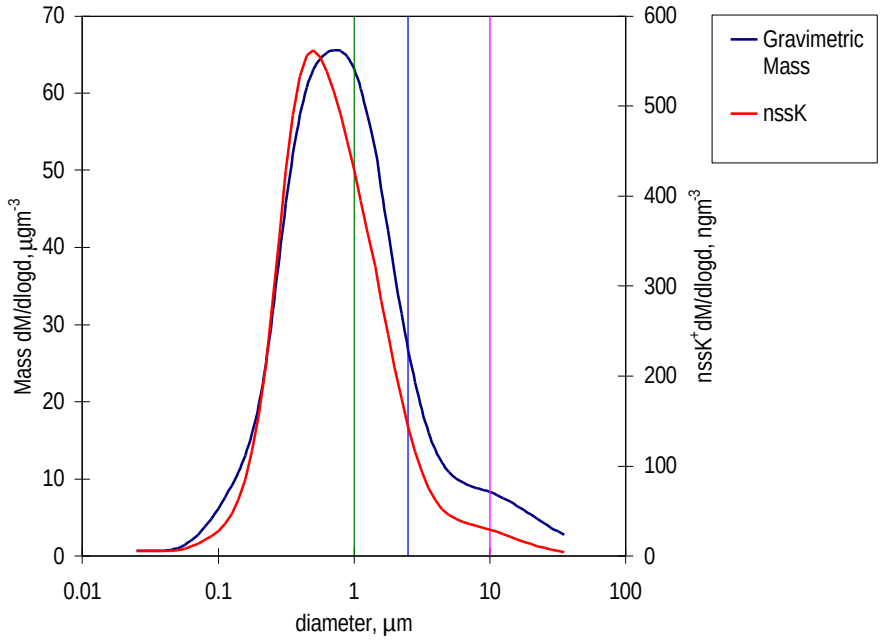

Figure 16. Mass distributions for $nssK^+$ and total mass, Launceston aerosol.

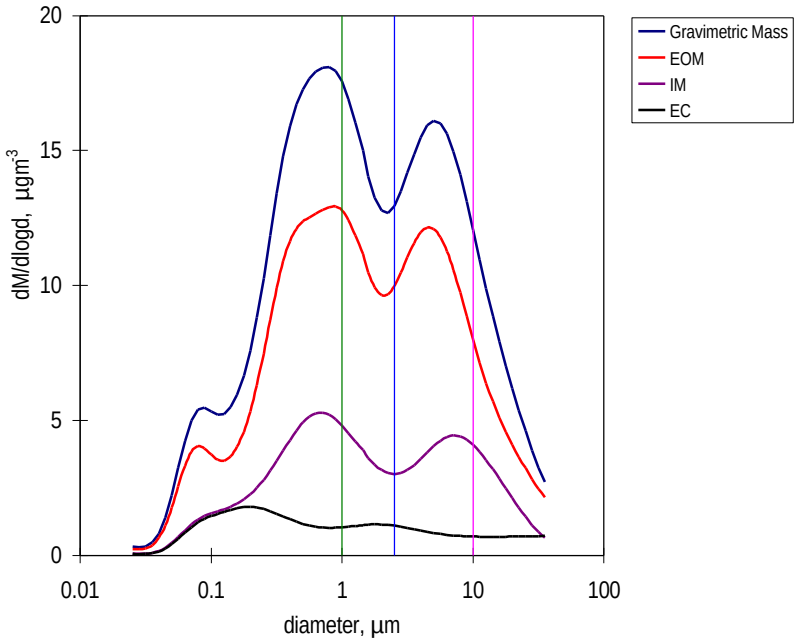

Figure 17. Major mass components, Canberra aerosol. EOM = estimated organic mass; IM = inorganic mass; EC = elemental carbon mass.

Since the MOUDI provides simultaneous information on different size ranges, such as the PM10, PM2.5 and PM1 size ranges delineated by the vertical lines in Figures 13 – 17, a self-consistent (*i.e.* from within a single sample) picture of the relationship between the different PM fractions is readily derived. Figure 18 contains a plot of PM2.5 vs PM10 from all MOUDI samples, revealing a very clear structural relationship, a particular feature of which is a decreasing role for PM2.5 as total aerosol mass (*i.e.* PM10 and PM2.5) levels decrease. The latter point is more clearly evident in Figure 19, which reveals a systematic variation the ratio of PM2.5/PM10 as a function of PM2.5.

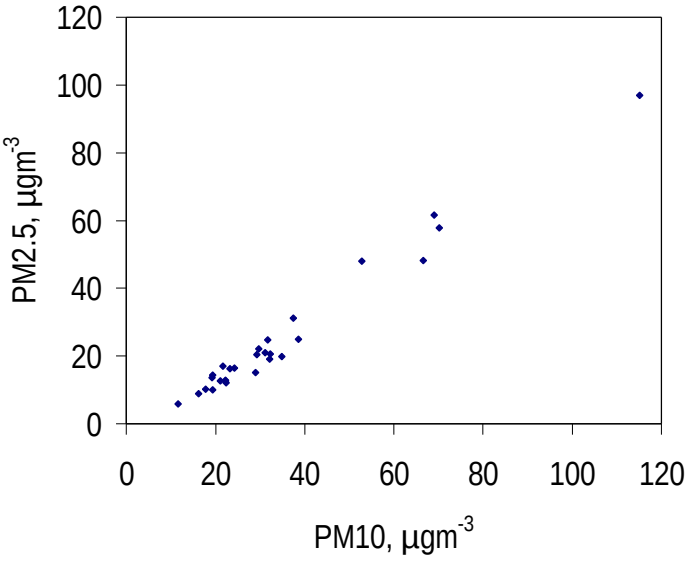

Figure 18. PM2.5 vs PM10 data, all sites.

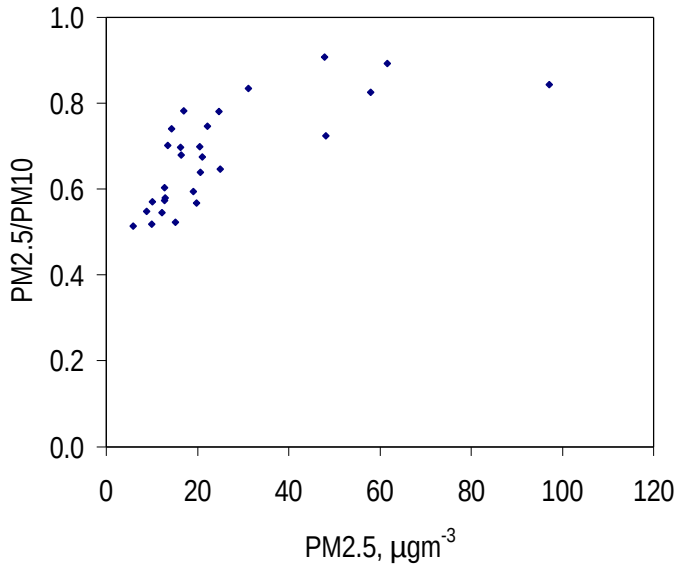

Figure 19. Ratio of PM2.5 to PM10 as a function of PM2.5 loading, all sites.

The apparently coherent trend in Figure 19 across all six sites in different parts of the country suggests that increasing aerosol mass, in other words aerosol pollution, may in general cause disproportionate elevation of PM2.5 loading in comparison with PM10 loading. Such a conclusion could offer an argument for a PM2.5 ambient aerosol standard in preference to the PM10 standard currently recommended for the air NEPM [NEPC, 1997].

Consistent with this observation the highest PM2.5/PM10 ratios were measured in Launceston and Canberra where PM2.5 levels were elevated, while the lowest were measured in Brisbane. This information is also summarised in Table 21, which in addition includes the ratios of PM2.5 and PM10 to TSP and PM1 to PM2.5, PM10 and TSP. In each city PM10 makes up a significant proportion of TSP (60-80%), while PM1 makes up between 30-50% of TSP.

Table 22 lists the mean proportions of major and tracer chemical species in each size fraction for each city. The tracer species listed identify sources that have been suggested to have an impact upon human health. Here we use Pb to trace vehicle exhaust, H^+, $nssSO_4^{2-}$, NO_3^- and NH_4^+ to trace strong acidity and $nssK^+$ as a tracer of woodsmoke.

On the basis of the relationships displayed by the major chemical species in Table 22, the 6 cities can be divided into 3 subsets. The first is comprised of Sydney, Melbourne and Adelaide, where EOM is a significant proportion of each mass size fraction (60-80%), and this proportion increases with decreasing size fraction. Inorganic mass (IM) comprises 15-30% of mass and conversely decreases with decreasing mass size fraction. Elemental carbon (EC) makes up 10% of the mass and increases with the smaller size fractions.

The second subset is made up of Canberra and Launceston and displays similar features to the first except that EOM is higher (75-85%) and EC is lower (<10%), and both are relatively constant over the size fractions. The third subset is made up of Brisbane, where EOM and IM are approximately equal (45%). Inorganic mass (IM) decreases with decreasing size fraction and EC increases significantly.

Adelaide displays the highest proportion of Pb in each size fraction, which is expected from the location of the sample site adjacent to a major roadway. All sites showed an increase in the proportion of Pb with decreasing size fraction, with Canberra and Launceston showing the smallest increase and Brisbane the largest. The acidity tracers, H^+, $nssSO_4^{2-}$ and NH_4^+ all show increasing proportions with decreasing particle size, again with Brisbane showing the largest increase. As expected based on the discussion presented earlier in conjunction with Figures 13 and 14, the change in the ratio of NO_3^- to mass with size fraction was opposite to that of $nssSO_4^{2-}$. The woodsmoke tracer, $nssK^+$, is more significant in PM1 than the larger fractions, with Brisbane having the highest overall fraction, followed by Canberra and Launceston. The high value in Brisbane can be reconciled by the high IM fractions measured, suggesting that $nssK^+$ in Brisbane may have additional sources, *e.g.* soil-dust.

Table 21. Matrices of mean mass ratios for each city.

Sydney	TSP	PM10	PM2.5	PM1
TSP	100%			
PM10	87%	100%		
PM2.5	65%	75%	100%	
PM1	51%	58%	77%	100%
Brisbane	TSP	PM10	PM2.5	PM1
TSP	100%			
PM10	82%	100%		
PM2.5	46%	56%	100%	
PM1	31%	38%	68%	100%
Melbourne	TSP	PM10	PM2.5	PM1
TSP	100%			
PM10	81%	100%		
PM2.5	51%	63%	100%	
PM1	36%	45%	72%	100%
Canberra	TSP	PM10	PM2.5	PM1
TSP	100%			
PM10	92%	100%		
PM2.5	74%	80%	100%	
PM1	53%	57%	72%	100%
Launceston	TSP	PM10	PM2.5	PM1
TSP	100%			
PM10	90%	100%		
PM2.5	70%	78%	100%	
PM1	46%	51%	65%	100%
Adelaide	TSP	PM10	PM2.5	PM1
TSP	100%			
PM10	83%	100%		
PM2.5	54%	64%	100%	
PM1	40%	48%	75%	100%

Table 22. Mean proportion of major and tracer chemical species to mass size fraction in each city.

Sydney				
Majors	TSP	PM10	PM2.5	PM1
Mass	100%	100%	100%	100%
EOM	70%	69%	72%	73%
IM-EC	21%	21%	16%	15%
EC	9%	10%	11%	12%
Tracers				
Pb	0.34%	0.38%	0.46%	0.50%
H^+	0.04%	0.04%	0.05%	0.05%
$nssSO_4^{2-}$	3.05%	3.45%	4.48%	4.95%
NO_3^-	2.95%	3.00%	1.93%	1.50%
NH_4^+	1.41%	1.59%	2.06%	2.32%
$nssK^+$	0.43%	0.46%	0.57%	0.62%
Brisbane				
Majors	TSP	PM10	PM2.5	PM1
Mass	100%	100%	100%	100%
EOM	46%	46%	50%	53%
IM-EC	47%	45%	36%	31%
EC	7%	9%	14%	17%
Tracers				
Pb	0.12%	0.13%	0.20%	0.25%
H^+	0.04%	0.05%	0.07%	0.08%
$nssSO_4^{2-}$	3.16%	3.83%	6.62%	8.31%
NO_3^-	13.84%	12.55%	7.97%	5.02%
NH_4^+	1.61%	1.87%	3.09%	3.99%
$nssK^+$	1.04%	1.02%	1.32%	1.37%
Melbourne				
Majors	TSP	PM10	PM2.5	PM1
Mass	100%	100%	100%	100%
EOM	64%	63%	71%	74%
IM-EC	29%	28%	18%	14%
EC	7%	8%	10%	11%
Tracers				
Pb	0.20%	0.25%	0.34%	0.38%
H^+	0.03%	0.03%	0.04%	0.04%
$nssSO_4^{2-}$	2.47%	2.95%	4.31%	5.42%
NO_3^-	3.62%	3.79%	2.30%	0.97%
NH_4^+	0.70%	0.84%	1.25%	1.65%
$nssK^+$	0.21%	0.23%	0.32%	0.38%
Canberra				
Majors	TSP	PM10	PM2.5	PM1
Mass	100%	100%	100%	100%
EOM	78%	79%	83%	83%
IM-EC	14%	13%	9%	8%
EC	8%	8%	8%	9%
Tracers				
Pb	0.22%	0.24%	0.27%	0.29%
H^+	0.03%	0.03%	0.03%	0.03%
$nssSO_4^{2-}$	2.81%	3.01%	3.65%	4.06%
NO_3^-	3.20%	2.99%	1.45%	1.04%
NH_4^+	1.17%	1.25%	1.54%	1.83%
$nssK^+$	0.56%	0.58%	0.64%	0.70%

Table 22 (continued). Mean proportion of major and tracer chemical species to mass size fraction in each city.

Launceston				
Majors	TSP	PM10	PM2.5	PM1
Mass	100%	100%	100%	100%
EOM	76%	78%	83%	84%
IM-EC	20%	17%	12%	11%
EC	4%	4%	4%	5%
Tracers				
Pb	0.12%	0.13%	0.15%	0.19%
H^+	0.02%	0.02%	0.02%	0.02%
$nssSO_4^{2-}$	1.34%	1.45%	1.68%	1.84%
NO_3^-	8.88%	7.67%	4.75%	3.87%
NH_4^+	1.62%	1.63%	1.65%	1.79%
$nssK^+$	0.72%	0.73%	0.79%	0.92%
Adelaide				
Majors	TSP	PM10	PM2.5	PM1
Mass	100%	100%	100%	100%
EOM	64%	66%	76%	80%
IM-EC	26%	23%	10%	5%
EC	10%	11%	15%	16%
Tracers				
Pb	0.88%	1.00%	1.12%	1.04%
H^+	0.02%	0.02%	0.03%	0.03%
$nssSO_4^{2-}$	0.55%	0.65%	1.00%	1.17%
NO_3^-	2.66%	2.87%	2.18%	1.71%
NH_4^+	0.53%	0.59%	0.80%	0.88%
$nssK^+$	0.21%	0.24%	0.35%	0.42%

7.3 Comparison of Measurements – ANSTO and CSIRO

Comparisons between data returned on the same days by the various AFP instruments deployed by ANSTO and CSIRO reveal differences beyond the estimated experimental uncertainties of the individual measurement systems. Clearly there are important implications for aerosol measurements across Australia, and difficulties inherent in comparing results from earlier studies, if differences exist between data returned by different instruments. In this section we explore the comparability of the data obtained by the various measurements systems. It is worth noting that the US EPA and Australian Standards suggest that co-location comparisons should be made with at least three samplers of each type side by side and more than 15 twenty four hour samples per site. In the context of this study these criteria were impossible to meet. Generally between 3 and 8 samples were obtained at the six sites from only one sampler of each type at each site. Also at some sites the particle mass loadings were so high that some samplers were operating outside their designed flow rate specifications with consequent effects expected upon mass loadings and PM2.5 and PM10 cut-points.

In Figures 20 and 21, data from the ANSTO PM10 and PM2.5 samplers are compared with data derived from the MOUDI. The agreement between the PM2.5 measurements is reasonable. The agreement between the PM10 data is less so, with the ANSTO unit often returning lower concentrations than the MOUDI. As mentioned earlier, this reflects a tendency for the filters used in the ANSTO PM10 sampler to block at high aerosol

concentrations, slowing the flow rate into the sampler and thus changing the collection characteristics of the unit. Side by side comparisons of PM2.5 data taken on the ANSTO stacked sampler and the ANSTO cyclone sampler over a 2 year period involving 200 filters has produced better correlations than those shown in Fig. 21. In these previous comparisons, the stacked filter to cyclone PM2.5 ratio was (0.89±0.19) for the mass and (0.95±0.12) for the sulfur concentrations.

Figures 22 and 23 compare the CSIRO PM2.5 TEOM data with PM2.5 data derived from the MOUDI and ANSTO samplers. Both the MOUDI and ANSTO instrument measured greater mass than the TEOM. This probably results from the loss of mass by the TEOM from volatilisation of semi-volatile material, as the inlet of the TEOM was heated to 50°C (Melbourne) or 35°C (subsequent cities). Figure 24 displays a comparison between the Solar-Vol PM2.5 sampler and the MOUDI. The agreement between these two instruments is good.

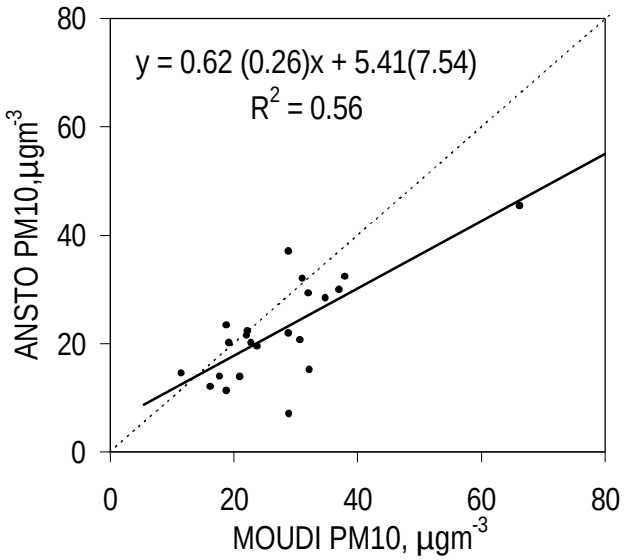

Figure 20. Relative performance of ANSTO PM10 sampler and the MOUDI. Numbers in parenthesis are the 95% confidence ranges.

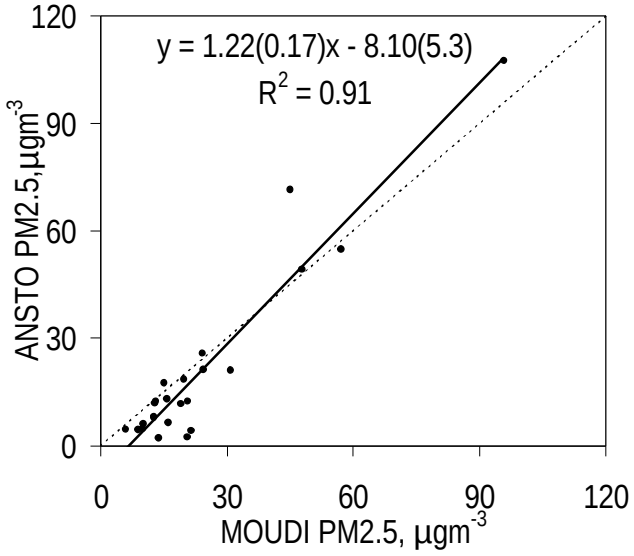

Figure 21. Relative performance of ANSTO PM2.5 sampler and the MOUDI. Numbers in parenthesis are the 95% confidence ranges.

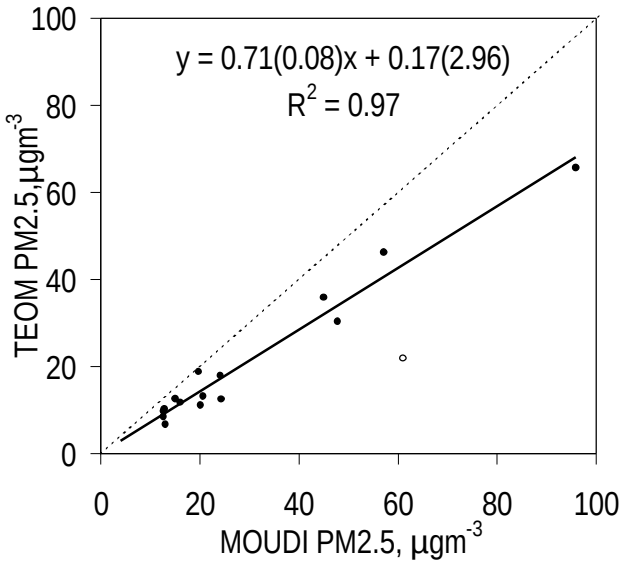

Figure 22. Relative performance of CSIRO PM2.5 TEOM and the MOUDI. Numbers in parenthesis are the 95% confidence ranges.

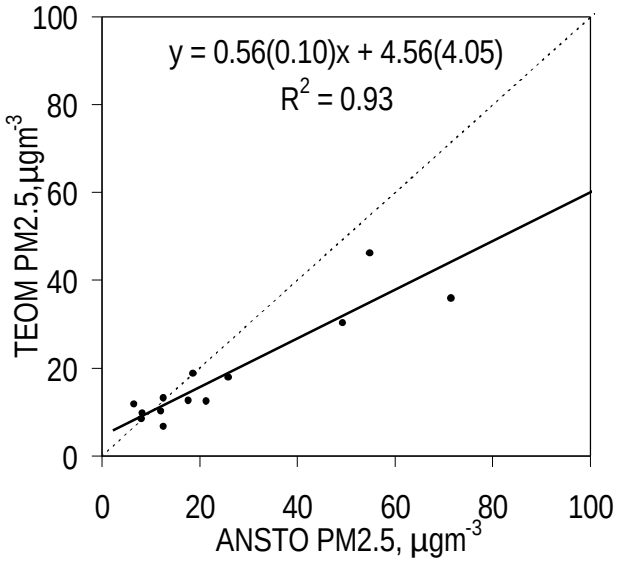

Figure 23. Relative performance of CSIRO PM2.5 TEOM and the ANSTO PM2.5 sampler. Numbers in parenthesis are the 95% confidence ranges.

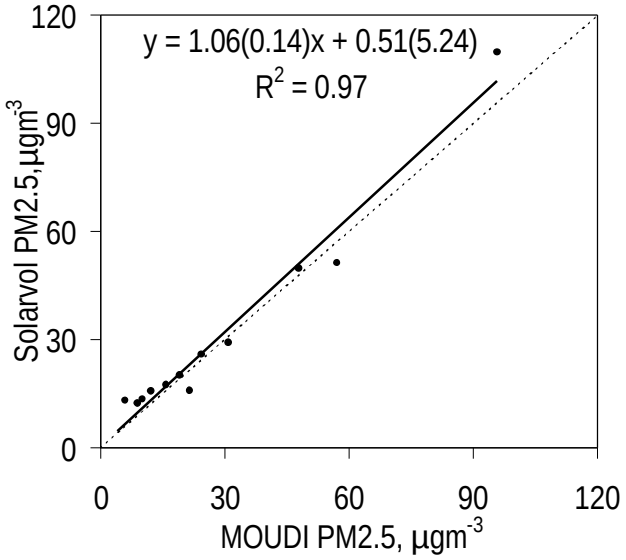

Figure 24. Relative performance of Solar-Vol PM2.5 sampler and the MOUDI. Numbers in parenthesis are the 95% confidence ranges.

The next comparison is made between the two continuously recording aerosol instruments, the nephelometer and the TEOM. Figure 25 shows an example of the relationship between b_{spd} and PM2.5 for hourly values. The relationships for each of the four cities in which both devices operated are summarised in Table 23. A linear relationship exists between the two parameters, with varying degrees of agreement at each site. It is notable that the Launceston and Canberra data in Table 23 clearly exhibit one slope, with the Melbourne and Adelaide data exhibiting another slope, a factor of 2 – 3 different. In later discussion it will be shown that these differences in scattering-mass relationship are caused primarily by systematic differences in aerosol size distribution caused by different dominant source types in Launceston/Canberra (smoke) and Melbourne/Adelaide (urban/automobiles).

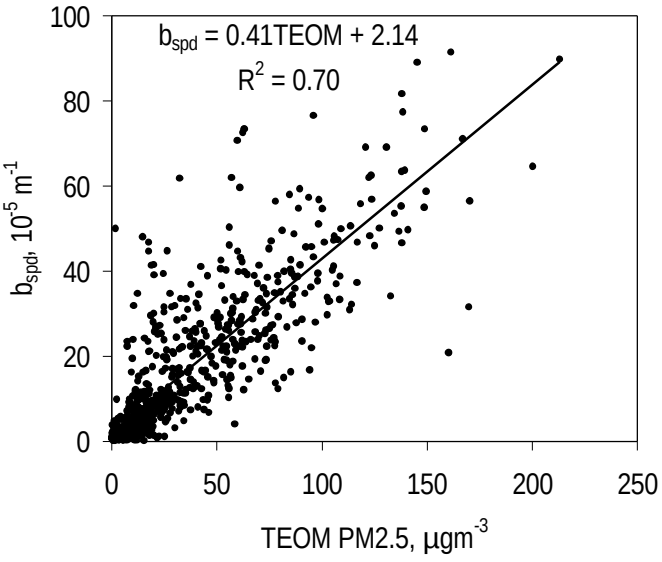

Figure 25. Relationship between bspd (measured by Nephelometer) and PM2.5 (measured by TEOM) for hourly values at Launceston.

Table 23. Summary of the relationship between b_{spd} (measured by Nephelometer) and PM2.5 (measured by TEOM) for hourly values at each site.

	slope	±95%	intercept	±95%	R^2
Melbourne	0.15	0.02	0.24	0.16	0.59
Canberra	0.40	0.04	1.5	1.3	0.55
Launceston	0.41	0.02	2.14	0.91	0.70
Adelaide	0.13	0.01	0.51	0.17	0.47

7.4 Comparison of Measurements – AFP and State/Territory Systems

In this section we compare data collected on the same days by the MOUDI and various instruments run by the relevant State/Territory regulatory authorities. It is important to note that some of the State/Territory data had not been fully quality controlled before provision to the AFP Study. Given time constraints the data have been used as supplied.

Figure 26 displays a comparison between mass concentration data measured by the State/Territory regulatory authorities and the MOUDI for the same sampling days. While agreement with the MOUDI appears to be good at high mass concentrations, there appears to be increasing fractional difference between the samplers at concentrations below 20 μgm^{-3}. Table 24 shows the mean % difference between the measurements compared in Figure 26. There is a wide variation in % difference across the table and in many cases the % difference is outside the combined experimental error that would be attributed to the individual measurement systems.

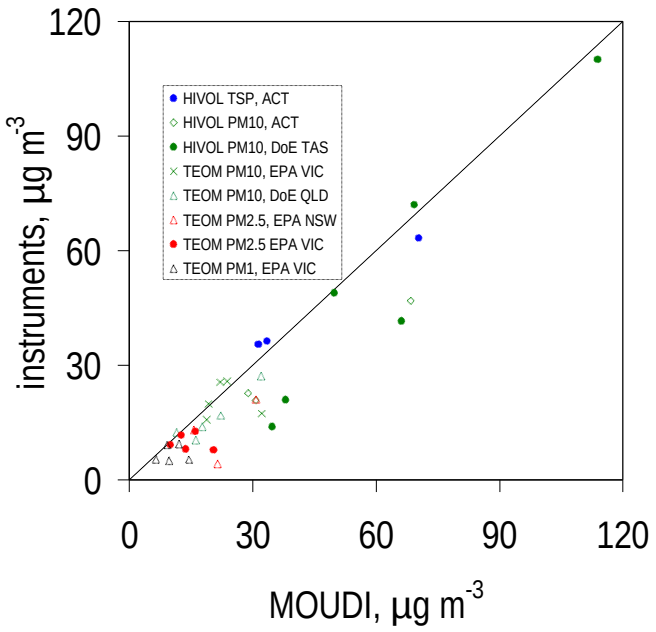

Figure 26. Relative performance of the State/Territory regulatory authority instruments compared to the MOUDI.

Table 24. Mean % difference between State/Territory regulatory authority instruments and the MOUDI for each city, based on differences between 24 hour mean data.

	TSP Hi-Vol	PM10 Hi-Vol	PM10 TEOM	PM2.5 TEOM	PM1 TEOM
Sydney				29% n=4	
Brisbane			21% n=5		
Melbourne			18% n=5	27% n=5	60% n=5
Canberra	10% n=3	28% n=3			
Launceston		14% n=6			
Adelaide					

7.5 Aerosol Concentration-Size Data - Integral Representation

Size-dependent aerosol concentration data were obtained with two high-resolution sizing instruments, a differential mobility analyser (DMA) and an active cavity laser size spectrometer (ASASP-X). Additionally, an integral measure was determined directly using an ultrafine particle counter (UCN counter). The two spectrometers span the particle diameter range from approximately 15 nm to 3 μm, with additional information on the concentration from 3 to 15 nm obtained from the ultrafine particle counter.

These differential systems provide a total of 88 particle size channels of data with redundancies (overlapping ranges) reducing this to around 65 channels. Data obtained from these spectrometers can also be presented in integral form as the number concentration of particles greater than a given diameter as in Figures 27 - 33. Values plotted are hourly averages of ASASP-X derived concentrations, which were determined each second hour.

In addition to particle number concentration Figures 27 - 33 include time series of hourly integrated mass concentration obtained from the CSIRO TEOM (PM2.5) and mass concentrations for diameter $D < 2.5$ μm calculated from the ASASP-X size distributions for an assumed dry particle density of 1.7 g cm^{-3} (all masses derived from the ASASP-X size distribution measurements that are discussed here, and elsewhere in the text, were obtained in this way, and are designated as M2.5, in recognition of the difference between actual physical particle diameter and aerodynamic diameter). In general the ASASP derived mass loadings are less noisy than the TEOM values and usually these two variables co-varied quite closely.

Several important features of the aerosol at the different locations can be readily discerned from the integral concentrations.

7.5.1 Total Particle Number Concentration (N for D > 3 nm)

Total particle numbers were typically in the range of 10,000 to 50,000 cm^{-3} with only minor city-to-city differences for all the study locations. Diurnal variation of about a factor of 5 in concentration is also evident in all locations. Peak concentrations usually occur around traffic peak times of 7 AM and 6 PM with greater concentrations during daytime than at night. Covariance of total particle number with mass concentrations (PM2.5) on a day-to-day or longer time scales (*e.g.* synoptic) is weak. A reasonably constant average total particle number concentration across a wide range of sites in different parts of the country had been observed

and explained almost two decades ago as a consequence of the non-linear physical processes regulating particle dynamics. Specifically, Ayers *et al*. [1981] measured the number flux of particles in the plumes downwind of a wide range of Australian cites and found a high correlation between particle flux and population, in other words a rather constant emission of particles per person irrespective of town size. Manton and Ayers [1982] carried out a simple modelling exercise to show that this is the behaviour expected from the processes of dispersion and coagulation in an evolving plume. The implication of these studies is that total particle number concentration and fine particle mass are regulated by different processes, so number-based and mass-based fine article properties should not be expected to be highly correlated.

7.5.2 Concentration of Particles D > 110, 140 & 306 nm.

Particles in this size range, part of the so-called accumulation mode, show a strong tendency to co-vary diurnally and have a significant superposed synoptic-scale variability. Particle number concentration in this size range also covaries reasonably closely with mass loading for D < 2.5 µm. For most of the study locations, concentrations of particles with D > 140 nm, for example, show 1 to 2 orders of magnitude variation over periods of a few days. Most concentrations for this lower size limit fall in the range of 100 -1000 cm^{-3} with prominent nocturnal peak concentrations to 10,000 cm^{-3} in both Canberra and Launceston.

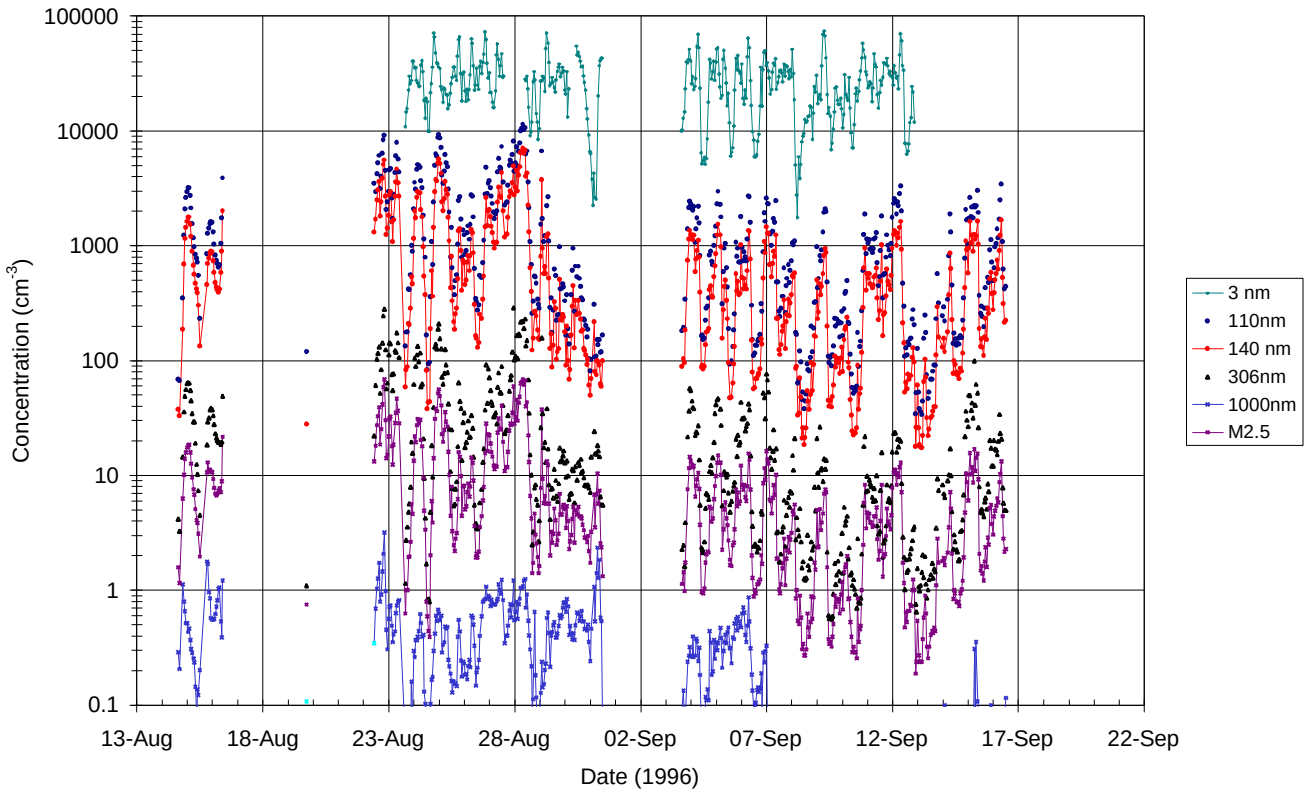

Figure 27. Sydney site, concentrations of particles with D > 3, 110, 140, 306 and 1000 nm, and calculated mass loading M2.5 (µg m^{-3}: for definition see text).

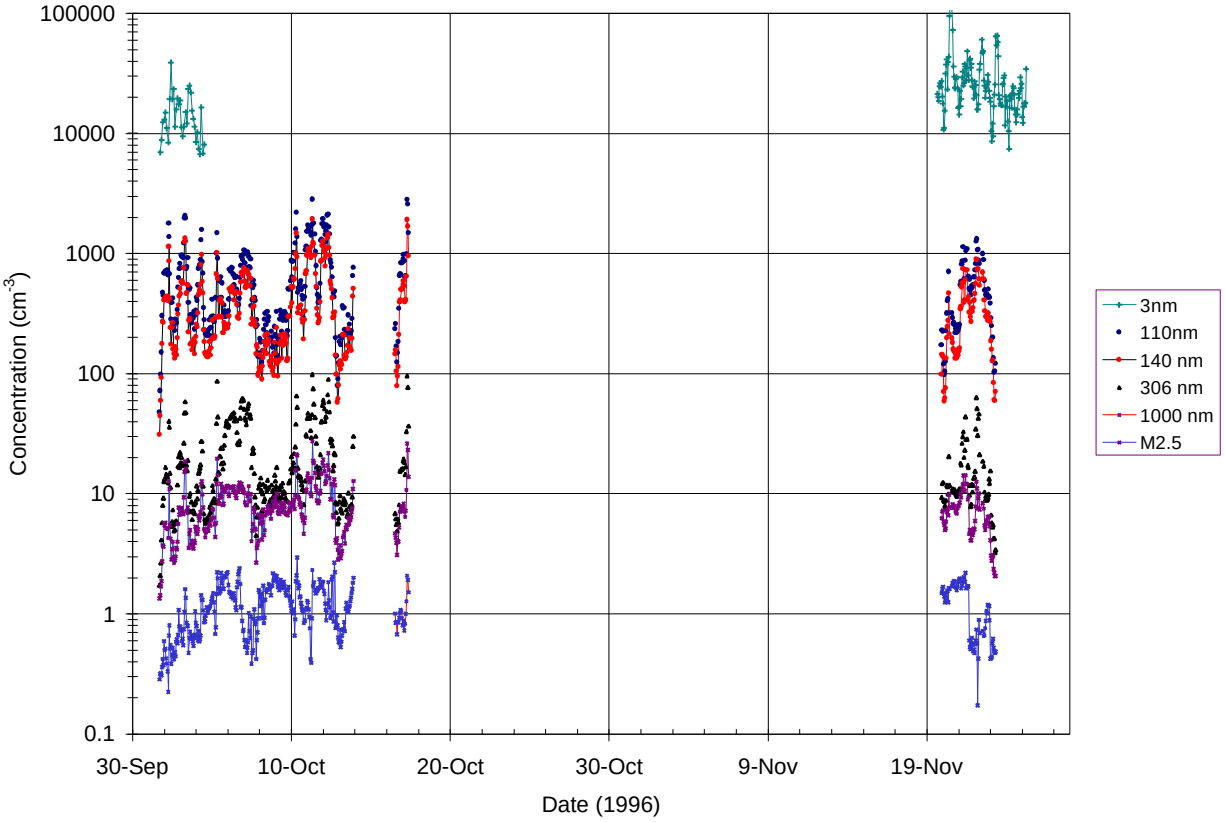

Figure 28. Brisbane site, concentrations of particles with D > 3, 110, 140, 306 and 1000 nm, and calculated mass loading M2.5 (µg m^{-3}: for definition see text).

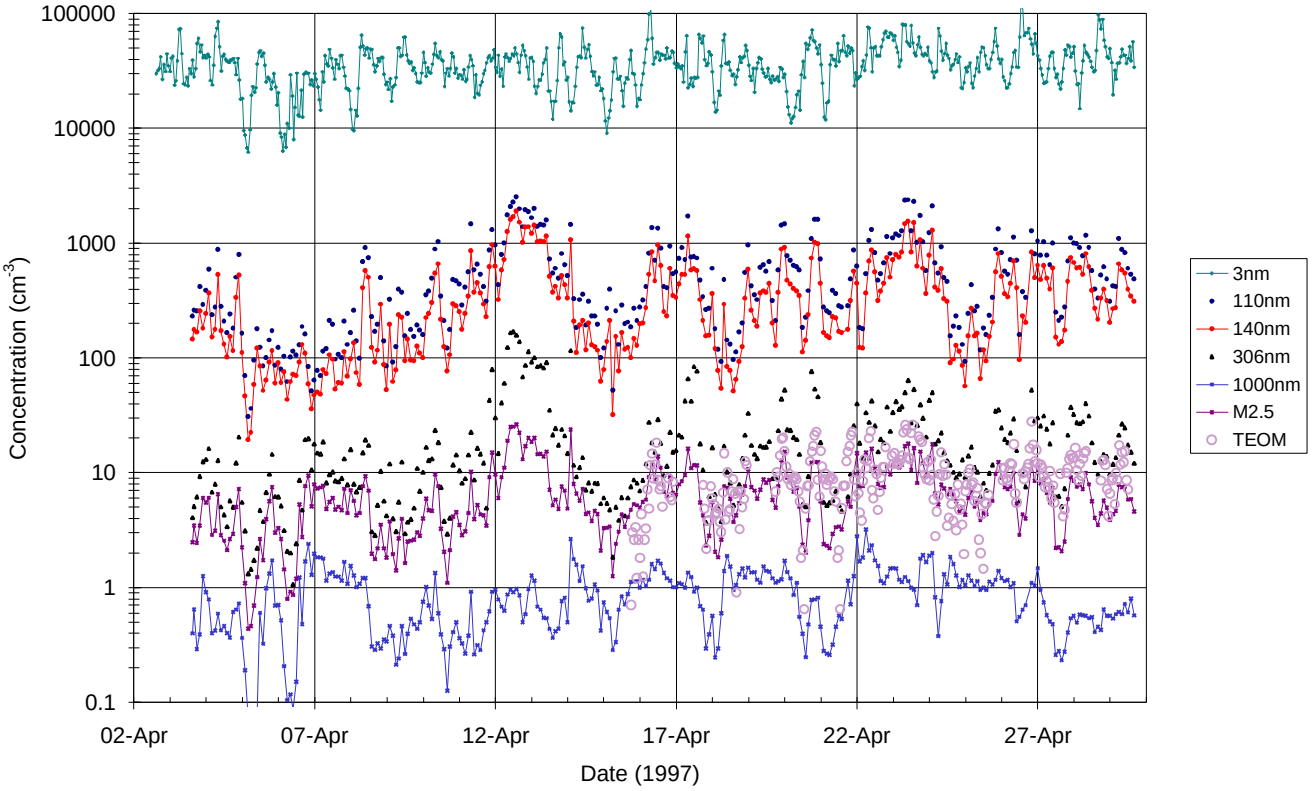

Figure 29. Melbourne site, concentrations of particles with D > 3, 110, 140, 306 and 1000 nm, and calculated mass loading M2.5 (µg m^{-3}: for definition see text). Also included, PM2.5 mass loading (µg m^{-3}) from the CSIRO TEOM.

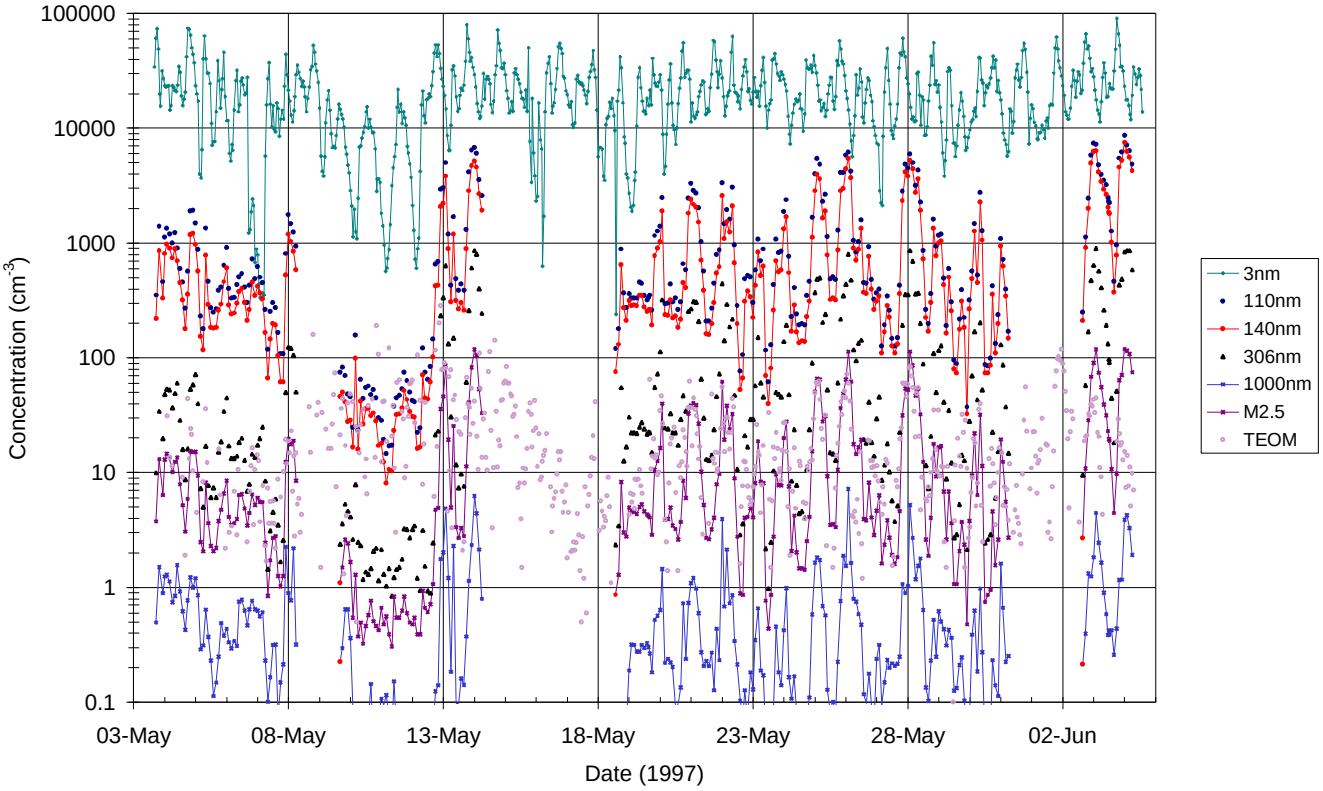

Figure 30. Canberra site, concentrations of particles with D > 3, 110, 140, 306 and 1000 nm, and calculated mass loading M2.5 (μg m^{-3}: for definition see text). Also included, PM2.5 mass loading (μg m^{-3}) from the CSIRO TEOM.

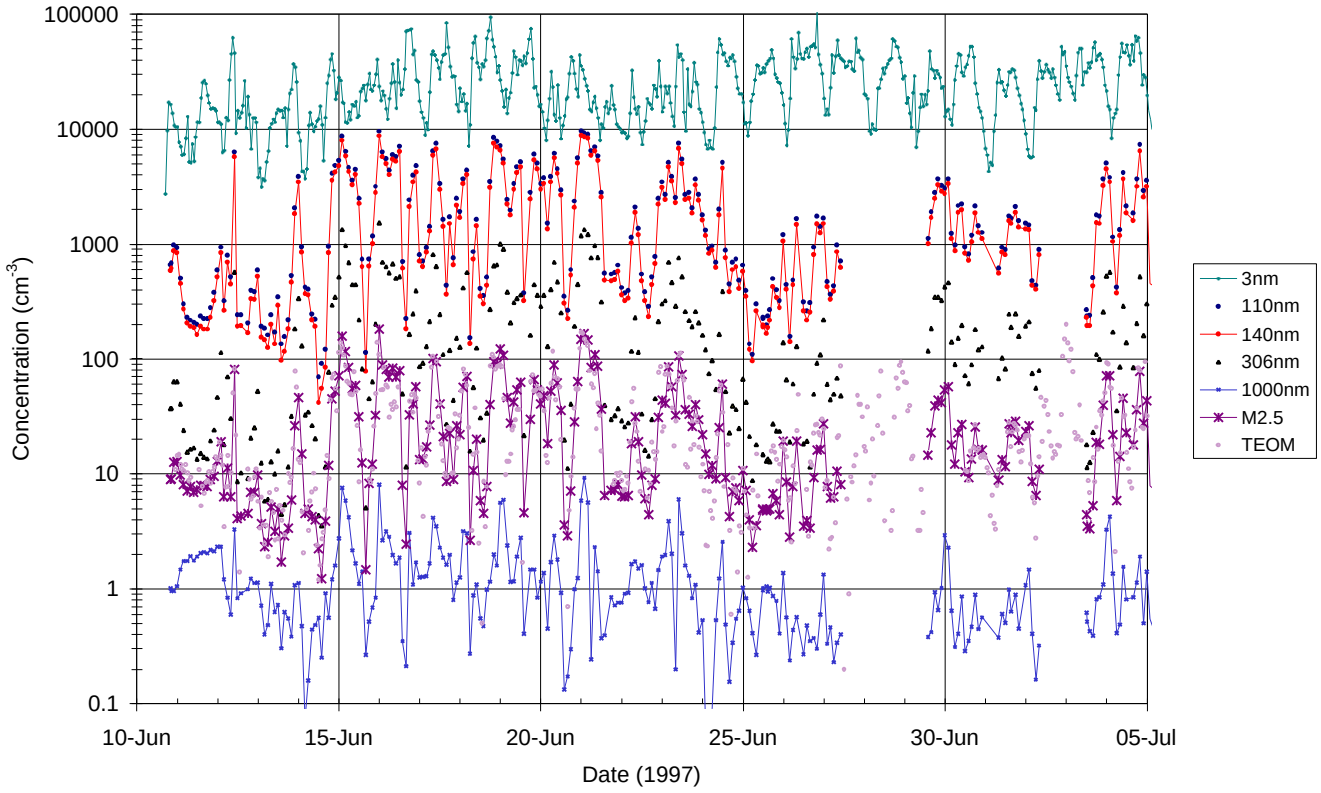

Figure 31. Launceston site, concentrations of particles with D > 3, 110, 140, 306 and 1000 nm, and calculated mass loading M2.5 (μg m^{-3}: for definition see text). Also included, PM2.5 mass loading (μg m^{-3}) from the CSIRO TEOM.

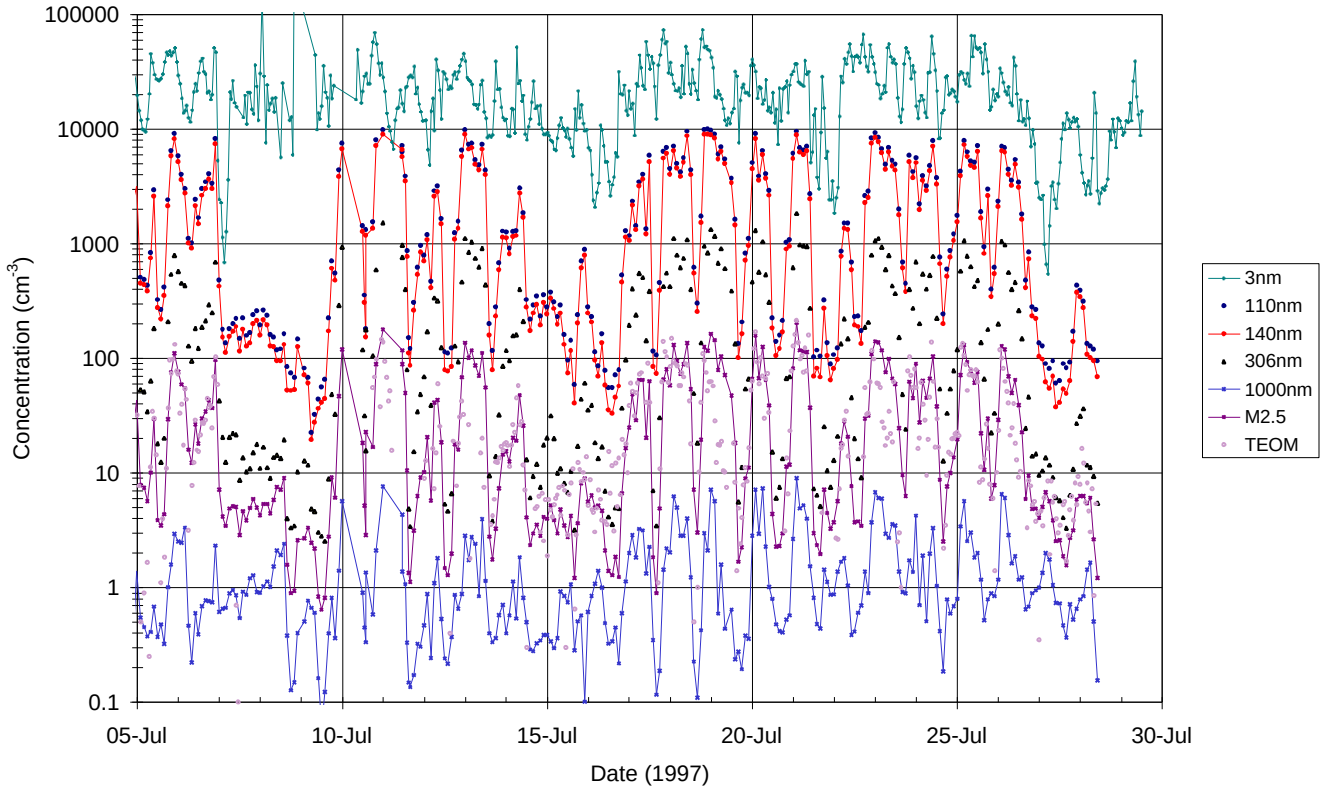

Figure 32. Launceston site, concentrations of particles with D > 3, 110, 140, 306 and 1000 nm, and calculated mass loading M2.5 (μg m^{-3}: for definition see text). Also included, PM2.5 mass loading (μg m^{-3}) from the CSIRO TEOM.

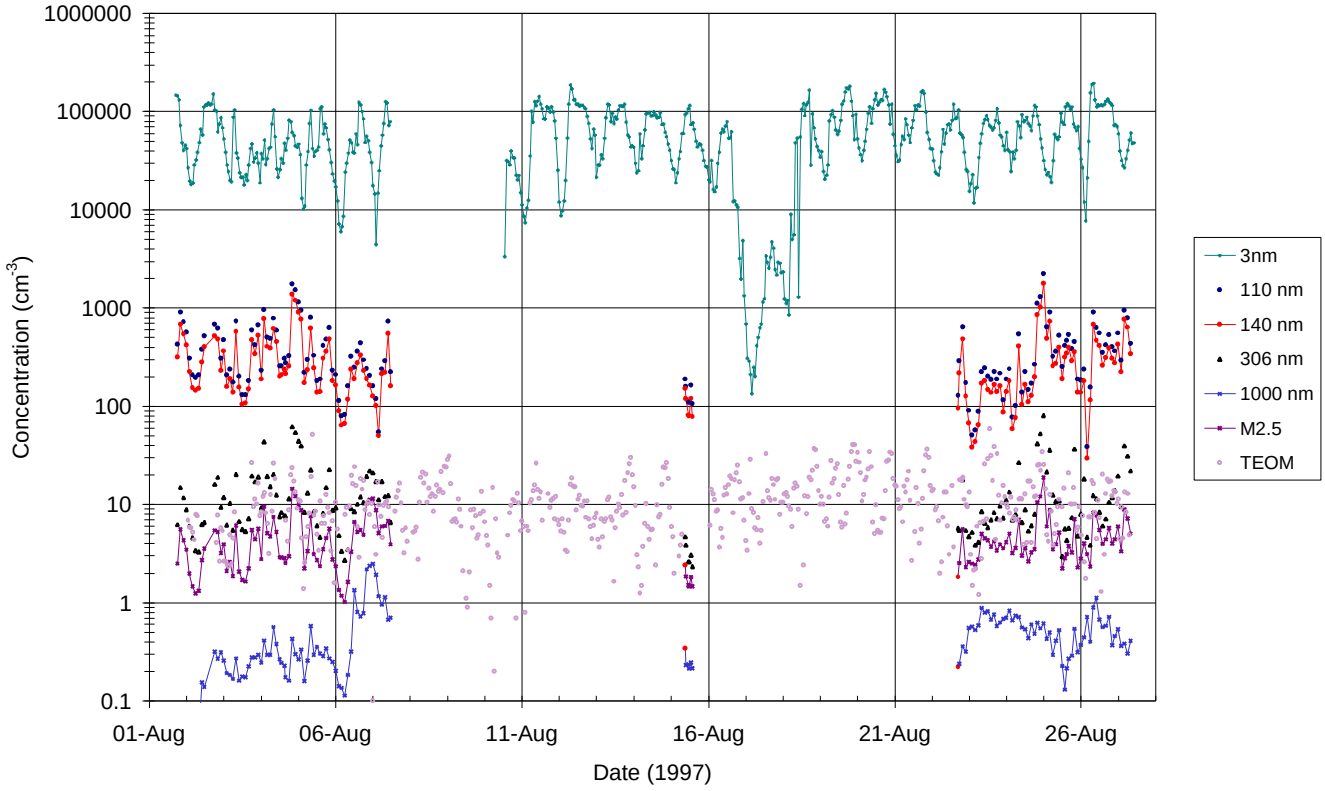

Figure 33. Adelaide site, concentrations of particles with D > 3, 110, 140, 306 and 1000 nm, and calculated mass loading M2.5 (μg m^{-3}: for definition see text). Also included, PM2.5 mass loading (μg m^{-3}) from the CSIRO TEOM.

7.5.3 "Ultrafine" Particle Concentration

Unfortunately there is no universal definition for ultrafine particles, although there is a relatively wide acceptance that ultrafine particles are less than around 100 nm diameter. In this context we can determine a good estimate of ultrafine particle concentration from the difference between concentrations of particles with D >3 nm and say D > 140 nm (green and red curves in Figures 27 - 33). One particularly important feature, shown clearly in the integral concentration plots, and evident at all the study locations, is that the number of these ultrafine particles essentially shows an inverse relationship with the previously discussed measures of the aerosol accumulation mode (*i.e*. number concentrations for D > 140 nm and PM2.5 mass loadings). Such lack of correlation is typical in aerosol systems where different sources and removal processes dominate different aerosol (size) modes.

7.5.4 Larger Particles e.g. D > 1 mm

The number of particles with diameter greater than 1 μm can be dominated by either the accumulation mode or the next larger coarse mode (usually a mechanically generated mode). This can be seen clearly in Figures 34 and 35. For Melbourne, at low scattering coefficient or mass loadings, particles with D > 1 μm are dominated by a mass mode with D_{mode} > 2 μm. In contrast, in Launceston, with high scattering coefficients and mass loadings, the number of particles in this size range is still largely controlled by the smaller mode (volume distribution mode around 300 nm D_{mode}). As a consequence the integral number concentration for D > 1 μm in Figures 27 - 33 sometimes co-varies with the accumulation mode concentrations, *i.e*. D > 140 nm and fine mass (PM2.5), but at times shows independent behaviour or even an inverse relationship. Overall whether these fractions co-vary or not is a function of the relative strengths of the coarse and accumulation size modes in different air masses.

7.6 Aerosol Concentration-Size Data - Differential Size Distributions

Examples of differential size distributions are given in Figures 34 and 35 for Melbourne and Launceston. Several thousand distributions were derived during the study and only selected samples are shown here. The two locations chosen represent fairly extreme conditions. In Melbourne scattering coefficients were quite low (typically < 50 Mm^{-1}, where 1 Mm^{-1} = 1 x 10^{-6} m^{-1}) and likely to be dominated by vehicle emissions whereas the Launceston data represent conditions where smoke aerosol dominates (similar conditions were observed in Canberra). Distribution selection was based on calculated scattering coefficient (at 530 nm); random selections of distributions were made in bands of scattering coefficient to show changes in size distribution (number and volume) with increasing particle loading. Distributions are coded by colour, corresponding to the particular scattering coefficient (in Mm^{-1}) in Figures 34 and 35.

Gross features of the size distributions at these two sites are similar. These include the mode structure - number modes with mode diameters less than 20 nm and around 200 nm, and a coarse mode at D > 2 μm. In Melbourne where particle loadings were significantly smaller than Launceston, the coarse mode is relatively stronger and more persistent. The coarse mode is also evident in the aerosol spectrometer data from Launceston but typically at reduced concentration. A more prominent mode, similar in magnitude to that observed in Melbourne is observed in some daytime distributions when scattering coefficients were low (usually less than about 30 Mm^{-1}).

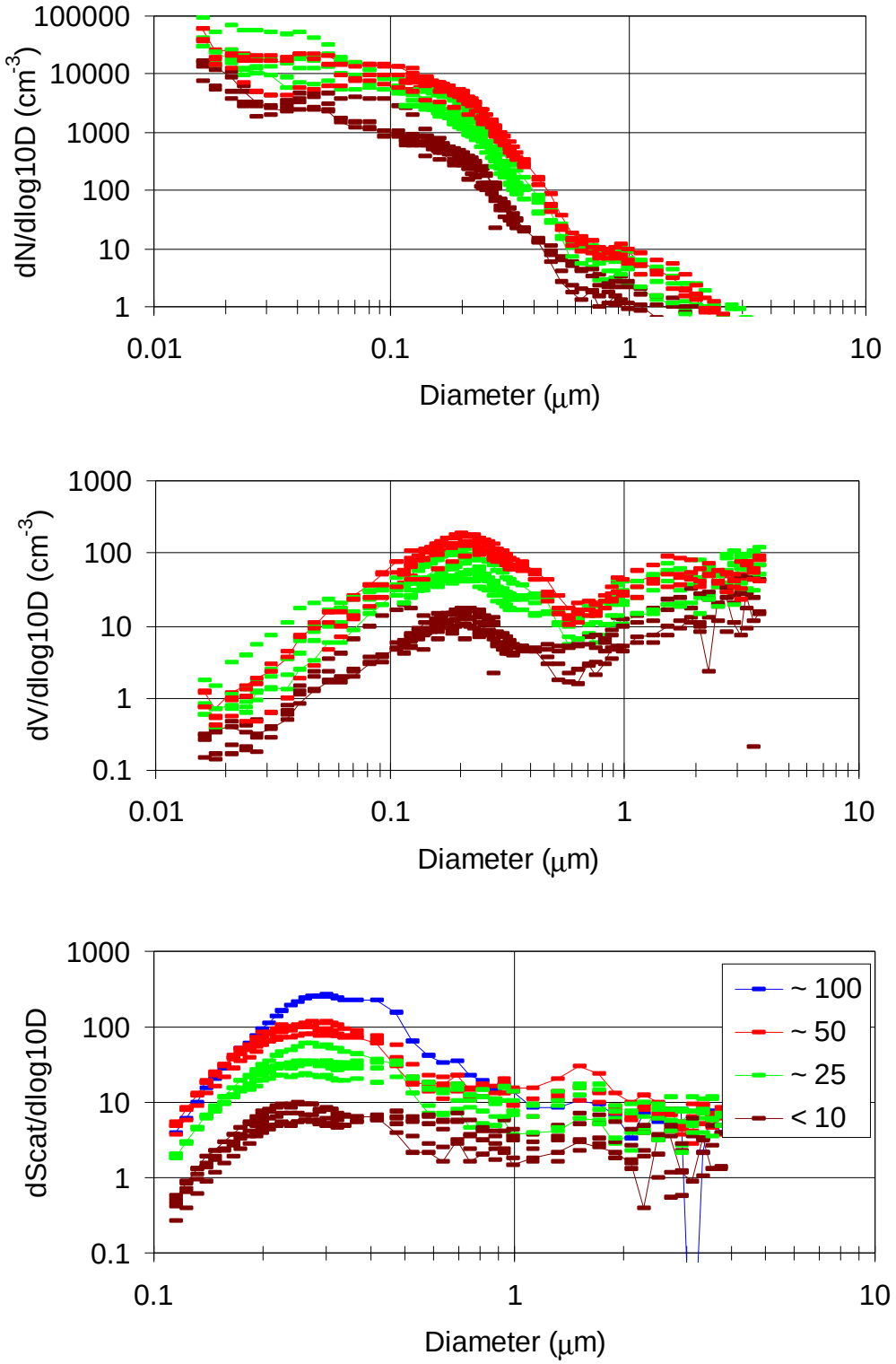

Figure 34. Number, volume and differential light scatter distributions for Melbourne. Distributions were selected by calculated scattering coefficient (Mm^{-1}; 1 Mm^{-1} = 1 x 10^{-6} m^{-1}) with the selected ranges indicated in the legend; a value of <10 represents clean air/good visibility; a value of ≥100 represents highly polluted air/poor visibility.

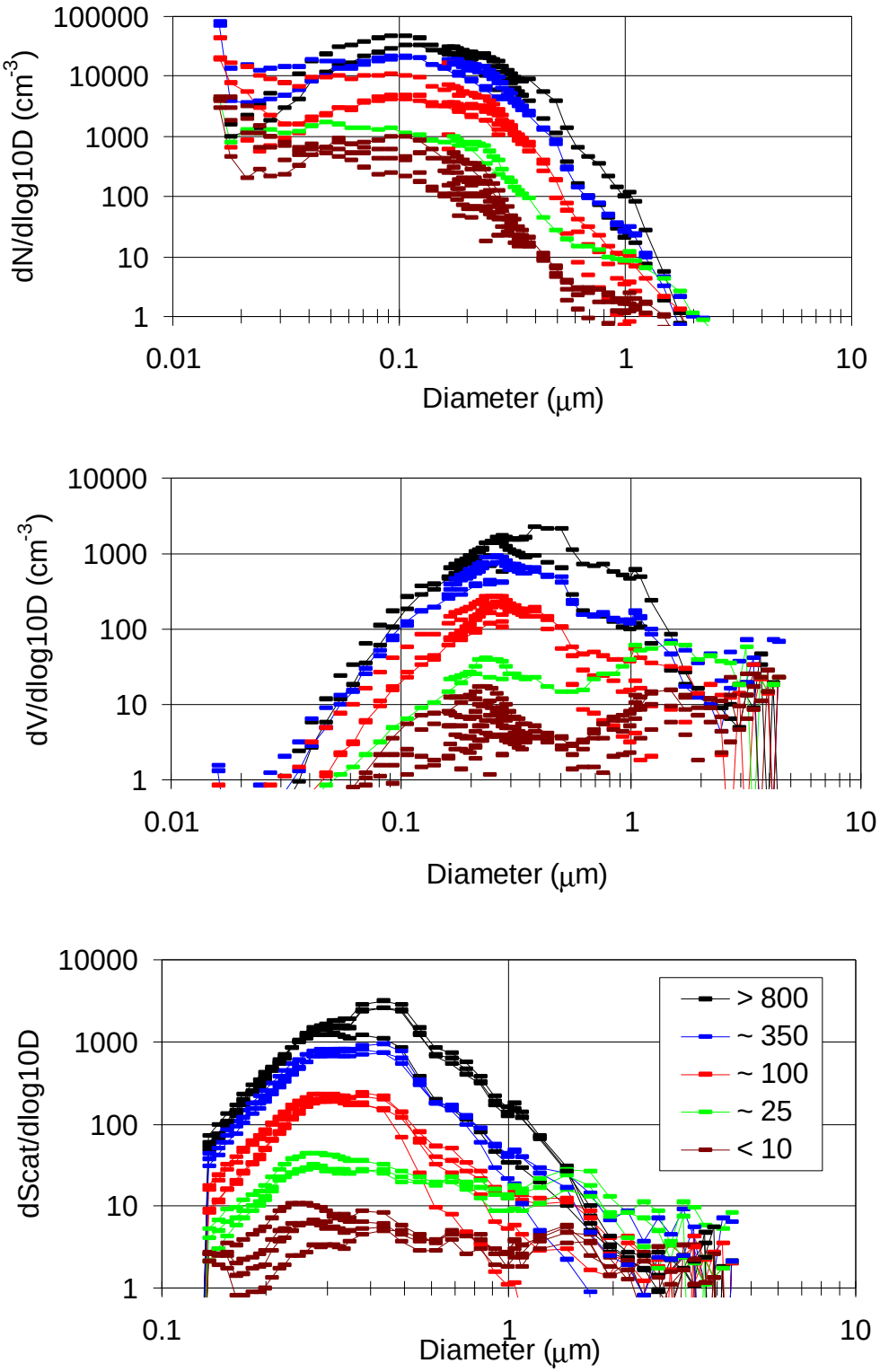

Figure 35. Number, volume and differential light scatter distributions for Launceston. Distributions were selected by calculated scattering coefficient (Mm^{-1}; 1 Mm^{-1} = 1 x 10^{-6} m^{-1}) with the selected ranges indicated in the legend; a value of <10 represents clean air/good visibility; a value of ≥800 represents significantly polluted air/poor visibility.

Differential distributions of the relative amount of light scattered per logarithmic size increment are also given, as a function of particle size, in Figures 34 and 35. Scattering efficiency distributions were determined for all size distributions using Mie theory for dielectric spheres, and utilising the same refractive index that was used to size particles in the ASASP-X size spectrometer. A wavelength of 530 nm was used for these calculations, the same wavelength that is employed to determine scattering coefficient in the nephelometers. This approach shows that in all the study locations light-scattering (and hence visibility reduction) is dominated by particles with diameter between around 100 - 500 nm with a peak sensitivity at around 300 - 400 nm diameter (for light of 530 nm wavelength). Two patterns were evident. At low mass and scattering levels there is frequently a non-negligible contribution out to large particle sizes, but for all cases of elevated scattering the peak centred around 300 nm diameter dominates. There is also a tendency for the modal diameter in the scattering distribution to increases with increase in particle loading.

8. Discussion

8.1 Nephelometer vs TEOM

Use of nephelometers to determine aerosol scattering coefficient at multiple sites in a number of Australian locales has a long history, going back as much as two decades. Although scattering coefficient as determined by a nephelometer is an integral property of the aerosol size distribution, the physics of the interaction between aerosol particles and visible radiation is weighted towards particles in the sub-micrometre size range, as shown in Figures 34 and 35 and discussed above.

The current discussion over choice of aerosol indicator variable for ambient air quality assessment has considered both PM10 and PM2.5, but rejected the latter partially at least on the basis that there is a paucity of Australian data available for PM2.5 [see discussion in NEPC, 1997]. It is relevant in this context to consider the possibility that the extensive historical records of b_{sp} might provide a surrogate historical record for PM2.5, because both integral measures tend to be dominated by the mode in the mass distribution at diameters below 1 µm (*e.g.* Figures 16 and 17).

The bivariate plot of hourly mean of b_{spd} (CSIRO nephelometer) vs PM2.5 (CSIRO TEOM) from Launceston shown in Figure 25 is typical of the clear structural relationships found between scattering coefficient and PM2.5 at each site where both measurements were made. The scatter in the relationship is decreased if 24 hour means are plotted (Figure 36).

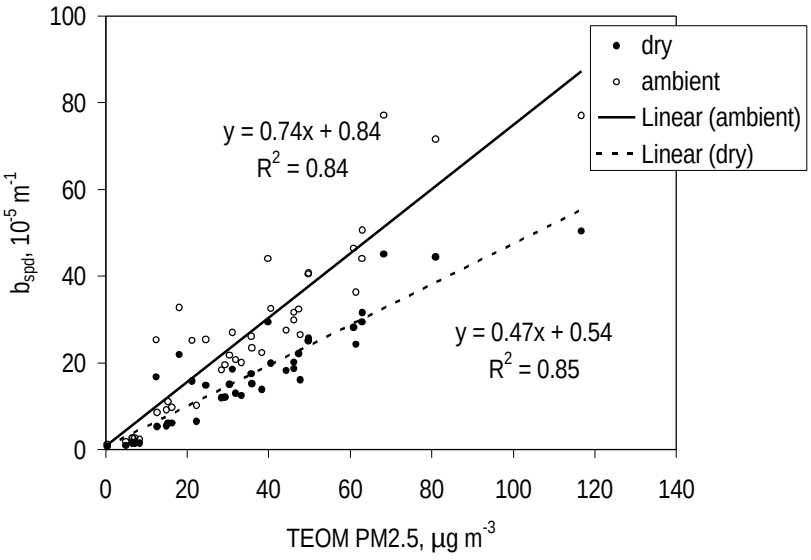

Figure 36. Relationship between b_{sp} (measured at ambient humidity) and b_{spd} (measured at <20% humidity) with PM2.5 (measured by TEOM) for 24 hour mean values from Launceston.

The clearly evident relationship confirms that in principal b_{spd} could act as a surrogate for PM2.5. However as shown by the regression data presented earlier in Table 23, the slope of the relationship can vary significantly from site to site, suggesting that site-specific aerosol properties determine the form of the relationship. Thus the value of the slope would need to be obtained for each specific site if b_{spd} were to be used in this way. This is discussed further in

section 8.3. There is also the possibility that at any site this relationship might vary with season (not investigated in the AFP study), so clearly caution would be required in any project aimed at harmonising the historical b_{sp} data records with new and ongoing PM2.5 records. Other complicating matters are the clear dependence of nephelometer output on humidity, and the implication from the TEOM results discussed in the section below, that humidity reduction by heating, also often used for nephelometers, may not be appropriate.

8. 2 TEOM vs Other Instruments

The increasing use of the TEOM as a convenient method of choice for monitoring aerosol mass loading in real-time (PM10, PM2.5 or PM1 using appropriate size-selective inlets) assumes implicitly that the TEOM is an appropriately accurate and precise aerosol measurement device. The fact that the TEOM has achieved US EPA "Equivalent method" status for PM10 measurement [Chow, 1995], and has been demonstrated to meet German regulatory performance requirements for TSP [RWTÜV, 1994], implies that the TEOM has performed well under a range of specified test conditions. However in the AFP study the CSIRO TEOM measured systematically lower 24 hour mean PM2.5 mass concentrations than either the MOUDI (Figure 22) or the ANSTO PM2.5 sampler (Figure 23) or the Solar-Vol. In the comparison with the MOUDI, the difference averaged 29% (based on the regression slope in Figure 22).

The performance of the CSIRO TEOM was checked against the performance of the co-located EPA TEOM at the Footscray site in Melbourne, as shown in Figure 37. The comparison, based on hourly mean data suggests that the CSIRO TEOM was not malfunctioning in a gross way – average deviation was only 8%. In view of the much larger 29% average difference between the CSIRO TEOM and the MOUDI, there appears to be the possibility of a systematic performance difference between measurements made by the TEOM method, and the traditional, time-integrated, filter-based gravimetric methods.

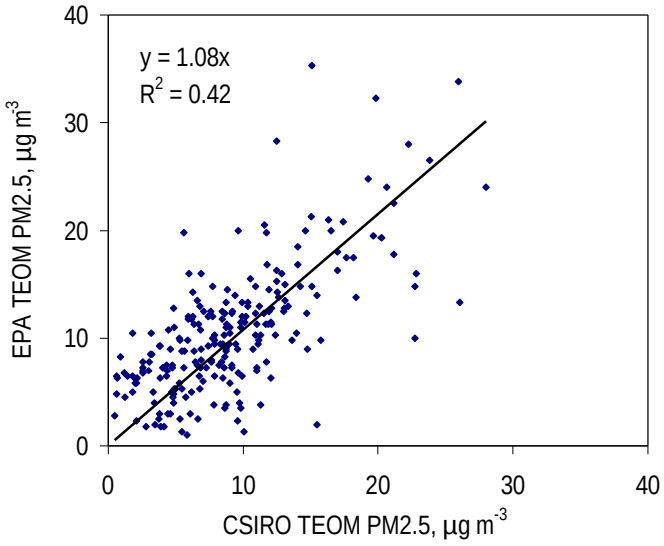

Figure 37. Relationship between hourly data determined in parallel by the CSIRO and Victorian EPA TEOMs operated at Footscray, Melbourne.

Recourse to the scientific literature confirms that systematically low TEOM response in comparison with the time-integrated manual aerosol mass determinations has been observed elsewhere, and has been traced to the use of heating in the TEOM, whereas the manual reference method based on high volume aerosol sampling (or low-volume equivalent methods such as the MOUDI and ANSTO samplers) collects aerosol at close to ambient temperature.

The heated sampling system on the TEOM serves the dual purposes of avoiding changes in the microbalance response due to temperature fluctuations, while at the same time volatilising water from the aerosols being sampled. However under certain conditions it has also been shown to volatilise semi-volatile material from the aerosol, leading to a systematically lower response, as found here in the AFP Study.

Three examples from the literature are the work Meyer *et al.* [1992], Meyer and Rupprecht [1996] and Allen *et al.* [1997]. Meyer *et al.* [1992] compared the responses of two PM10 measurement systems co-located at a Californian mountain site in winter, when domestic heating by wood burning causes wood smoke to dominate the PM10 aerosol. Wood burning is known to produce smoke containing significant quantities of semi-volatile organic material.

The systems deployed were a pair of TEOM model RP1400 instruments, and a Sierra Anderson model 1200 high volume aerosol sampler (an approved US EPA reference method for PM10). One TEOM was operated at 50^{o}C, the other heated to 30^{o}C, while the high volume sampler operated at ambient temperature (range ~ -5 to 7^{o}C). PM10 loading ranged from ~30 – 130 $\mu g\ m^{-3}$, with six 24 hour average values measured.

Meyer *et al.* [1992] report regressions between the three sampling devices as follows, with $PM10_{50}$ depicting the TEOM at 50^{o}C, $PM10_{30}$ depicting the TEOM at 30^{o}C, and $PM10_{SSI}$ depicting the Anderson Hivol:

$$PM10_{50} = 0.55\ PM10_{SSI} + 1.5;\ \text{with}\ R^2 = 0.98$$

$$PM10_{30} = 0.66\ PM10_{SSI} + 7.2;\ \text{with}\ R^2 = 0.99$$

$$PM10_{30} = 1.29\ PM10_{50} + 2.3;\ \text{with}\ R^2 = 0.95.$$

Meyer *et al.* [1992] concluded that these results "strongly suggest" that partial volatilisation of semi-volatile aerosol components was caused by the heated sampling system employed on the TEOMs, and that the extent of volatilisation increased with temperature employed.

Similar results were achieved in a study by Meyer and Rupprecht [1997], in which two TEOMs run at different temperatures and filter face velocities were compared. A factor of two difference in PM10 mass concentration was found between a TEOM operated at 50^{o}C (and 41 cms^{-1} flow rate) and a TEOM operated at 30^{o}C and 14 cms^{-1}, prompting the authors to call for standardisation in any TEOM PM10 reference method.

Considerably more comprehensive results consistent with this conclusion were reported by Allen *et al.* [1997] who compared 24 hour TEOM data with manual methods, both PM10 and PM2.5, at 10 urban sites across the US and Mexico, in both winter and summer seasons, with 24 – 74 data points per season. On the basis of this considerable dataset the authors state that in "urban areas, a substantial fraction of ambient PM can be semi-volatile material. A larger fraction of this component of PM10 may be lost from the TEOM-heated filter than the Federal Reference Method" (the manual method). Allen *et al.* [1997] indicate that the semi-volatile material may be organic in nature or inorganic, in the form of ammonium nitrate, depending on site and season. They also suggest that the semi-volatile fraction of PM2.5 is larger than that in PM10, so that fractional differences between the TEOM and manual methods may be larger for PM2.5 than for PM10.

In the AFP study the data generated by the CSIRO PM2.5 TEOM and the PM2.5 MOUDI, displayed in Figure 22 above, showed a mean TEOM/MOUDI ratio (from the regression slope) of 0.71. Allen *et al.* [1997] reported mean TEOM/Manual method ratios from four sets of PM2.5 data and one set of PM2.1 data in addition to ratios for their PM10 sites. Their PM2.5 and PM2.1 ratios to PM10 were 0.64, 0.78, 0.84, 0.89 and 0.84. Clearly the mean AFP Study PM2.5 ratio generated here using the CSIRO TEOM, at 0.71, sits very well with the US results.

We conclude that volatilisation of semi-volatile aerosol components in the heated sampling system of the CSIRO PM2.5 TEOM probably caused the average of ~29% lower TEOM values in comparison with the co-located MOUDI PM2.5 measurement. Even if the CSIRO TEOM were systematically in error (low) in calibration by the 8% mean difference between it and the Victorian EPA TEOM at Footscray (Figure 37), there would still remain a ~20% underestimation in comparison with the MOUDI[8].

Additional data illuminating the above discussion come from a comparison of the MOUDI data with data from the co-located TEOMs operated independently by the Victorian, NSW and Queensland agencies. Figure 38 presents the sets of 24 hour average data produced, with the MOUDI PM10, PM2.5 and PM1 data compared with the relevant EPA TEOM data (a separate TEOM was used for each PM measurement). It is evident from the Figure that the Victorian EPA PM2.5 and PM1 TEOMs on average underestimate the MOUDI results, at about the level found from the CSIRO TEOM-MOUDI comparison. The three data points from the NSW EPA PM2.5 TEOM also show substantially lower values than the MOUDI, consistent with the CSIRO and Victorian EPA PM2.5 and PM1 data. These comparisons support the conclusion that loss of semi-volatile material in the heated TEOM may be widespread for the PM2.5 and PM1 fractions, as reported by Allen *et al*. [1997]. On the other hand the comparison between the MOUDI and the Victorian EPA PM10 TEOM does not show such a consistent disparity. Allen *et al*. [1997] suggest that a smaller difference between the TEOM and gravimetric data for PM10 may reflect the increased contribution of non-volatile aerosol material (*e.g*. sea salt and soil dust) and in the larger size fraction. A similar explanation may underlie the results for the Queensland TEOM results, since as shown in Table 22 the Brisbane aerosol had by far the lowest estimated organic matter (*i.e*. potentially semi-volatile) fraction and by far the highest inorganic (*i.e*. involatile) fraction.

We conclude that caution should be exercised by any Australian jurisdiction moving from manual to TEOM-based aerosol mass measurements. A comprehensive comparison between co-located samplers of each type should be carried out at each site, over at least one full annual cycle, so that systematic differences in measured results are defined quantitatively as a function of season. It would also be prudent at locations where the TEOM reads significantly low to determine the nature of the semi-volatile component involved. Otherwise there will be the risk that any apparent improvements in PM air quality might reflect nothing more than a change in measurement method, and/or secular change in the mix of aerosol volatile and non-volatile aerosol components.

[8] Note that the CSIRO TEOM had been calibrated and found to be within 1% of manufacturer specifications.

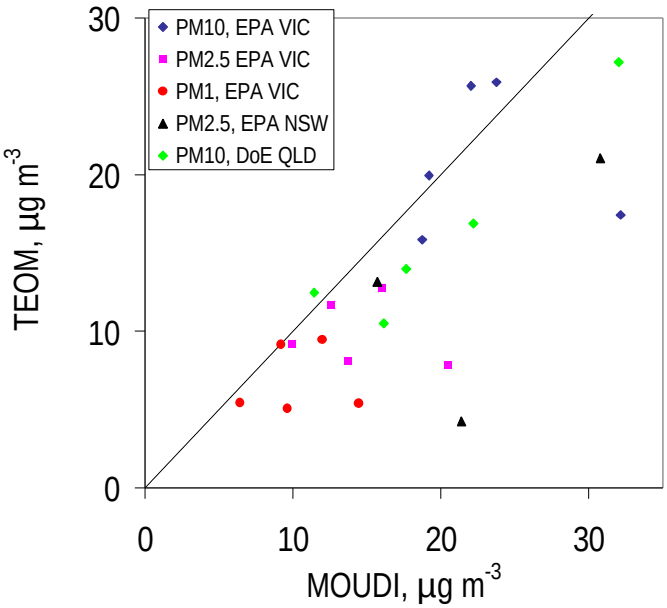

Figure 38. Relationship between 24 h average values of PM10, PM2.5 and PM1 determined by TEOMs run by relevant Victorian, NSW and Queensland agencies, and the equivalent data from the co-located MOUDI.

8.3 Scattering Efficiency – Use of Nephelometers for Mass Estimation

Mass scattering efficiency is the ratio of scattering coefficient to mass in a given size range and is an important climatological parameter. The reciprocal of the scattering efficiency is also frequently used as an empirical factor for converting scattering coefficient to mass loading, as a surrogate for gravimetric mass determination. Values of mass loading (or the empirical conversion factor), determined from the CSIRO nephelometer (dry) and CSIRO TEOM (PM2.5) were found in this study to have a significant location-dependent variation as well as showing considerable scatter at a given location (see Table 23 and Fig. 25).

To investigate the extent to which the theoretical relationships between aerosol size distribution, light extinction and aerosol mass are able to be measured in practice, the high-resolution aerosol size-distributions were employed to calculate both dry scattering coefficient at 530 nm and particle mass (assuming a dry density of 1.7 g cm^{-3}) for each ASASP-X size distribution. A comparison between the aerosol scattering coefficient calculated from the size distribution, and that observed directly with the nephelometer, is presented in Figure 39. A complementary plot in Figure 40 compares calculated aerosol PM2.5 mass with measured mass from the CSIRO PM2.5 TEOM. Both the ASASP-X and TEOM are heated to dry the aerosol, so only minor systematic difference due to heating is expected, and none was evident. The figures illustrate results from Launceston, however the excellent agreement shown was typical for all sites.

Hourly values of calculated mass scattering efficiency for all locations are given in Figures 41 - 46. Calculated mass scattering efficiency varied with air mass change, and also varied on a daily cycle due to diurnal patterns in sources and atmospheric mixing.

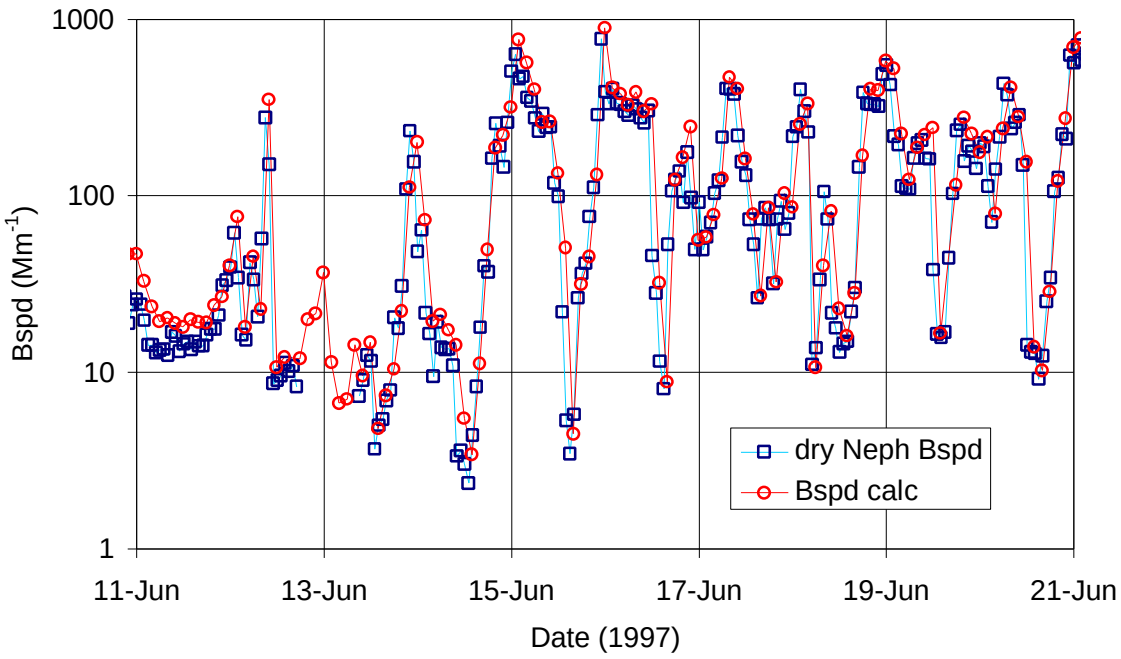

Figure 39. Comparison of calculated and observed aerosol scattering coefficient, Launceston.

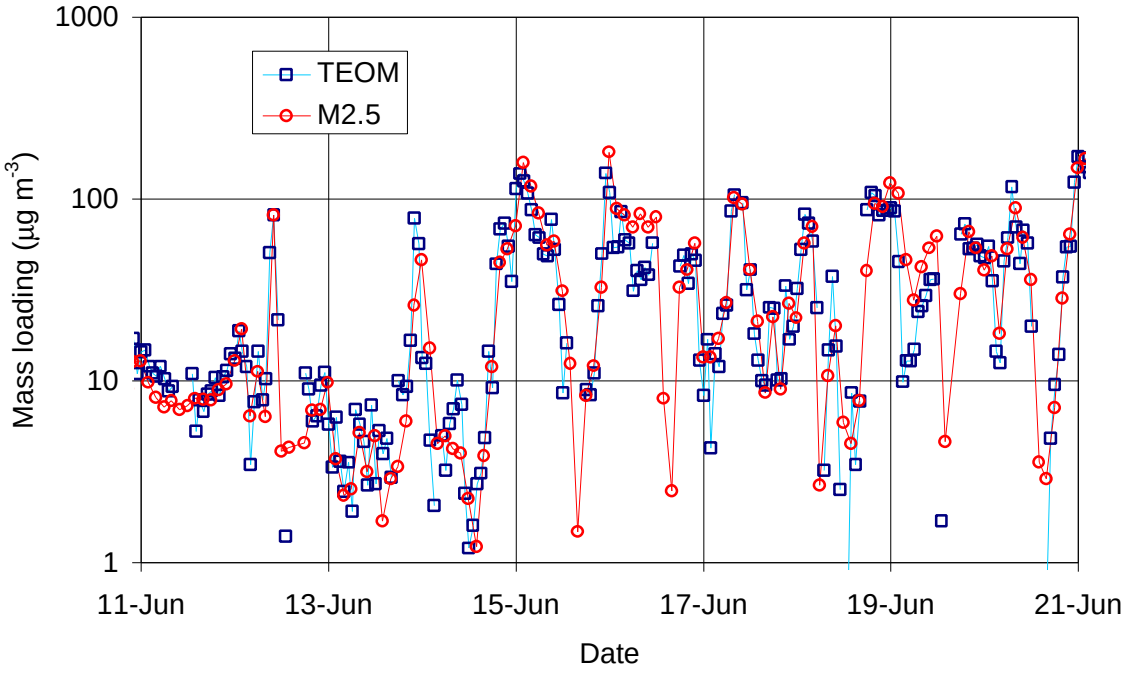

Figure 40. Comparison of calculated and observed M2.5 loading (for definition see text), Launceston.

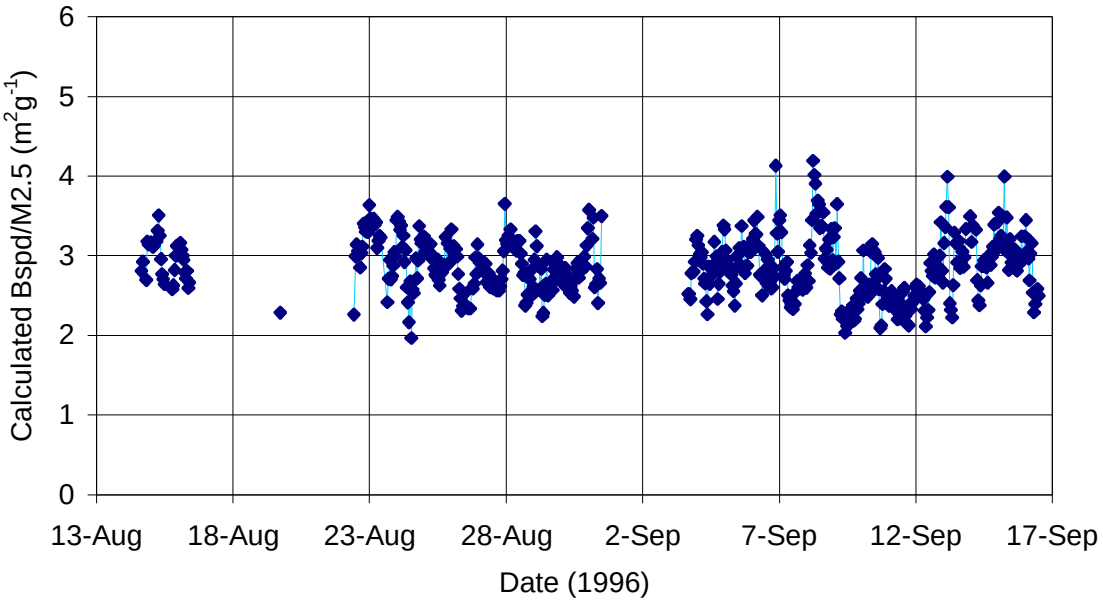

Figure 41. Mass scattering efficiency calculated using ASASP-X size distributions for the Sydney site (for λ=530 nm, ρ=1.7 µg cm^{-3}).

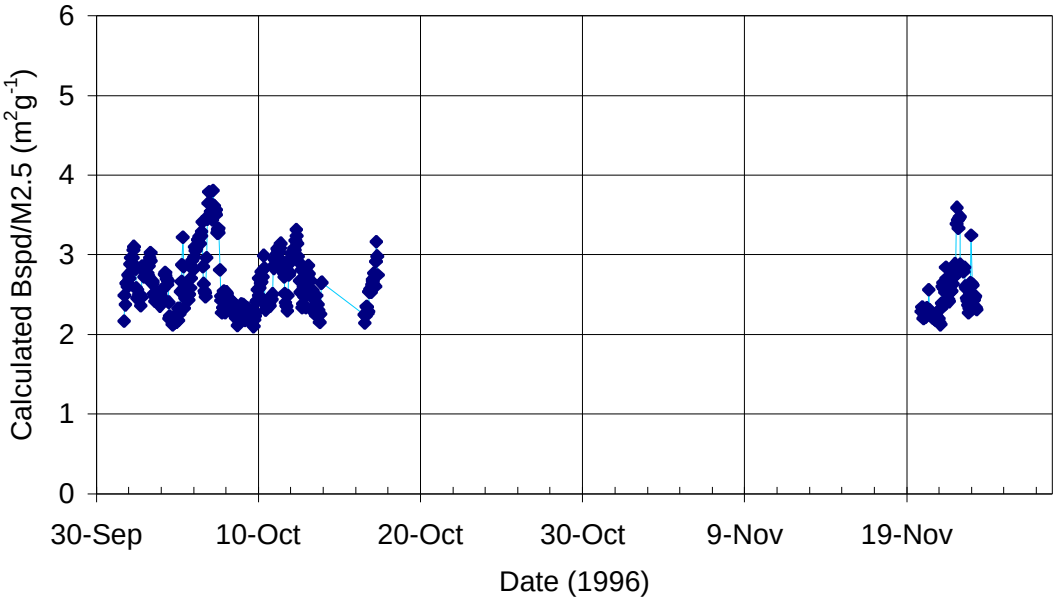

Figure 42. Mass scattering efficiency calculated using ASASP-X size distributions for the Brisbane site (for λ=530 nm, ρ=1.7 µg cm^{-3}).

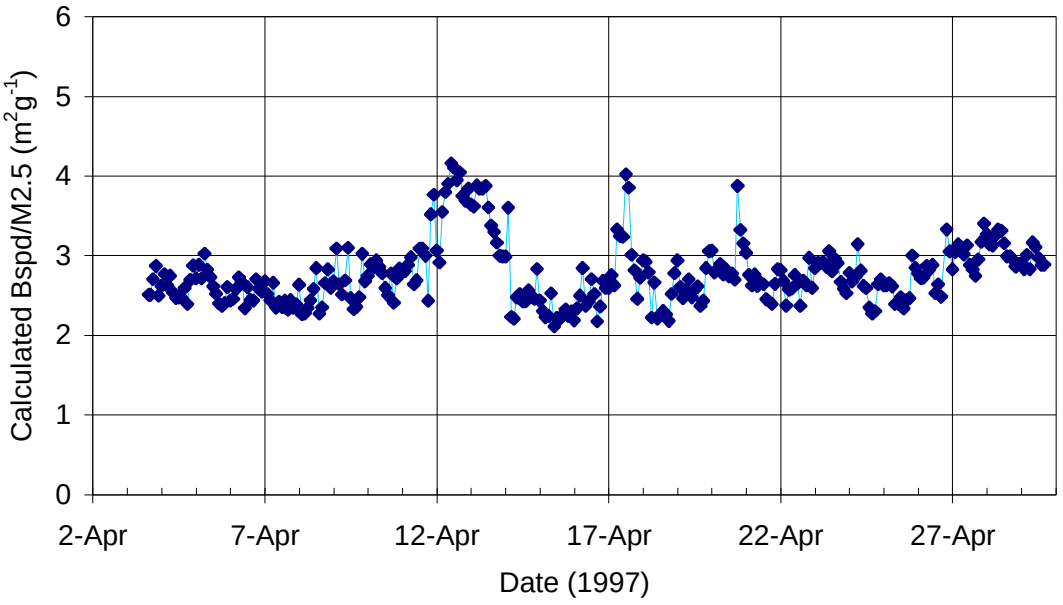

Figure 43. Mass scattering efficiency calculated using ASASP-X size distributions for the Melbourne site (for λ=530 nm, ρ=1.7 µg cm^{-3}).

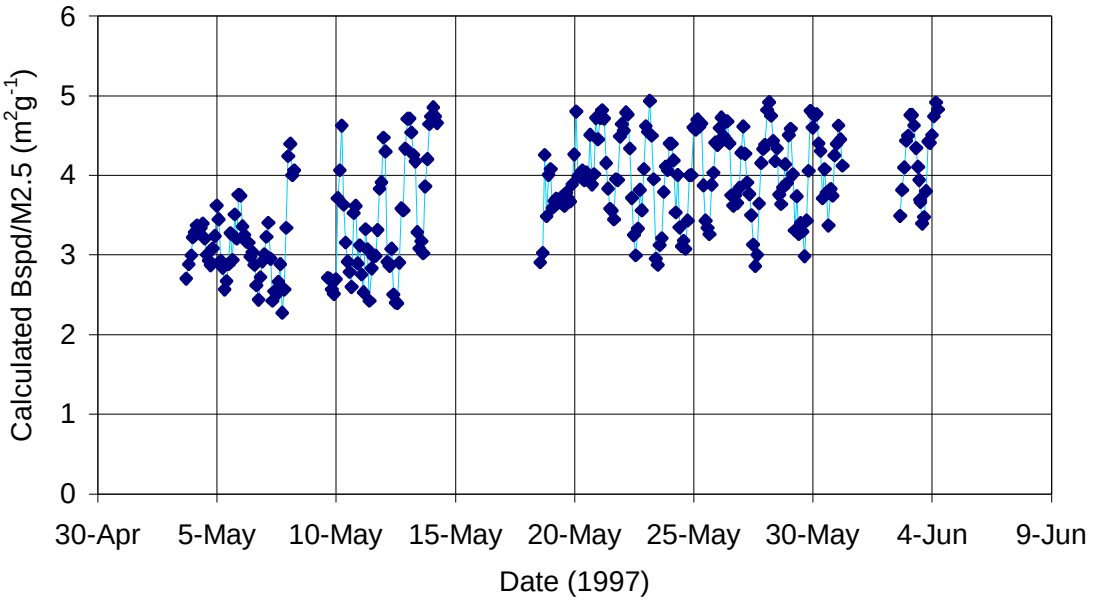

Figure 44. Mass scattering efficiency calculated using ASASP-X size distributions for the Canberra site (for λ=530 nm, ρ=1.7 µg cm^{-3}).

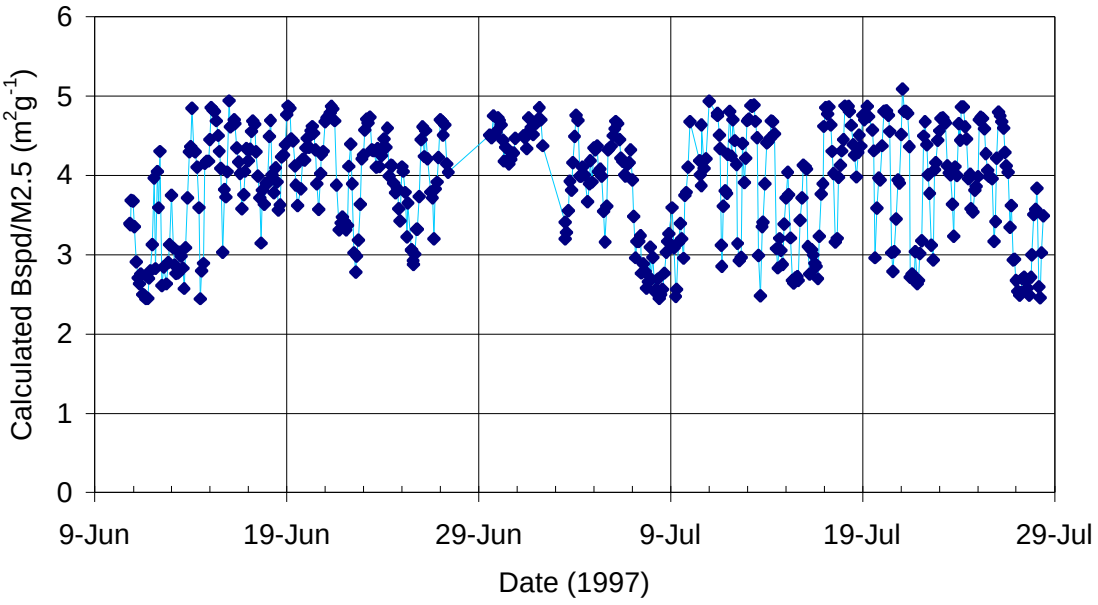

Figure 45. Mass scattering efficiency calculated using ASASP-X size distributions for the Launceston site (for λ=530 nm, ρ=1.7 µg cm^{-3}).

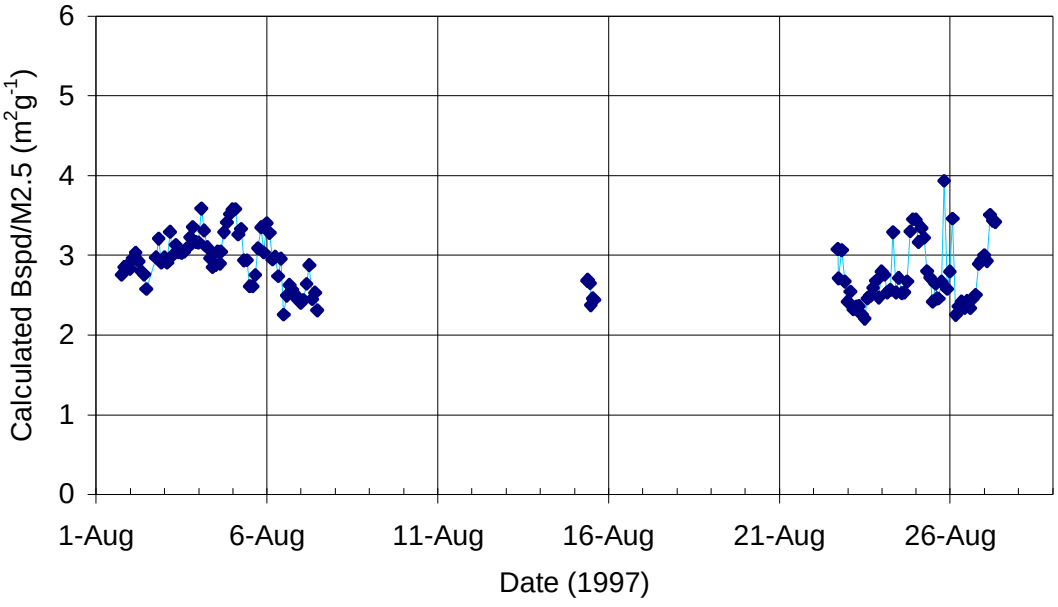

Figure 46. Mass scattering efficiency calculated using ASASP-X size distributions for the Adelaide site (for λ=530 nm, ρ=1.7 µg cm^{-3}).

For locations where large nocturnal loadings of smoke were observed, in particular Canberra and Launceston, corresponding mass scattering efficiencies based on particle size approach a value of 5 $m^2 g^{-1}$ during the night. The values reduce to around 2.5 to 3 $m^2 g^{-1}$ during the day when particle loadings reduce with day-time decrease in the smoke source and increased ventilation due to the daytime increase in vertical mixing.

For locations more dominated by vehicle sources, *e.g*. the Adelaide and Melbourne sites, calculated mass scattering efficiencies are typically around 2.5 to 3.5 $m^2 g^{-1}$. The difference in mass scattering efficiency by a factor of two compared with Launceston and Canberra is due solely to local size distribution (*i.e*. aerosol source-type) differences. It points to the need for care in use of scattering data to infer fine mass in the absence of other aerosol data. Errors of a factor of two or more in inferred mass would be possible, based on these AFP Study data.

8.4 State/Territory Agencies: Instrument Comparison

One significant motivation for this study was a desire to investigate the relative performance of a variety of aerosol measurement instruments previously employed in Australia in both monitoring and research activities in the different jurisdictions. Such a broad-scale assessment has not been undertaken previously in this country, but it is noteworthy that where such instrument comparisons have been undertaken elsewhere using ambient aerosol, differences in performance between co-located measurement systems have often been found to be significantly larger than would be expected based on the performance of the individual systems under ideal (or laboratory test) conditions [*e.g*. see discussion included in Chow, 1995]. The case of the TEOM discussed in the previous section illustrates this point well.

Protocols for assessment of aerosol system performance have been developed, most notably by the US EPA, which defines a given measurement system meeting a tightly specified protocol as being a Federal Reference Method. Additional protocols that are met by non-reference methods allow classification of alternate measurements methods/systems as Equivalent Methods. For example the TEOM 1400 and 1400a series instruments are registered as an Equivalent Method for PM10 determination. Although PM2.5 and even PM1 measurements now figure significantly in both technical and policy debates concerning the atmospheric aerosol [*e.g*. Chow, 1995; Vedal, 1997], the regulations focus almost exclusively on PM10 in terms of performance specifications. A convenient and thorough overview of the recent US position is provided by Chow [1995].

In Australia the situation is somewhat less developed. The two Australian Standards relevant to the AFP Study are AS 3580.9.6-1990 and AS 3580.9.7-1990, defining the methods and performance requirements for PM10 determination by manual gravimetric analysis of High Volume sampler filters and Dichotomous sampler filters, respectively. These Australian Standards derive heavily from the relevant US literature.

The resources and time available to the AFP Study precluded carrying out performance evaluations in the form detailed in the US EPA Methods or Australian Standards: it was simply impossible to meet the defined hardware requirements (co-location of three samplers of each type), or sampling requirements (≥15 twenty-four hour samples per site, with a minimum of five samples having PM10 greater than 50 μg m^{-3}). Therefore an alternative, pragmatic approach was adopted in the AFP Study.

A key element in this was the use of a single “reference package” of aerosol measurement systems that would be deployed sequentially in parallel with local authority measurement systems in six different state/territory locations across the country. The aim was

to enable comparison of the performance of different aerosol measurement systems operated in different parts of the country, by different groups, via comparison of these disparate systems with a single, unchanging suite of aerosol samplers set up and overseen identically in each location by unchanging (CSIRO/ANSTO) operators.

A second element in the AFP Study design concerned the contents of the "reference package". A conscious decision was made to include a range of aerosol measurement systems, representative of systems deployed previously in Australia in aerosol studies, to permit a second level of instrument performance comparison. In this case the variability associated with different instrument systems operated by different groups was removed: a single set of instruments operated by a single group would be compared, across a range of aerosol types at six different locations/seasons.

Although the AFP study did not adopt quantitatively the performance assessment criteria of the US EPA Methods/Australian Standard Methods, these methods may provide a convenient guideline for assessment of relative instrument performance. The criteria for comparison between data from co-located candidate samplers and reference samplers from AS 3580.9.6-1990 (Method 9.6 referring to the gravimetric determination of PM10 using a Hivol sampler) are given in Table 25.

Table 25. Criteria for acceptance of PM10 samplers, AS 3580.9.6-1990.

Specification	***Criteria***
Slope of the regression relationship	1 ± 0.1
Intercept of the regression relationship	0 ± 5 µg m^{-3}
Correlation of the reference sampler and candidate sampler	≥ 0.97

For the purposes of the following comparison the MOUDI is adopted as the reference sampler. This choice is based on the facts that the MOUDI is a very well understood and well-characterised instrument (see earlier chapters), its response does not depend on size selective inlet characteristics, and it operated on the most days, at all sites. Moreover, it consistently showed the lowest variance and highest correlations in bivariate comparisons with all other mass-determining instruments, indicating subjectively, at least, that it was the most precise of the mass-determining instruments employed.

Regressions were computed for the four instruments in the AFP "travelling package" for which there were 12 or more concurrent instrument-MOUDI 24 hour-average data points, distributed across the different sites. Regression results are provided in Table 26. It is apparent from the Table that only the Solar-Vol data would meet our chosen "indicative" criteria (slope, intercept and correlation coefficient) listed in Table 25.

Table 26. Regression relationships between AFP instruments and the MOUDI, with 95% confidence ranges.

	Slope	Intercept	R	n
ANSTO PM10	0.62±0.26	5.4±7.5	0.75	22
ANSTO PM2.5	1.22±0.17	-8.1±5.3	0.95	24
Solar-Vol PM2.5	1.06±0.14	0.5±5.2	0.98	12
TEOM PM2.5	0.71±.08	0.2±3.0	0.98	15

For the comparisons with data generated by the various state/territory authorities regression is not appropriate, as the 3 - 6 concurrent data points which were generated per site are insufficient. As an alternative indicator of relative performance the absolute mean difference between the MOUDI and the alternative sampler was calculated in each case, with results as shown in Table 27. An appropriate context within which to view these data is provided by the US EPA criteria for precision of PM10 measurements summarised by Chow [1995]. This is that repeated co-located measurements should agree within 5μg m^{-3} for measurement at less than 80 μg m^{-3}, typical of the majority of the AFP sampling. It is evident from Table 27, and the visual presentation of the individual data points in Figure 26, that disagreement by more than ± 5 μg m^{-3} was regularly found for individual data pairs.

Table 27. Absolute mean differences between agency samplers and the MOUDI, μg m^{-3}.

	Mean Difference		s.d.	n
HIVOL PM10, ACT	12.4	±	8.1	3
HIVOL PM10, TAS	11.6	±	10.3	6
TEOM PM10, VIC	4.8	±	5.6	5
TEOM PM2.5, NSW	6.3	±	5.0	4
TEOM PM10, QLD	4.1	±	1.8	5
TEOM PM2.5, VIC	4.6	±	4.9	5
TEOM PM1, VIC	3.1	±	2.3	5

Overall these comparisons suggest that the co-located samplers employed by the various groups involved in this study regularly did not achieve the level of precision that evidently underpins the relevant US or Australian standards. It is noteworthy that the Australian Standards contain the following statements: “The test data obtained indicated that two co-located samplers should provide results which agree within 3.3% relative standard deviation” (AS 3580.9.6-1990, PM10 measurements using a Hivol sampler), and “The test data obtained indicated that two co-located samplers should provide results for the fine fractions (PM2.5) ….to agree within 5.5% relative standard deviation, and for the coarse fractions (PM2.5-PM10) ….to agree within 2.2% relative standard deviation. The total PM10 fractions collected should agree within 1.5% relative standard deviation” (AS 3580.9.7-1990, PM10 measurements using a dichotomous sampler). It would appear from the AFP data that in practice, in routine operation under ambient monitoring conditions, these levels of precision may be proving difficult to meet.

8.5 Non-ideality of Size Selective Inlets

One aspect of aerosol sampling, the influence on collected mass of size selective inlet characteristics, has not been studied before in Australia even though it has the potential to affect comparisons between different sampling devices. To consider this question we follow the proforma of the relevant US method, that is to compute the difference between the aerosol mass that would be collected by an ideal inlet and the mass that would be collected by a given instrumental inlet, when challenged with a known aerosol mass distribution. While the US

procedure employs an idealised mass distribution [Chow, 1995] to carry out this analysis, here the availability of well quantified ambient mass distributions from the MOUDI enables the "sampling effectiveness" of given inlets employed in the AFP to be determined on the actual aerosols encountered in the study.

The two samplers employed in this work for which inlet collection functions were available were the Solar-Vol PM2.5 sampler [Ecotech, 1996] and the ANSTO PM2.5 sampler [John and Reischl, 1980]. The collection efficiencies as a function of aerodynamic particle diameter are displayed in Figure 47 along with the ideal PM2.5 inlet characteristic.

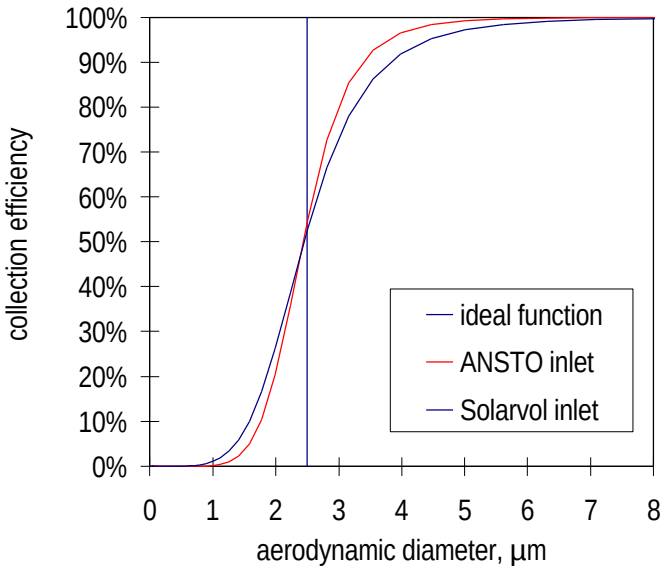

Figure 47. Inlet characteristics of the ANSTO and Solar-Vol PM2.5 samplers.

Figure 48 illustrates the effect of applying the Solar-Vol and ANSTO cyclone inlet functions to a mass distribution determined from the Brisbane site using the MOUDI.

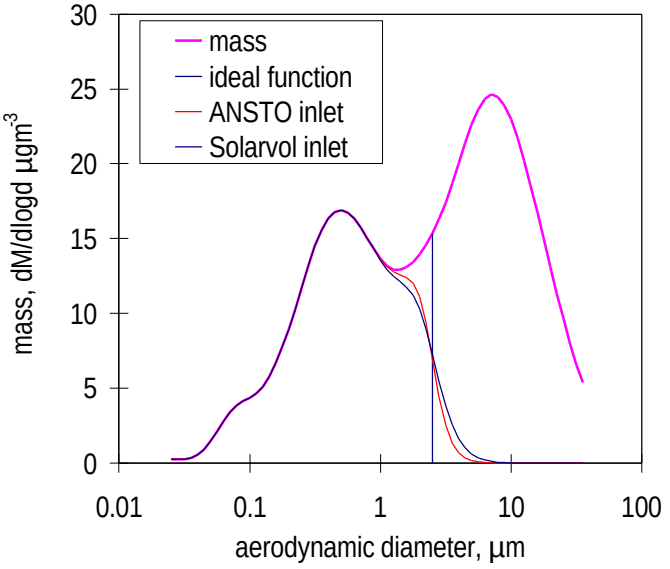

Figure 48. Calculated mass distribution collected by the ANSTO and Solar-Vol PM2.5 samplers, derived from convolution of the sampler inlet functions (Figure 33) with a measured mass distribution (from the MOUDI).

Application of the Solar-Vol and ANSTO inlet functions to a total of 28 MOUDI mass distributions taken across the six AFP sampling sites resulted in an average loss of PM2.5 mass of 1.1% (standard deviation 1.5%) for the Solar-Vol, and 0.7% (standard deviation 1.4%) for the ANSTO sampler. According to the US criterion summarised by Chow [1995] for PM10 the effect of the inlet should be less than 10% in comparison with the ideal sampler. Both the Solar-Vol and the ANSTO sampler meet this requirement. It is pertinent to add that at the levels of PM2.5 measured at all sites except Launceston, systematic discrepancies of order 1% computed here are too small to explain the much larger random discrepancies sometimes exceeding ±5 μg m^{-3}, discussed in the previous section.

8.6 PM10/PM2.5/PM1 Mass Relationships

In the literature discussions of the possible effects of the atmospheric aerosol on human health the question of causation is acknowledged by all sides to be vexed [*e.g.* Seaton *et al.*, 1995; Vedal, 1997, NEPC, 1997; Wilson and Suh, 1997; see also multiple comments in *J. Air & Waste Management*, Vol. 47, 1997]. Variations in each of PM10, PM2.5 and PM1, as well as individual components such as acid sulfate, organic compounds, and even non-mass-based parameters such as "ultrafine" (or CN) number concentration have been proposed as parameters linked with adverse human health outcomes. The absence of clearly identifiable causation in the face of published study results linking adverse heath effects with PM10 has caused considerable difficulty in policy development both in the US [Vedal, 1997; Wilson and Suh, 1997], and in Australia where a PM2.5 ambient standard has been mooted but was discarded in favour of PM10 [NEPC, 1997], perhaps at least partially on the basis that PM10 may act adequately as a surrogate for PM2.5.

The MOUDI data obtained in the AFP Study provide an opportunity to investigate the relationships between the alternative mass-based parameters. A particular advantage of the MOUDI data is that the PM10, PM2.5 and PM1 values may all be derived from a single measurement, thus avoiding errors introduced by differences in sampler performance that are unavoidable if different samplers are required for each PM measurement. As discussed in Section 7.2, PM10 contains at the large size end a significant component of refractory material, produced by mechanical processes, including wind-blown soil dust (Figure 14) and sea-salt (Figure 15). PM2.5 and PM1 fractions contain less of this mechanically-produced aerosol, and relatively more of the products of combustion processes, such as vehicular emissions (Figure 12) and wood-burning (Figure 16), as well as gas-particle conversion products responsible for aerosol acidity (Figure 13). The details of how each size fractions is represented by these sources for each city are discussed also discussed in Section 7.2 and listed in Table 22.

Figures 49 - 51 show the bivariate relationships between the PM10 and PM2.5 size fractions in the 24 hour mean MOUDI samples taken across all six AFP sites. Figures 52 – 54 show the comparable plots for the PM2.5 and PM1 fractions.

The first three figures show that the MOUDI PM2.5 fraction of PM10 is well correlated with PM10, however the PM10-PM2.5 fraction of PM10 is only weakly correlated with both PM10 and PM2.5 aerosol fractions. In the case of the PM2.5 and PM1 fractions of the aerosol (Figures 52 - 54) not only do these two fractions correlate well, but the PM2.5-PM1 fraction also correlates well with both PM2.5 and PM1.

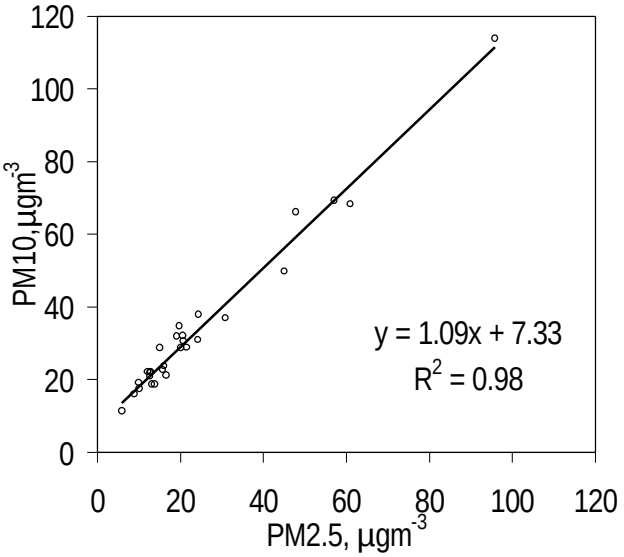

Figure 49. PM10 vs PM2.5, all AFP samples (24 hour mean values).

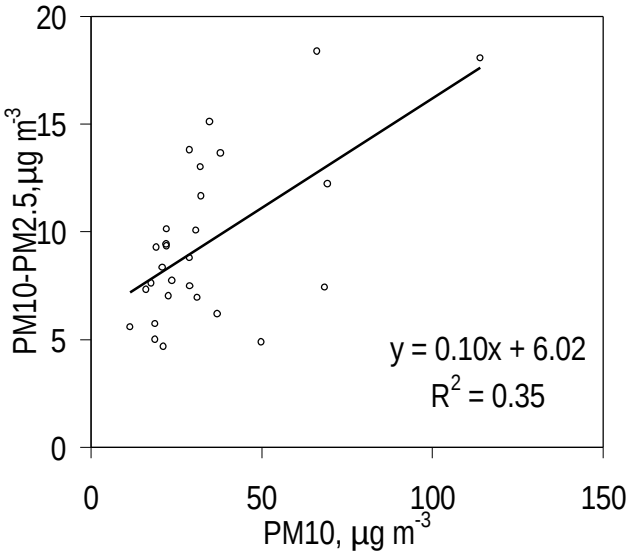

Figure 50. PM10-PM2.5 vs PM10, all AFP samples (24 hour mean values).

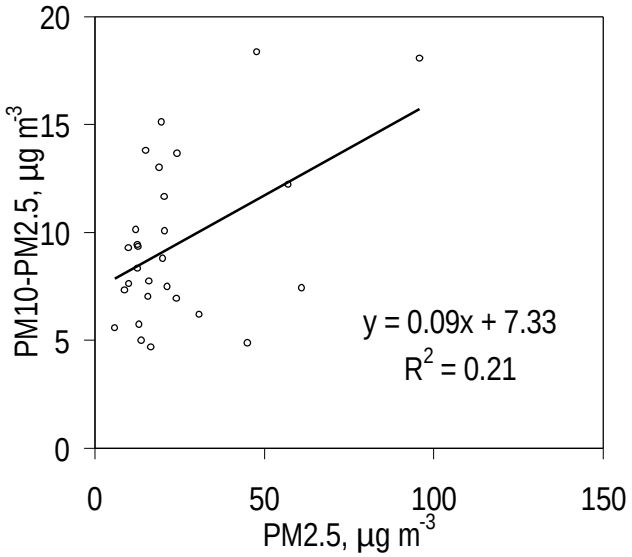

Figure 51. PM10-PM2.5 vs PM2.5, all AFP MOUDI samples (24 hour mean values).

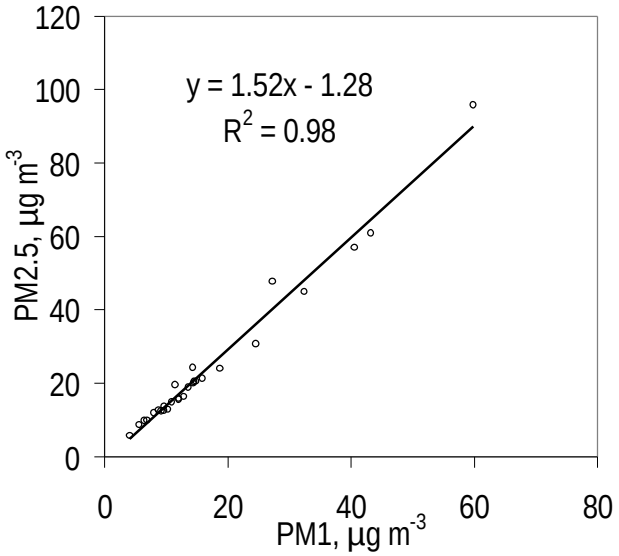

Figure 52. PM2.5 vs PM1, all AFP MOUDI samples (24 hour mean values).

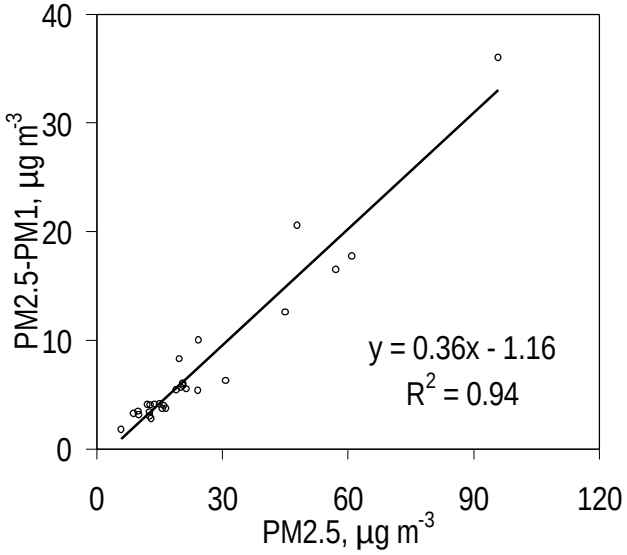

Figure 53. PM2.5-PM1 vs PM2.5, all AFP MOUDI samples (24 hour mean values).

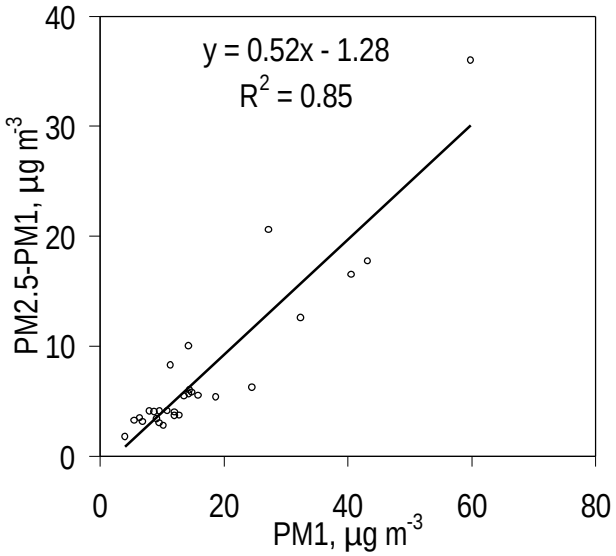

Figure 54. PM2.5-PM1 vs PM1, all AFP MOUDI samples (24 hour mean values).

These results suggest that in the AFP samples variability in PM10 is dominated by variability in the PM2.5 fraction, rather than the PM10-PM2.5 fraction. If the results from the six AFP sites apply to Australian environments generally, then it suggests the possibility that statistical associations between health outcomes and variance in PM10 in Australia may be due to PM2.5, rather than the PM10-PM2.5 component of PM10. If such a hypothesis were tested and found to be sustained, this would provide an argument for an ambient aerosol standard based on PM2.5 mass concentration rather than the current PM10 mass concentration.

On the other hand, the high correlations between each of PM2.5, PM1 and PM2.5-PM1 suggest that in terms of analysis of variance in conjunction with health indicator variables, there would be little to gain by moving from PM2.5 to PM1. Perhaps there may even be something lost if it were the case that PM1 mass concentration measurement systems were less precise than PM2.5 measurements systems because of the smaller mass being sampled.

We conclude that the AFP data give some support to PM2.5 rather than either PM10 or PM1 as the most appropriate indicator of aerosol pollution if a single, integrated exposure parameter is required.

8.7 PM2.5/Ultrafine Particle Mass Relationship – MOUDI Data

In the literature discussions of the possible effects of the atmospheric aerosol on human health the role of ultrafine particles has been questioned [*e.g.* Seaton *et al*. 1995], however ultrafine particle concentrations are not routinely recorded or reported in any Australian jurisdiction as far as we are aware. In general, for reasons discussed elsewhere in this report we do not expect ultrafine particle number concentrations to be correlated with the ambient mass-based data that are reported, *i.e*. PM10 and PM2.5. The AFP ultrafine particle measurements discussed in a subsequent section confirm this. However the availability of the MOUDI mass distributions enables an additional analysis in terms of ultrafine particle mass, since the mass distributions returned by the MOUDI generally show evidence of the ultrafine particle mode in the vicinity of 0.1 µm (100 nm) aerodynamic diameter. Figure 17 depicts a well resolved ultrafine mass mode from a sample taken in Canberra, while Figure 55 below shows a more typical partially resolved ultrafine mode, from a Brisbane sample.

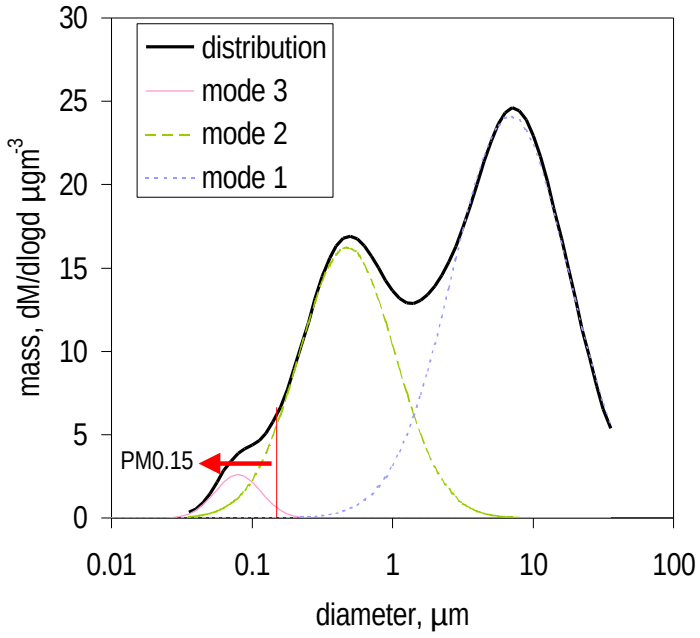

Figure 55. Mass distribution, Brisbane aerosol. For definitions see text.

Given the variable degree to which the ultrafine mass mode was evident, two measures of ultrafine particle mass were estimated from the available MOUDI mass distributions. The first was calculated in analogy to PM10 and PM2.5, that is the area below 150 nm diameter was determined, yielding PM0.15. A second measure was estimated by fitting three log-

normal distributions to each overall MOUDI mass distribution, allowing ultrafine particle mass to be estimated as the area under the log-normal mode centred near 0.1 μm (Figure 55).

Correlations between both measures of ultrafine particle mass and both PM10 and PM2.5 were calculated, essentially addressing the question as to whether either of these commonly determined aerosol parameters also acted as a surrogate for ultrafine particle mass. All correlations were found to be weak, as illustrated by Figure 56 which shows the comparison with PM2.5.

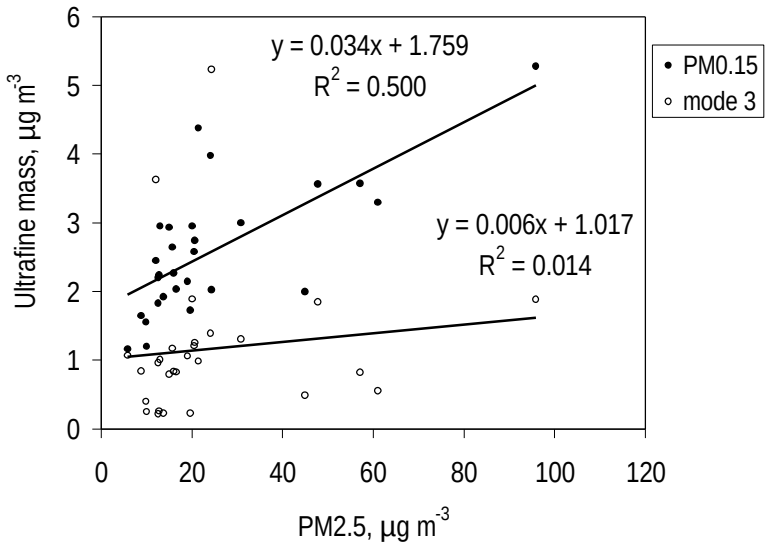

Figure 56. Relationships between two measures of ultrafine particle mass and PM2.5

We conclude that the currently measured mass-based aerosol indicators PM10 and PM2.5 do not act effectively as surrogates for ultrafine particle mass in the AFP MOUDI samples.

8.8 Aerosol Elemental Carbon

Elemental carbon (EC) is one individual aerosol component that makes up a significant part of PM10 and PM2.5 aerosol mass. It is commonly measured in aerosol assessment/source apportionment studies. In urban air it is frequently used as one of several tracers for automotive emissions, especially diesel emissions. It may also be used in the estimation of aerosol organic matter by difference (*i.e.* organic mass = total mass – EC – inorganic mass), so accurate measurement of aerosol EC levels is desirable.

However experience internationally has been that aerosol carbon determinations, both for EC and organic carbon (OC), are difficult to carry out with accuracy and precision. Comparisons between different co-located measurement systems often yield differences of a factor of two or more [*e.g.* Hering *et al.*, 1990; Horvath, 1997; Heintzenberg *et al.*, 1998].

Within the Australian context the possibility of such variation between measurement systems is important, since previous aerosol assessment studies carried out in different parts of the country by different groups have yielded significantly different levels of EC content in PM2.5 aerosol. For example, the ASP Study carried out in NSW reported an average EC contribution to PM2.5 mass of 23% [ERDC, 1995], whereas the Perth Haze Study [Gras,

1996] found the EC contribution to average only half as much. Given the international experience concerning the difficulty of accurately determining EC, it is legitimate to ask whether there is a real difference in the contributions of EC sources to PM2.5 in Sydney and Perth, or whether this apparent difference was simply the result of measurement imprecision.

The two EC measurement systems that underpinned previous major Australian aerosol studies were both deployed in parallel in the AFP Study, and are described in the experimental section earlier. Neither determine EC directly, but carry out a measurement of aerosol optical absorbance, from which EC is estimated on the assumption that visible light absorbance is dominated by EC, to which is attributed a mass absorbance of ~10 m^2 g^{-1}. The laser integrating plate method operated by ANSTO has underpinned aerosol studies in NSW and Brisbane [ERDC, 1995; Chan *et al.*, 1997], while the alternative method employed by CSIRO in aerosol studies carried out in the Latrobe Valley, in Melbourne and in Perth [Ayers *et al.*, 1990; Gras *et al.*, 1992; Gras, 1996] has some different characteristics, *e.g.* it is based on a monochromatic, but much lower intensity LED light source and employs a different filter substrate. As noted earlier in the experimental section a third LED-based absorbance reader was developed for the AFP Study by CSIRO for specific application to the MOUDI samples.

Daily mean (24 hour) EC data were obtained from four sampling systems during the AFP Study, though not all systems were in operation at all sites: the ANSTO PM10 and PM2.5 samplers from which EC was obtained using the ANSTO laser integrated plate absorbance reader; the Ecotech Solar-Vol PM2.5 sampler from which EC was determined using the original CSIRO absorbance reader; and the MOUDI for which EC was determined using the new CSIRO absorbance reader.

Figures 57 - 60 contain bivariate plots comparing the available data pairs from the various EC sampling/measurement systems. Table 28 contains the same data presented as mean values with ~95% confidence interval (twice the s.e.).

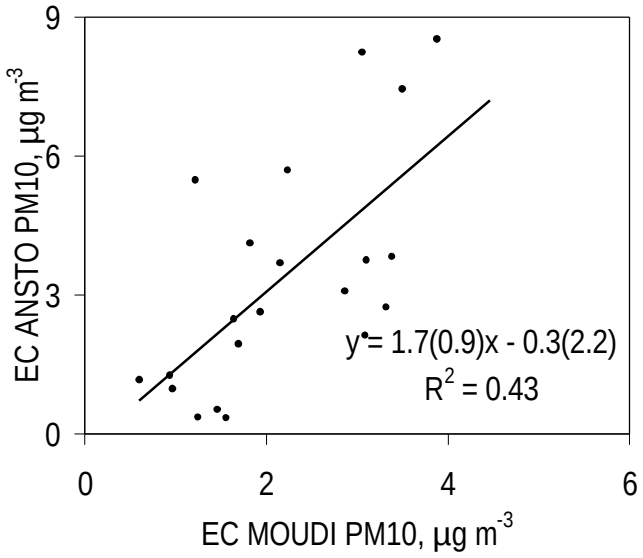

Figure 57. ANSTO vs MOUDI PM10 EC values (24 hour mean values). The values in parentheses are the 95% confidence intervals.

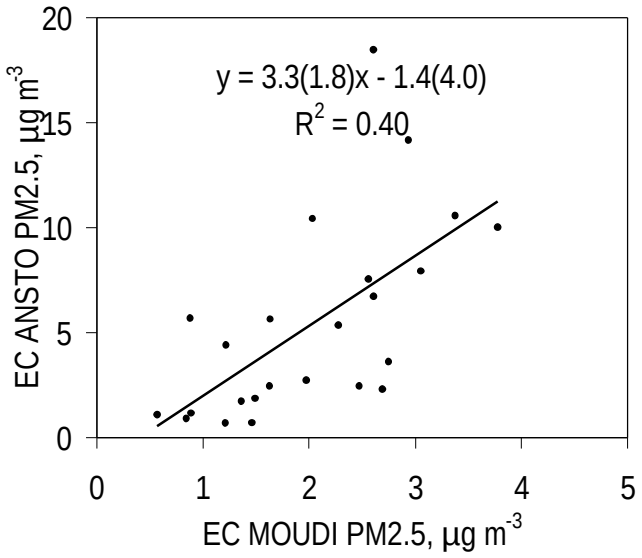

Figure 58. ANSTO vs MOUDI PM2.5 EC values (24 hour mean values)). The values in parentheses are the 95% confidence intervals.

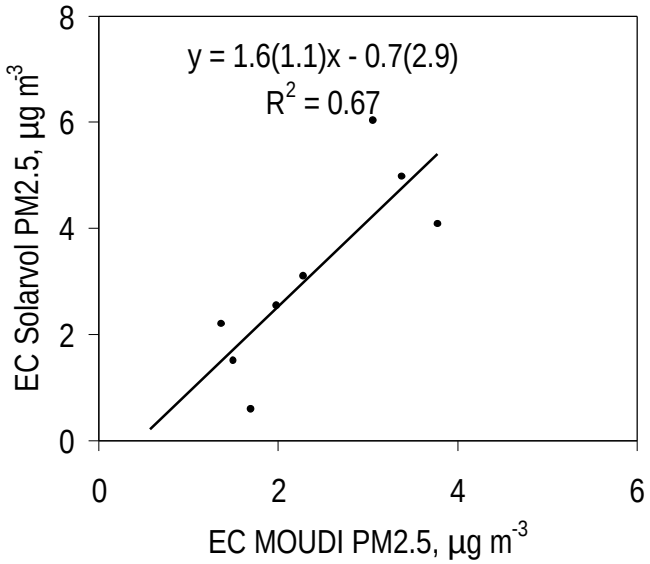

Figure 59. Solar-Vol vs MOUDI PM2.5 EC (24 hour mean values). The values in parentheses are the 95% confidence intervals.

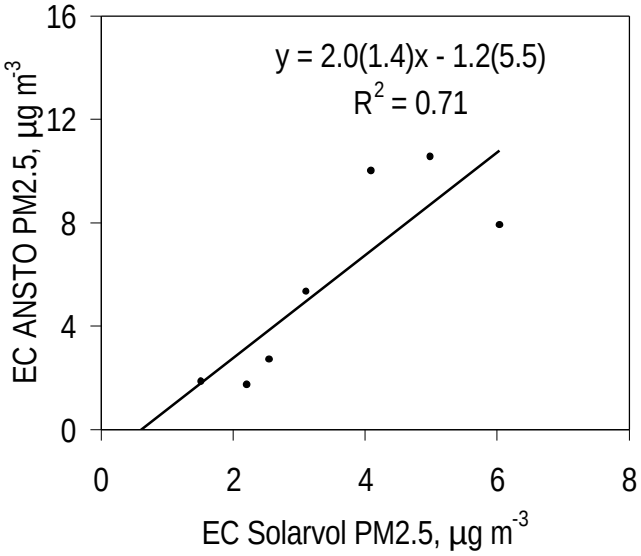

Figure 60. ANSTO vs Solar-Vol PM2.5 EC (24 hour mean values). The values in parentheses are the 95% confidence intervals.

Table 28. Mean EC values (µg m^{-3}) with ~95% confidence intervals. The slight differences apparent for a given sampler in the different comparisons reflects the differing numbers of data pairs in each case.

PM10					
MOUDI			ANSTO		
Mean		95%	Mean		95%
2.2	±	0.4	3.4	±	1.1
PM2.5					
MOUDI			ANSTO		
Mean		95%	Mean		95%
2.0	±	0.4	5.3	±	2.1
MOUDI			Solar-Vol		
Mean		95%	Mean		95%
2.4	±	0.4	3.1	±	0.8
Solar-Vol			ANSTO		
Mean		95%	Mean		95%
3.5	±	0.7	5.7	±	1.7

Two features of the data stand out. First, that the precision of the EC estimations, judged by the scatter in the plots, is considerably worse than that of the gravimetric mass determinations presented and discussed earlier (Figures 20 - 24). Second, there is an indication of systematic variations in response of the systems, with the ANSTO samplers generally yielding higher EC estimates than the CSIRO samplers. For the PM2.5 data, the MOUDI results are lowest, the Solar-Vol results are on average higher, with the ANSTO PM2.5 EC data being the highest. These measurement systems not only employ different optical setups, but also quite different aerosol sample accumulations, which in turn means different optical geometries for the collected aerosol material. It is known that matrix effects (such as the contribution to extinction made by light scattering in the collected sample and filter material) can vary significantly depending upon optical arrangement, filter type and sample loading [*e.g.* Horvath, 1997; Petzold *et al*., 1997; Heintzenberg *et al*., 1998]. In the AFP Study the ANSTO PM2.5 sampler collects aerosol at >7 times the flowrate used by the Solar-Vol, on a different filter type only one quarter the area of the Solar-Vol filter. As a result, the ANSTO aerosol sample will have 30x physical thickness compared with the Solar-Vol. Yet another arrangement occurs with the MOUDI samples, as these are not uniformly distributed over the collection surface but pile up in "spots" below each impaction jet. The effect of this on the light measurements is not well understood.

At this stage it is impossible to determine which of the systems return the most accurate estimate of aerosol EC loading. However it is clear that differences of factors of 2-3 (differences of this order or more are evident in the plots) significantly affects the usefulness of the data. For example, a number of studies in which total aerosol carbon was determined by high temperature combustion of the aerosol material and determination of CO_2 evolved, have demonstrated "mass closure". In other words, aerosol mass determined gravimetrically has been shown to agree (within experimental uncertainty) with the independently determined sum of inorganic components plus total carbon, TC (EC plus OC).

Consistency of aerosol data is often assessed in terms of this idea of "mass closure", or a test of whether total sample mass determined gravimetrically is accounted for by the sum of the major, independently determined aerosol components – organic matter, inorganic matter and elemental carbon. Good mass closure has been demonstrated in the USA, for example, by the work of Malm *et al*. [1994] who used the same cyclone sampler and analysis procedures, including the same laser integrating plate methods (LIPM) as ANSTO. They have also performed independent EC measurements finding good agreement with LIPM techniques. A two year study commencing in 1992 by ANSTO, at 25 sites across NSW, produced mass closure to (84±13)% which did not include 8% measured water vapour [ERDC 1995]. More recent work at selected sites in NSW for local Councils has produced mass closure to (92±9)% all using the LIPM techniques for EC measurements. If the EC measurements were high by a factor of two then the relatively good mass closure agreements would become significantly worst for all these studies. The mass closure measured for the AFP study on all the ANSTO PM2.5 samples using these methods was (96±26)%. The relatively high standard deviation reflects the low numbers of samples and the fact that some samplers were run outside their operating specifications on some days during the study period.

Figure 61 demonstrates another Australian example of this "mass closure". Yet another recent example is provided by the Perth Haze Study [see Figure 25 in Gras, 1996].

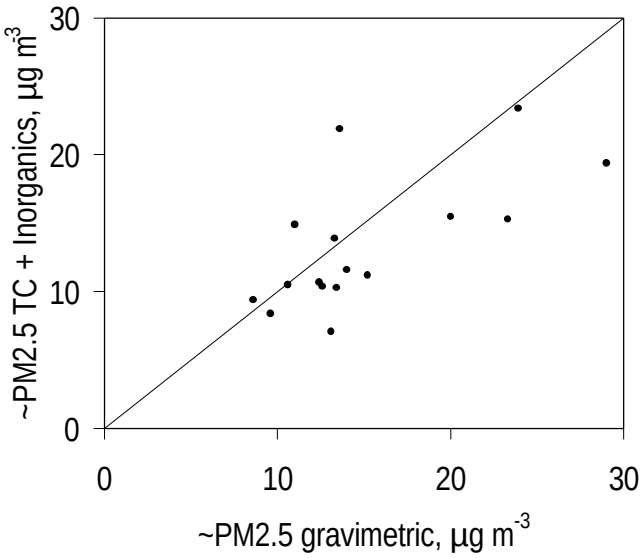

Figure 61. Mass closure from the Latrobe Valley Aerosol/Visibility Study (1986-1988): sum of inorganic and total carbon components vs gravimetric aerosol mass [Ayers *et al*., 1990].

Although reported in the studies quoted above, the confirmation that gravimetrically determined mass can be explained as the sum of inorganic plus organic components is not trivial. The total carbon determinations are difficult, time consuming and costly, so it has been a practical choice for some purposes to not directly determine TC, instead relying on the assumption of mass closure to enable estimation of aerosol organic matter as the difference between gravimetric mass (GM), and the sum of inorganic components (IM) plus EC. In other words Estimated Organic Matter content (EOM) is determined as follows:

$$EOM = GM - IM - EC.$$

Clearly, large disparities in EC or IM would make such a procedure problematic, therefore calculation of EOM for the AFP samples constitutes a sensitive test of the consistency of the GM, IM and EC data. Here we carry out such a consistency test, comparing EOM data calculated from different AFP samplers. We anticipate, in particular, that systematic differences in results from different EC measurement systems would flow through to the EOM calculation to yield systematic EM differences in EOM of the opposite sense. This was found to be the case, as illustrated Figure 62, which contrasts EOM data calculated from the ANSTO PM2.5 EC data (highest EC results) with the MOUDI PM2.5 EC data (lowest EC results).

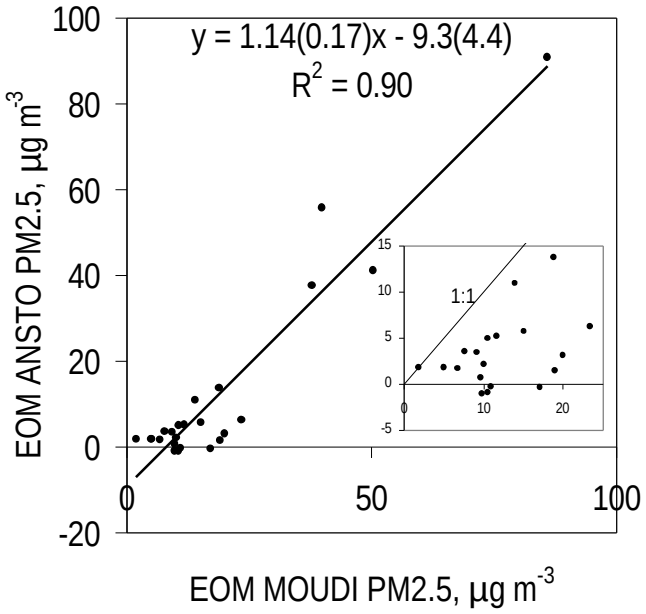

Figure 62. EOM derived from the ANSTO PM2.5 sampler vs EOM from the MOUDI PM2.5 data (24 hour mean values).

At higher PM2.5 mass loadings the EOM values agree reasonably well, but at the more frequently encountered lower levels, as shown in the inset, there is a very large systematic bias towards the MOUDI having much higher EOM, and little correlation – a consequence of subtracting off systematically lower EC values than for the ANSTO sampler. There is also some evidence in the fact that the ANSTO EOM values go to zero, and even negative, that the ANSTO EC values may be systematically high for the lower mass samples.

As noted earlier it is not possible to do more here than to highlight the differences between the different measurement systems. An obvious conclusion to be drawn from these results is that aerosol EC values from the various aerosol studies carried out previously in Australia should be interpreted and compared with caution.

The same conclusion is almost certainly true of aerosol organic matter data. For example it may be that the above definition of EOM is not such a good one for low values of EOM and other techniques such as the one described earlier in section 7.1, where the total hydrogen and sulfur measurements are used, could be more appropriate. However this method also has certain underlying assumptions built into the data estimation procedure. Thus while the question of organic matter estimation in aerosol samples has not been considered in detail here, it would appear prudent to conclude for OC, as in the case of EC, that extant Australian data should be interpreted and compared with caution.

9. Conclusions and Recommendations

A comprehensive range of fine particle physical and chemical properties has been determined during one month at each of six sites in Eastern Australia (located in Sydney, Brisbane, Melbourne, Canberra, Launceston and Adelaide). The particle measurement systems deployed by CSIRO and ANSTO were operated in parallel with the routine particle measurements carried out by the relevant State/Territory agency, enabling an evaluation of the comparability of data from the various measurement systems.

9.1 Comparability of Measurement Systems

At the fine particle levels encountered in the six locations studied, the various measurements of aerosol mass concentration regularly differed by more than the expected levels of measurement system uncertainty. In routine operation, the levels of performance for co-located samplers implied in the Australian PM10 standards [AS 3580.9.6-1990/AS 3580.9.9-1990] and relevant US standards [summarised by Chow, 1995] were not always achieved.

The key source of variance between aerosol measurement systems appears to be the extent to which semi-volatile aerosol material is collected and determined. One component of this is atmospheric water, which may readily exchange with aerosol material sampled on filters in response to change in humidity. Although this fact is well known and allowed for in the standard (gravimetric) PM10 methods, tighter control of humidity during the gravimetric analysis of filters appears desirable. In this regard, it is noteworthy that the least variance between gravimetric data pairs was achieved by the MOUDI (Micro-Orifice Uniform Deposit Impactor) and Solar-Vol samplers: both were operated by the CSIRO group, which had the strictest control of humidity during filter weighing.

A second component of semi-volatile aerosol material occurs in the organic fraction. In general, systematically lower PM2.5 and PM1 values were determined by TEOM (Tapered Element Oscillating Microbalance) measurement systems in comparison with the manual, gravimetric systems. The discrepancy was of order 30% between the CSIRO PM2.5 TEOM and the MOUDI in the AFP Study. The principal difference between these systems is that the TEOMs operate with the inlet air stream heated to well above ambient temperature (commonly to 50^{o}C) whereas the manual gravimetric systems collect aerosol material at ambient temperature. Evidence in the international literature supports the view that volatilisation of semi-volatile organic material in the heated inlet is a cause of systematically lower TEOM data.

Comparison of the two measurement systems used extensively to estimate aerosol elemental carbon (EC) content in previous Australian fine particle studies revealed a systematic difference approaching a factor of two. Differences of this magnitude have been found internationally in comparisons between aerosol carbon measurement systems, underlining the difficulties inherent in these measurements.

Taking into consideration all these findings we recommend that:

(1) a nationally coherent approach to particle measurement systems should be developed, incorporating performance standards for PM parameters that are amenable to validation on a regular basis (for example by comparison of operational instruments in routine use with a single national “calibration” sampler operated by a single agency);

(2) consideration should be given to seeking a common sampling system for particle measurements in all jurisdictions, to avoid differences between different sampler types and different operational procedures;

(3) care should be exercised in the use of heating to achieve humidity control for measurement systems such as the nephelometer or TEOM; where heating is used operationally the extent of loss of semi-volatile aerosol material should be assessed by comparison with manual, gravimetric measurements undertaken at ambient temperature;

(4) consideration should be given to employing alternate methods of humidity control (drying) in Australian fine particle measurement systems;

(5) comparisons between absolute EC levels reported from previous Australian fine particle studies should be made with caution; research should be undertaken to evaluate available methods of aerosol carbon measurement with a view to developing a single method of measurement for aerosol carbon that is appropriate for Australian conditions.

9.2 Relationships Between PM10, PM2.5 and PM1

The MOUDI has been used in the AFP study to provide data on aerosol mass and chemical composition over the TSP, PM10, PM2.5 and PM1 aerosol fractions simultaneously, without the additional error that must intrude if these four parameters are measured by four separate instruments.

While PM10 and PM2.5 data show a strong structural relationship, variability in PM10 was found to be dominated by variability in the PM2.5 fraction, rather than the PM10-PM2.5 fraction. Thus, the statistical relationships noted between health outcomes and PM10 are most likely caused by the PM2.5 component of the size fraction, rather than the PM10-PM2.5 fraction. This would appear to provide an argument for an ambient aerosol standard based on PM2.5 mass concentration rather than the current PM10 mass concentration. It suggests that stronger relationships might be observed between PM2.5 and health outcomes, than are currently observed between PM10 and health outcomes, if more PM2.5 data were available, *i.e*. if PM2.5 data were regularly monitored and reported.

On the other hand, the high correlations between each of PM2.5, PM1 and PM2.5-PM1 suggest that in terms of analysis of variance in conjunction with health indicator variables, there would be little to gain by moving from PM2.5 to PM1.

Therefore, we recommend that:

(6) PM2.5 measurements should be undertaken routinely in Australia (initially in conjunction with existing PM10 measurements so as to provide a quantitative basis for determining which is the better indicator of health effects of atmospheric particles);

(7) given high correlations found between PM1, PM2.5-PM1 and PM2.5, PM1 measurements offer no clear advantage over PM2.5 measurements as a mass-based indicator of potential health effects of ambient particles.

9.3 Continuous Particle Measurement Systems: Nephelometer, TEOM, Ultrafine Particle Measurement Systems

The advantages of a continuous monitoring systems compared with 24 hour average sampling on a 6 day cycle should be self-evident. Where high particle loadings occur on an event basis, as in most Australian cities, this avoids the 5 in 6 probability of missing events, provides greater insights into physical processes, opens the prospects for examining lagged particle-health relationships (over varying lag times) and allows much better statistics for

health determinations where statistics are usually severely limited. However any measurement system has limitations as well as advantages, as noted above in the case of the TEOM.

Use of nephelometers to determine aerosol scattering coefficient (b_{spd}) at multiple sites in a number of Australian locales has a long history, going back as much as two decades. Although scattering coefficient as determined by a nephelometer is an integral property of the aerosol size distribution, the physics of the interaction between aerosol particles and visible radiation is weighted towards particles in the sub-micrometre size range. Within the context of an emerging focus internationally on the PM2.5 aerosol fraction, it is relevant to consider the possibility that the extensive historical records of b_{spd} might provide a surrogate historical record for PM2.5, because this latter mass-based integral measure tends also to be dominated by a mode in the mass distribution at diameters below 1 μm.

In the AFP Study we have confirmed that linear relationships can be found between b_{spd} (measured by nephelometer) and PM2.5 (measured by TEOM) in each city studied. However differences in the scattering-mass relationships were identified, caused by site-specific aerosol (size distribution) properties. Thus if b_{spd} were to be used as a surrogate historical record for PM2.5 the slope of the relationship would have to be determined for each site. An additional complication is that at any given site this relationship may vary with season (not investigated in the AFP study), so clearly caution would be required in any project aimed at harmonising the historical b_{spd} data records with new and ongoing PM2.5 records. Other complicating matters are the significant dependence of nephelometer output on humidity, and the strong implication from the TEOM results that humidity reduction by heating, often used for nephelometers as well as for the TEOM, may not be appropriate.

Ultrafine particle number concentration is also readily amenable to continuous measurement: such measurements were included in the AFP Study. The AFP study data show that ultrafine particle number concentrations do not correlate with the ambient mass-based data normally reported, *i.e*. PM10 and PM2.5, nor with measures of ultrafine particle mass derived from MOUDI data (*i.e*. estimates of PM0.15). We conclude that mass-based integral properties of the aerosol do not provide surrogates for ultrafine particle number concentration.

Taking into consideration these findings we recommend that:

(8) a rigorous determination of the relationship between b_{spd} and PM2.5 must be carried out at each locality (over at least one complete annual cycle) where historical b_{spd} data are to be used as a surrogate for fine mass data.

(9) ultrafine particle number concentrations cannot be inferred from mass-based aerosol measurements so must be determined directly using independent ultrafine particle (or condensation nucleus) measurement systems.

9.4 Gaps in Knowledge

The AFP study has highlighted a number of areas where further understanding is required to underpin sound policy development. The most important lack of knowledge concerns semi-volatile aerosol material. A related issue, given the probable role of organic material as a major fraction of the semi-volatile aerosol material, and the possible role of toxic organic constituents in health effects, is a lack of certainty about the amount and types of carbonaceous material in the aerosol. In this regard we recommend that:

(10) studies be undertaken to characterise the semi-volatile component of aerosol material in the major urban airsheds in Australia, in terms of its contribution to PM10 and PM2.5 mass loading, its composition, sources, and variability with location and season;

(11) uniform methods be developed and agreed between jurisdictions for the determination of carbonaceous aerosol material, in particular the components elemental carbon (EC) and organic carbon (OC).

Discussions between the AFP Study team and representatives of the various State/Territory agencies assisting with the measurement program suggest that a number of aspects of fine particle monitoring and assessment may have been the subject of in-house investigations carried out by some of these agencies. Useful information may have been generated, but remains not widely known or available. Therefore we recommend that:

(12) agencies be encouraged to make available to a central database, located in Environment Australia, copies of all published and unpublished work in their possession related to aerosol monitoring and assessment in Australia.

Finally, taking into consideration all the foregoing comments we recommend that:

(13) given the current uncertainty world-wide over the implications for human health of exposure to fine particles, the uncertainty over choice of ambient indicator for fine particles, the disparity of approaches taken to date by different agencies within Australia, and the evident differences between results from different measurements systems employed in the AFP Study, a national conference on fine particle monitoring and assessment should be held. The aim would be to bring together the relevant regulatory agencies and research institutions to seek a consensus on the development of a nationally uniform approach to fine particle monitoring and assessment within Australia.

10. Acknowledgments

The AFP Study involved the co-operation of a large number of individuals. We would like to thank several people for their help in obtaining access to the measurement sites, including Steve McPhail and George Richmond (EPA, NSW), David Wainwright (DoE, QLD), Trevor Bardsley and Cathy Wilson (EPA, VIC), Tony Hodgson (Environment, ACT) and Wayne Riley (ACT Analytical Laboratories), Frank Carnovale and Frank Cattel (DoE, TAS) and Bill Piesse (Launceston City Council), Rob Mitchell (EPA, SA) and the St George School, Therbaton.

The AFP research team gratefully acknowledges all the State and Territory Authority personnel who assisted with field work, including Phil Kingston, Brendan Finn and Brian Haynes (DoE, QLD), Ian Fox and Kerry Boulder (ACT Analytical Laboratories) and Robert Trimble (DoE, TAS). We would also like to thank Neville Clark (Flinders University) for his help in the field.

Paul Selleck, Jenny Powell, Kate Boast and Tom Firestone (CSIRO) and Eduard Stelcer (ANSTO) are gratefully thanked for the contributions to the analysis of samples and data. Rob Gillett, Mark Hibberd and Andrew Larkin are thanked for valuable discussons.

11. References

Allen G., C. Sioutas, P. Koutrakis, R. Reiss, F.W. Lurmann and P.T. Roberts [1997], Evaluation of the TEOM method for measurement of ambient particulate mass in urban areas, *J. Air Waste Management Assoc*., **47**, 682-689.

AS3580.9.6 [1990], Australian Standard methods for sampling and analysis of ambient air. Method 9.6: Determination of suspended particulate matter-PM10 high volume sampler with size-selective inlet-Gravimetric method. Standards Australia, North Sydney, 11p.

AS3580.9.7 [1990], Australian Standard methods for sampling and analysis of ambient air. Method 9.6: Determination of suspended particulate matter-PM10 dichotomous sampler - Gravimetric method. Standards Australia, North Sydney, 11p.

Ayers G.P., E.K. Bigg, D.E. Turvey and M.J. Manton [1981], Urban influence on condensation nuclei over a continent, *Atmos. Environ.*, **16**, 951-954.

Ayers G.P., Gras J.L., Gillett R.W. and Bentley S.T. [1990], The Latrobe Valley Aerosol/Visibility Study : a summary of results, *Clean Air [Aust.]*, **24**, 18 - 26.

Brook J. R., T. F. Dann and R. T. Burnett [1997], The relationship among TSP, PM10, PM2.5 and inorganic constituents of atmospheric particulate matter at multiple Canadian locations, *J. Air Waste Management Assoc*., **47**, 2-19.

Chan Y.C., R. W. Simpson, G. H. Mactainsh, P. D. Vowles, D. D. Cohen and G. M. Bailey [1997], Characterisation of chemical species in PM2.5 and PM10 aerosols in Brisbane, Australia, *Atmos. Environ.*, **31**, 3773-3785.

Chow J. C. [1995], Measurement methods to determine compliance with ambient air quality standards for suspended particles, *J. Air Waste Management Assoc*., **45**, 320-382.

Ecotech [1996], Solar-Vol 1100 Particulate Sampler for PM10, PM2.5, TSP-Reference Manual, Ecotech Pty Ltd, Blackburn, Australia, pp 26.

ERDC [1995], Contributions of fuel combustion pollution by airborne particles in urban and non-urban environments. Report no. ERDC 259. Energy Research and Development Corporation, Canberra, Australia.

Gras J.L., R.W. Gillett, S.T. Bentley, G.P. Ayers and T. Firestone [1992], CSIRO-EPA Melbourne Aerosol Study, Final Report to EPA of Victoria.

Gras J.L. [1996] The Perth Haze Study. Report to the Department of Environmental Protection of Western Australia, CSIRO.

Heintzenberg, J., R. J. Charlson, A. D. Clarke, C. Liousse, V. Ramaswamy, K. P. Shine, M. Wendisch and G. Helas [1998], Measurements and modelling of aerosol single-scattering albedo: Progress, problems and prospects, *Bietr. Phys. Atmosph*., **70**, 249-263.

Hering S.V. *et al.* [1990], Comparison of sampling methods for carbonaceous aerosols in ambient air, *Aerosol Sci. and Technol*., **12**, 200-213.

Horvath H. [1997], Experimental calibration for aerosol light absorption measurement using the integrating plate method – summary of data, *Aerosol Sci*., **28**, 1149-1161.

John W. and G. Reischl [1980], A cyclone for size-selective sampling of ambient air, *J. Air Poll. Control Assoc*., **30**, 872-877.

Lin C. I., M. Baker and R. C. Charlson [1973], Absorption coefficient of atmospheric particles, *Appl. Optics*, **12**, 1357-1363.

Malm C. W., J. F. Sisler, D. Huffman, R.A. Eldred and T.A. Cahill, [1994], Spatial and seasonal trends in particulate concentration and optical extinction in the United States, *J. Geophys. Research, **99,*** 1347-1370.

Manton M.J. and G.P. Ayers [1982], The evolution of an aerosol plume from a town, *Boundary Layer Met.,* **22**, 171-181.

Marple V. A., K. L. Rubow and S. M. Behm [1991], A microorifice uniform deposit impactor [MOUDI]: Description, calibration and use, *Aerosol Sci. and Technol.,* **14**, 434-446.

Meyer M., J. Lijek and D. Ono [1992], Continuous PM10 measurements in a woodsmoke environment, PM10 Standards and Nontraditional Particulate Source Controls, J. C. Chow and D. M. Ono, Eds , *Air Waste Management Assoc*., TR-22, Vol 1 pp24-38.

Meyer M. and E. G. Rupprecht [1997], Particulate matter sampling methods: The importance of standardisation, *J. Aerosol Sci*., **27**, supp 1, S349-S350.

NEPC [1997], Towards a National Environment Protection Measure for Ambient Air Quality, National Environment Protection Council paper on ambient air quality.

Petzold A., C. Kopp and R. Neissner [1997], The dependence of the specific attenuation cross-section on black carbon mass fraction and particle size, *Atmos. Environ.,* **31**, 661-672.

RWTÜV [1994], Performance testing of the Rupprecht and Patashnick TEOM Series 1400a Ambient Particulate Monitor, Report to R&P from RWTÜV Anlagentechnik GmbH, Essen, Germany.

Seaton A., W. MacNee, K. Donaldson and D. Godden [1995], Particulate air pollution and acute health effects, *Lancet*, **345**, 176-178.

Twomey S. A. and R. A. Zalabsky [1981], Mulitifilter technique for examination of the size distribution of the natural aerosol in the submicrometer range, *Environmental Sci. Tech*., **15**, 177-184.

Vedal S. [1997], Ambient particles and health: the lines that divide, *J. Air Waste Management Assoc*., **47**, 551-581.

Wilson W. E. and H. H. Suh [1997], Fine particles and coarse particles: concentration relationship relevant to epidemiologic studies, *J. Air Waste Management Assoc*., **47**, 1238-1249.

Winklmayr W., H-C, Wang and W. John [1990], Adaptation of the Twomey algorithm to the inversion of cascade impactor data, *Aerosol Sci. Tech*., **13**, 322-331.

Working Party [1996], Report into Air Pollution Environmental Health and Respiratory Diseases, Launceston and Upper Tamar Valley, Tasmanian 1991-1994, by the Air pollution Environmental Health and Respiratory Diseases Working Party, published by Launceston City Council.

12. Glossary of selected terms

Term	*Meaning*
Aerodynamic diameter	defined property of any given atmospheric particle: the diameter of a spherical particle of density 1 g cm^{-3} that would have the same aerodynamic behaviour as the given particle [Chow, 1995]
Aerosol	generic term for a suspension of liquid or solid droplets/particles in a fluid; the atmospheric aerosol consist of particles ranging in size from molecular clusters (≤1 nm in diameter) to large cloud and drizzle drops (~100 μm in diameter)
ASASP-X	Particle Measuring Systems Inc. (PMS) active-cavity-laser particle size spectrometer that uses light scatter in an open-cavity laser system to size individual particles over the diameter range of 100 nm to 3 μm (nominal) into 60 size channels (in four overlapping ranges)
b_{sp}	aerosol light scattering coefficient at ambient humidity
b_{spd}	aerosol light scattering coefficient for dry particles
b_{abs}	aerosol light absorption coefficient
CN	Condensation Nuclei; synonymous with the older term Aitken nuclei; effectively equivalent to the total number concentration of atmospheric particles larger than the condensation nucleus counter minimum particle size threshold, typically ~3 nm particle diameter
CCN	Cloud Condensation Nuclei; the subset of CN that act as centres for cloud droplet nucleation at the small supersaturations (typically 0.1 - 1%) encountered in natural clouds; usually consists of particles containing soluble salts with diameter greater than about 10 – 50 nm
coarse particles	old term mostly used by aerosol physicists to denote atmospheric particles larger than about 1 μm in diameter
cut-point	usually specified as 50% cut-point, or the aerodynamic particle diameter at which the sampling efficiency falls to 50%; i.e. the diameter at which an aerosol sampling device collects 50% of incoming particles and transmits 50% of incoming particles
DMA	Differential Mobility Analyser determine the mobility of an particle which is dependent on the size of the particle. In this study when attached to a CN or UCN counter particle size distributions in the range 15 nm - 300 nm could be determined
EC	Elemental Carbon
EOM	Estimated Organic Matter (EOM) is determined as follows: EOM=GM-IM-EC

Term	*Meaning*
fine particles	old term mostly used by aerosol physicists to denote atmospheric particles smaller than about 1 µm in diameter
GM	Gravimetric Mass
IC	Ion Chromatography; a method of analysis applicable to aqueous ionic species; sensitive method applied to aerosol samples after the samples are dissolved in high purity water
IM	Inorganic Mass calculated (after Brook *et al*. 1997): $IM=H^{+}+Na^{+}+1.41K^{+}+NH_4^{+}+1.63Ca^{2+}+Mg^{2+}+Cl^{-}+NO_3^{-}+NO_2^{-}+SO_4^{2-}+PO_4^{3}+Pb+Br+1.79V+2.2Al+1.24Zn+2.5Si+1.58Fe+1.94Ti+Cr+Mn+Co+Ni+Cu$
M2.5	mass concentrations calculated from ASASP-X size distributions for particle diameter less than 2.5 µm and an assumed density of 1.7 g cm^{-3}
MOUDI	Micro Orifice Uniform Deposit Impactor: aerosol sampling device used in this study to determine aerosol mass-size distribution over the range ~0.05 - 20 µm in diameter [Marple *et al.*, 1991]
nephelometer	device used to measure b_{sp} in real-time; based on illuminating a length of ambient air with a strong collimated light source in the visible region, and collecting off-axis scattered light with a sensitive photomultiplier/amplifier
particles	generic term; widely understood common meaning; often used interchangeably with "aerosol", as in "atmospheric particles" and "atmospheric aerosol"
particulates	variation of the word "particles" usually applied in the regulatory or "air quality" communities, infrequently used by aerosol physicists; a term to be avoided as a useless gloss
PIXE	Proton Induced X-ray Emission; a method of elemental analysis based on exciting a sample with a high energy proton beam and collecting the emitted x-rays, for which specific x-ray energies are unique to each element; useful for elements above an atomic number of 13
PM10	the subset of atmospheric particles having aerodynamic diameters less than 10 µm
PM2.5	the subset of atmospheric particles having aerodynamic diameters less than 2.5 µm
PM1	the subset of atmospheric particles having aerodynamic diameters less than 1 µm
STP	Standard Temperature and Pressure: standard gas (atmospheric) conditions defined to be 273.15 Kelvin and 101.3 hPa

Term	*Meaning*
TEOM	Tapered Element Oscillating Microbalance; device used to determine real-time aerosol mass concentrations; use of different inlets enables measurement to represent any one of TSP, PM10, PM2.5 or PM1; based on collecting aerosol on a tapered quartz element, the oscillation frequency of which depends sensitively upon collected aerosol mass
TSP	Total Suspended Particle mass; mass concentration of particles of all sizes; usually expressed in units of μg m^{-3} at STP
UCN	Ultrafine Condensation Nuclei (see ultrafine particles)
ultrafine particles	new term entering scientific usage in the 1990's referring to particles in the aerodynamic diameter range from ~2nm to ~100 – 200 nm